EFFECTS OF SHORT AND LONG TERM STORAGE SYSTEMS ON SIZE DETERMINATION OF RENEWABLE ENERGY SYSTEMS IN MICRO-GRIDS

SUSTAINABLE ENVIRONMENT AND ENERGY SYSTEMS

MIDDLE EAST TECHNICAL UNIVERSITY

NORTHERN CYPRUS CAMPUS

BY

LOIY AL-GHUSSAIN

IN PARTIAL FULFILLMENT OF THE REQUIREMENTS FOR

THE DEGREE OF MASTER OF SCIENCE

IN

SUSTAINABLE ENVIRONMENT AND ENERGY SYSTEMS

JUNE 2017

Approval of the Board of Graduate Programs

Prof. Dr. Oya Yerin Guneri
Chairperson

I certify that this thesis satisfies all the requirements as a thesis for the degree of Master of Science

Asst. Prof. Dr. Carter Mandrik
Program Coordinator

This is to certify that we have read this thesis and that in our opinion it is fully adequate, in scope and quality, as a thesis for the degree of Master of Science.

Asst. Prof. Dr. Onur Taylan
Supervisor

Prof. Dr. Derek Baker
Co-Supervisor

Examining Committee Members

Assoc. Prof. Dr. Murat Fahrioglu	Electrical and Electronics Engineering, METU NCC	
Asst. Prof. Dr. Onur Taylan	Mechanical Engineering, METU NCC	
Prof. Dr. Derek K. Baker	Mechanical Engineering, METU	
Prof. Dr. Serkan Abbasoglu	Energy Systems Engineering, Cyprus International University	
Prof. Dr. Ali Tasiran	Economics, METU NCC	

I hereby declare that all information in this document has been obtained and presented in accordance with academic rules and ethical conduct. I also declare that, as required by these rules and conduct, I have fully cited and referenced all material and results that are not original to this work.

Name, Last Name: Loiy Al-Ghussain

Signature:

ABSTRACT

EFFECTS OF SHORT AND LONG TERM STORAGE SYSTEMS ON SIZE DETERMINATION OF RENEWABLE ENERGY SYSTEMS IN MICRO-GRIDS

Al-Ghussain, Loiy

M.Sc., Sustainable Environment and Energy Systems

Supervisor: Asst. Prof. Dr. Onur Taylan

Co-Supervisor: Prof. Dr. Derek Baker

June 2017, 81 pages

Energy resources and global warming are two of the most important concerns for the whole world, where the necessity of finding clean and cheap energy resources have high priority nowadays. Renewable Energy Systems (RES), such as PV power plants and wind turbines, have the ability to meet the demand of the world; however, the energy generation of these kind of systems does not fully match with the electrical energy demand. Having a diversity of RESs with Energy Storage System (ESS) will increase the matching between the energy generation and the energy demand. The purpose of this thesis is to determine the sizes of different Renewable Energy Micro-Grid (REMG) systems with four main ESS scenarios with and without taking the ESS depth of discharge (DOD) into consideration; (1) without ESS, (2) with short term ESS-batteries, (3) with long term ESS-Pumped Hydro Storage (PHS), (4) with hybrid short and long term ESSs- batteries and PHS- for a university campus on a Mediterranean island in order to achieve the maximum yearly RES fraction (F_{RES}) with Cost of Electricity (COE) equal or lower than the local grid tariff. Moreover, this study aims to determine the optimal ESS sizing methodologies with different RESs in order to achieve this goal. In addition, a sensitivity analysis of the models is carried out to determine the sensitivity of the RESs to the fluctuation of meteorological data in addition to the variation in the demand. Moreover, the effect of the integration of different ESS scenarios on the COE, F_{RES}, demand supply fraction (DSF) and the feasible sizes of PV, wind, PV/wind hybrid systems is studied in addition to the effect of the DOD of the ESS on these parameters. The results indicate that the PV/wind hybrid system with 4.19 MW PV, 8 MW wind and 89.51 MWh PHS has the highest F_{RES}- 88.04%- among the other RESs while the PV/wind hybrid system with 3.44 MW

PV, 8 MW wind, 833 kWh battery and 89.51 MWh PHS has the highest DSF- 80.74%- with COE equal to the grid tariff. Moreover, the results indicate that the integration of ESS affects the economic and technical parameter of the RES where these effects vary based on the RES type, ESS type and RES capacity. Furthermore, the results show that the DOD of the ESS is a vital parameter that affects the optimal ESS sizing methodologies and the economic and technical parameters of the RES.

Keywords: energy storage systems, PV systems, wind systems, PV/wind hybrid systems, depth of discharge.

ÖZ

MİKRO-ŞEBEKELERDEKİ YENİLENEBİLİR ENERJİ SİSTEMLERİNİN BOYUTLANDIRMASINDA KISA VE UZUN VADELİ ENERJİ DEPOLAMA SİSTEMLERİNİN ETKİSİ

Al-Ghussain, Loiy

Yüksek Lisans, Sürdürülebilir Çevre ve Enerji Sistemleri

Tez Yürütücüsü: Yrd. Doç. Dr. Onur Taylan

Ortak Tez Yürütücüsü: Prof. Dr. Derek K. Baker

Haziran 2017, 81 sayfa

Enerji kaynakları ve küresel ısınma, temiz ve ucuz enerji kaynaklarının bulunmasının büyük önem taşıdığı günümüz dünyasındaki en önemli kaygılar arasındadır. Fotovoltaik (PV) enerji santralleri ve rüzgâr türbinleri gibi yenilenebilir enerji sistemleri (RES) dünyanın talebini karşılama yeteneğine sahiptir; bununla birlikte, bu tür sistemlerin enerji üretimi, elektrik enerjisi talebi ile tamamen uyumlu değildir. Enerji Depolama Sistemi (ESS) ile çeşitli RES'lere sahip olmak, enerji üretimi ve enerji talebi arasındaki eşleşmeyi artıracaktır. Bu tezin amacı, bir Akdeniz adası olan Kıbrıs'ta bulunan bir üniversite kampüsü için ESS'nin boşalma derinliğini (DOD) dikkate alarak ve almayarak dört ana ESS senaryosuna sahip farklı yenilenebilir enerji mikro-şebeke (REMG) sistemlerinin boyutlarını belirlemektir; (1) ESS olmadan, (2) kısa vadeli ESS-piller, (3) uzun vadeli ESS-pompa hidro depolama sistemi (PHS), (4) hibrid kısa ve uzun vadeli ESS'ler -piller ve PHS- kullanarak önerilen sistemlerden elektrik enerjisi üretim maliyeti (COE)'ni yerel tarife eşit veya daha düşük tutarak yıllık RES oranını (F_{RES}) azami seviyeye çıkarmaktır. Ayrıca bu çalışma, belirtilen amaca ulaşmak için farklı RES'lere sahip en iyi ESS boyutlandırma yöntemlerini belirlemeyi amaçlamaktadır. Buna ek olarak, elde edilen sonuçların meteorolojik verilerin ve elektrik talep dengesinin değişimine olan duyarlılığını belirlemek için modellerin hassasiyet analizleri yapılmıştır. Bununla birlikte, hibrid sistemleri de içeren farklı ESS senaryolarının ve DOD değerlerinin COE, F_{RES}, talep karşılama oranı (DSF) ve PV, rüzgâr, PV/rüzgâr hibrid sistemlerinin uygulanabilir boyutları üzerindeki etkileri incelenmiştir. COE'nin şebeke tarifesine eşit ya da düşük olduğu sonuçlar incelendiğinde, 4.19 MW PV, 8 MW rüzgâr türbini ve 89.51 MWh PHS'ten oluşan hibrid sistemin incelenen RES'ler arasında %88,04 ile en yüksek F_{RES} oranın

verirken 3.44 MW PV, 8 MW rüzgâr türbini, 833 kWh pil ve 89.51 MWh PHS'ten oluşan hibrid sistemin %80,74 ile en yüksek DSF oranını verdiği belirlenmiştir. Üstelik sonuçlar ESS'nin RES'lere dâhil edilmesinin, RES'lerin ekonomik ve teknik parametrelerini etkilediğini göstermektedir. Bu etkiler RES türü, ESS tipi ve RES kapasitesine göre değişmektedir. Dahası, sonuçlar ESS'nin DOD değerinin, en iyi ESS boyutlandırma yöntemlerinin belirlenmesini ve RES'nin ekonomik ve teknik parametrelerini etkileyen önemli bir parametre olduğunu göstermektedir.

Anahtar Kelimeler: enerji depolama sistemi, PV sistemleri, rüzgâr sistemleri, PV/rüzgâr hibrid sistemler, deşarj derinliği.

DEDICATION

To my beloved parents for their continuous supports.

ACKNOWLEDGEMENT

First of all, I would like to thank Allah Almighty who guided me and inspired me throughout my studies and my work. I would like also to give many thanks to my mentor and supervisor Dr. Onur Taylan who thought me how to write scientific papers, guided me throughout my entire master studies and enriched my knowledge in the field of solar and wind energy systems. I would like also to thank my co-supervisor Prof. Derek Baker who provided me with precious guidance and supported me with his valuable feedbacks on my thesis. Furthermore, I would like to thank Dr. Behzat kentel for giving the opportunity to become a teaching assistant in the mechanical engineering program.

Moreover, I would like also to thank my beloved father and mother for their sacrifices and for their supports to me in order to achieve the highest educational level. I would like also to thank my siblings who provided me with their support to reach this level. I would like also to thank Ahmad Al-Hudud for his continues support and prayers.

Finally, I would like to thank my friends; Sajed Sadati, Fahad Haneef, Humayun Ahmad, Obaidullah Mohiuddin, Ali Hamza, Mohammad Saleh, Mohammad Abujubbah and Remember Samu for their support and help during my study. And also, I would like to thank Abdulallah Ali, Hamed, Zaid, Ahmad Darweesh and all my friends from the mosque community for the enjoyable times we spent together.

TABLE OF CONTENTS

LIST OF FIGURES

LIST OF TABLES

NOMENCLATURE

A_{CO_2}	The yearly avoided amounts of CO_2 emissions, ton
A_m	The single Photovoltaic module area, m^2
C_i	The capital cost of the renewable energy system, USD
CF	The annual capacity factor, %
COE	Cost of Electricity of the renewable energy system, USD/kWh
D	The electrical demand, kWh
D_{excess}	The amount of excess energy from the renewable energy system, kWh
D_{grid}	The demand met by the electricity grid, kWh
D_{RES}	The demand met by the renewable energy system at time n, kWh
DOC	The depth of charge of the energy storage system, %
DOD	The depth of charge of the energy storage system, %
DSF	The annual demand Supply Fraction, %
E_A^n	The available energy in the ESS at time n, kWh
E_{gen}	The total yearly energy produced by the renewable energy systems, MWh
$E_{gen,PV}$	The electrical energy generated by the PV power plant, kWh
$E_{gen,wind}$	The electrical energy generated by the wind turbine(s), kWh
E_{stor}^{max}	The maximum capacity of the energy storage system, kWh
E_{stor}^n	The energy stored in the energy storage system at time n, kWh
F_{RES}	The annual renewable energy fraction, %
$G_{S.C}$	The solar constant, W m^{-2}
GT	The local grid tariff, USD/kWh
H	The number of hour in a year that the RES has totally met the demand
I	The global insolation on a horizontal surface, Wh m^{-2}

I_o	The extraterrestrial horizontal insolation, Wh m^{-2}
$I_{b,n}$	The hourly beam insolation, Wh m^{-2}
$I_{b,t}$	The hourly beam insolation on a tilted surface, Wh m^{-2}
I_d	The diffuse insolation on a horizontal surface, Wh m^{-2}
$I_{d,t}$	The diffuse insolation on a tilted surface, Wh m^{-2}
I_{Ref}	The reference insolation at nominal conditions, Wh m^{-2}
I_T	Global insolation on a tilted surface, Wh m^{-2}
K	The shape parameter of the Weibull distribution of the wind speeds
k_T	The clearness index
L	The lifetime of the system, years
L_{loc}	The longitude of the location, degree
L_{st}	The standard meridian for the local time zone, degree
$LCOE$	The levelized cost of electricity of the renewable energy system, USD/kWh
M_i	The value of the optimal methodology used to size the, kWh
M_t	The yearly fixed maintenance cost of the hybrid system, USD
N	The number of wind turbines
$N_{modules}$	The number of modules in the PV power plant
$NOCT$	The nominal operating photovoltaic cell temperature, ^oC
NPV	Net present value, $
n	Time in a year, hour
P	The installed capacity of the PV power plant, kW
P_e	The average electrical power generated at each hour from the wind turbine, kW
$P_{e,R}$	The rated electrical power of the wind turbine, kW

PR	The performance ratio of the PV system, %
PBP	Simple payback period, years
R_{CO_2}	The CO_2 intensity of electricity, kg/kWh
R_t	The annual net revenues from the system, USD
R_{t1}	The annual net revenues for the first year, USD
r	The annual discount rate, %
T_{amb}	The ambient temperature, ºC
T_{PV}	The module temperature, ºC
$\mathrm{T_{Ref,NOC}}$	The reference module temperature at nominal conditions, ºC
$\mathrm{T_{Ref,STC}}$	The reference module temperature at nominal conditions, ºC
T_z	The local time zone, hour
u_C	The cut-in wind speed of the wind turbine, m/s
u_F	The cut-out wind speed of the wind turbine, m/s
u_R	The rated wind speed of the wind turbine, m/s
u_Z	The speed at hub height, m/s
u_1	The average wind speed at ground level, m/s
$\bar{u}$	The mean wind speed at hub height, m/s
Z	The hub height, m
Z_1	The height of the ground level, m/s

Greek Letters

α	Wind shear coefficient
α_s	The solar altitude angle, degree
β	The tilt angle of the photovoltaic modules, degree
$\mathrm{\beta_{Ref}}$	The temperature coefficient of the photovoltaic module, 1/°C
γ	The surface azimuth angle, degree

γ_s	The solar azimuth angle, degree
δ	The declination angle, degree
η_r	The round-trip efficiency of the energy storage system
η_{PV}	The photovoltaic module efficiency, %
$\eta_{PV,Ref}$	The reference efficiency of the photovoltaic module, %
θ	The incident angle, degree
θ_z	The zenith angle, degree
σ	The standard deviation of the wind speeds sample, m/s
ϕ	The latitude angle, degree
ω	The hour angle, degree

Subscripts and Superscripts

l	Long term energy storage system
s	Short term energy storage system

Acronyms and Abbreviations

COE	Cost of Electricity
DNI	Direct Normal Irradiation
DOD	Depth of Discharge
DSF	Demand Supply Fraction
ESS	Energy storage system
GHGs	Greenhouse Gases
GHI	Global Horizontal Irradiation
LCOE	Levelized Cost of Electricity
METU NCC	Middle East Technical University Northern Cyprus Campus
NPV	Net Present Value
PBP	Simple payback period
PHS	Pumped Hydro Storage System

PV	Photovoltaic
RES	Renewable Energy System

CHAPTER 1

INTRODUCTION

1.1 Background Information

The economic growth and the development of the country is highly dependent on the availability of energy resources where energy is considered as the engine for the economic growth and social development [1]. After the industrial revolution in 1760s [2], human starts the excessive use of fossil fuel in order to meet the increasing demand on the energy without any concerns about the consequences of such use. Nowadays the world is suffering from the consequences of humankind activities and the reckless strategies adopted in the name of development and economic growth which led not just to the degradation of the vulnerable earth's resources but also to the disruption and destruction of the ecological life systems causing the extension of several species. As a result of the excessive use of fossil fuel, the concentration of greenhouse gases (GHGs) was significantly increased causing the increase in the earth's average surface temperature or what is known by the "Global Warming".

Before Kyoto protocol in 1997 [3], energy security was the only energy related concern for the countries; however, after Kyoto protocol global warming became the second vital energy related concern. Governments seek to find clean energy resources that can meet the demand of their countries with affordable prices. Renewable energy systems are considered as one of the most suitable alternatives for fossil fuels as it is abundant [4] ,[5] and cost competitive with other conventional resources [6]. After 2005, when Kyoto protocol interred into force, the share of renewables- without including the hydro power systems- increased from 2% [7] to 7.3% [8], where Photovoltaic (PV) and wind systems have witnessed significant growth with annual growth rate of 60% and 20% respectively [4].

Solar and wind energy systems are two of the most common types of renewable energy systems that have the potential to meet the demand of the whole world with affordable costs [8],[9]. However, wind and solar power generation systems are unreliable since both resources are variable and do not match the demand by 100% [10]–[12]. The integration between solar and wind systems increase the reliability of the system and partially solve the production fluctuation issue where it was proved that wind and solar systems work in a synergistic way.

In addition, the integration reduces the cost of electricity generated by the system [10], [12], [13].

The mismatch and the production fluctuation of Renewable Energy Systems (RESs) can be solved by either conventional energy systems [5] or by the integration of energy storage systems (ESS), where it was reported in [9], [11], [12], [14], [15] that the ESSs can improve the RES reliability and increase the matching between the energy generation and the demand with lower cost where the surplus can be stored and used in the deficit periods instead of depending on the grid. Furthermore, it was reported in [11] and [16] that ESSs will be play a vital role in the development of RES in the future and the increase in the energy penetration from RES into the grids where ESSs will allow the RES sources to provide dispatchable service.

ESSs are divided into two main categories based on the discharge time or storage time; short term such as batteries and flywheels with fast response time- called access oriented ESSs- and long term like pumped hydro systems (PHS) and compressed air energy storage (CAES) which do not have fast response time in general and it is called capacity oriented ESSs [17]. The short term ESSs are used to overcome the energy fluctuations throughout the day up to few hours while the long term ESSs are used to overcome hourly up to daily energy fluctuations [5]. Figure 1.1 shows the discharge time and the power rating ranges of different short and long term energy storage systems.

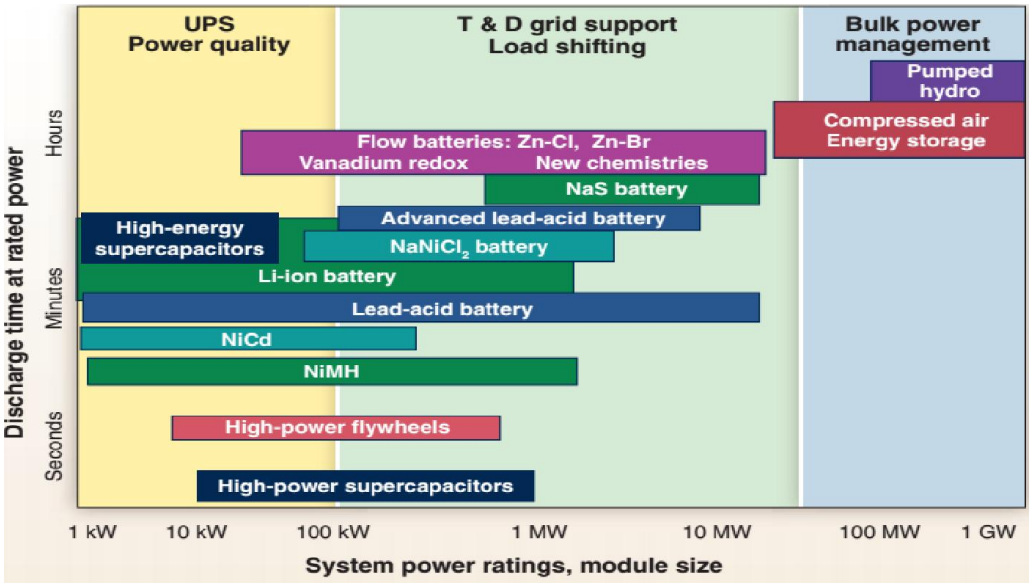

Figure 1.1. General comparison of the discharge time and the power rating ranges of different short and long term energy storage systems [14].

As mentioned before, the integration between wind and solar system can mitigate the fluctuations in the power generation and thereby reduces significantly the energy storage requirements [10], [18], [19]. In addition, the integration allows the development of microgrid systems based on renewable energy resources where it could be either grid connected or standalone microgrid, i.e. islanding the microgrid from the local electricity grid where the system will be able to meet the demand alone without the need of the local grid [20]. The sizing of the hybrid system components play an important role in the economic feasibility of the power generation systems [10], [18], [21] as well as the sizing of the ESSs [15]. Thereby the main challenge will be the determination of the optimal size of RESs and the ESSs to achieve economic and technical feasibility of the system.

1.2 Study Objectives

This study has three main goals where the state of art of what have been done and what is the gap- as defined in chapter 2- led to these goals. The first goal is to determine the optimal sizes of PV, wind and hybrid PV/wind systems with and without energy storage system based on maximizing the fraction of demand met by the RES with cost of electricity (COE)- takes into account the demand met by the grid where it is mathematically defined in section 3.2- lower or equal to the local grid tariff in Middle East Technical University (METU NCC) where the average demand throughout the system life will be used. In addition, this study aims to determine the optimal methodologies for sizing long and short term ESSs when integrating them with PV, wind and hybrid PV/wind systems based on two scenarios related to the Depth Of Discharge (DOD) of the ESSs; the first scenario is with taking into consideration the DOD, i.e. DOD <100% and the second is neglecting the DOD, i.e. DOD=100%.

The second goal is to analyze the effect of the integration of short and long term ESSs with DOD <100% on the COE, RES fraction (F_{RES}) and the demand supply fraction (*DSF*)- it is mathematically defined in section 3.6- of PV, wind and hybrid PV/wind systems in METU NCC, where the optimal sizes and methodologies will be used. Furthermore, the effect of the DOD of the short and long term ESSs on the COE, F_{RES} and *DSF* of hybrid PV/wind systems with hybrid ESS in METU NCC will be studied.

Finally, a sensitivity analysis is carried out to inspect the performance of the optimal PV/wind hybrid system in METU NCC due to the variation in the solar, wind resources and the demand where the inspection will be based on the change in the COE, F_{RES} and *DSF* of the system. The measured wind and solar resources between 2013 and 2016 and the demand

in 2011, 2014, 2015 and the forecasted demand of 2037 i.e., (the maximum demand throughout the life of the system) is used for this purpose and compared with the results obtained using TMY data. Moreover, the sensitivity analysis will be used to inspect the effect of the integration of the ESSs on the amount of change in the performance of the PV/wind system.

1.3 Work Organization

Chapter 2 presents a literature review of several studies that assessed the technical and economic feasibilities of the installation of different RES configurations with energy storage system in addition to some studies that proposed a sizing methodologies for the RESs and ESSs. The aim of the literature review is to address the state of art of what have been made in this field and what is the gap. In addition, the literature addresses some of the drawbacks and the limitations of HOMER software- which is one of the most famous RES modeling software, and led to developing a new model instead of using HOMER. Chapter 3 presents the methodology and the theory used in modeling the RESs- PV, wind and the PV/wind hybrid system- and the ESSs. In addition, it presents the methodology used to assess the economic and technical feasibility of the system in METU NCC. In Chapter 4 the optimal ESS sizing methodologies with different RES are presented and the optimal sizes of the RES configurations with their technical and economic feasibility is discussed. Furthermore, the effect of the integration of short term and long term ESSs with the different RES configurations is analyzed in addition to the effect of the DOD on the technical and economic feasibility of the PV/wind hybrid system in METU NCC. Moreover, Chapter 4 includes the results of the sensitivity analysis made to examine the performance of the PV/wind hybrid system with different ESS configuration to the change in the RES resources and the change in the demand. Finally, Chapter 5 presents the major conclusions obtained through this study in addition to some future works that can be built upon this study.

CHAPTER 2

LITERATURE REVIEW

2.1 Separate PV and Wind Systems

PV technologies is witnessing a tremendous growth rate in the global market [22] where the optimization of the sizing of such technology is vital for economic and technical metrics. Furthermore, the integration of ESSs with PV systems became a promising option which requires more investigation. Several studies proposed optimal sizing methodologies for PV systems with ESS and also assessed the technical and economic feasibility of the integration of the ESSs [15], [23]–[28]. For instance, Li et al. [23] studied the integration of stand-alone PV systems with batteries and fuel cells. They concluded that PV system with batteries and fuel cell was the optimal configuration with the lowest cost, higher system efficiency and the lowest number of PV modules compared with single storage configurations. Furthermore, Kaldellis et al. [24] studied the integration between PV and different energy storage system for remote islands. They concluded that the PV/storage has cost of electricity generation lower than the cost from existing thermal power plant in most of the cases in several Greek islands. Moreover, Manokalos et al. [25] studied the installation of standalone PV power plant with PHS and batteries in Merssini village in Greece. They concluded that small-scale PHS has low efficiency with high initial cost compared with batteries.

Similar to the PV systems, wind energy has a significant growth rate in the global energy sector [29] where the sizing of these systems took the intention of many scholars. Moreover, like PV systems scholars see in the integration of ESSs a path for more deployment of these systems and so the scholars presented several studies focusing on the optimization of wind turbine systems with different ESSs [30]–[33]. For instance, Papaefthymiou and Papathanassiou [31] investigated the optimal size of wind/PHS hybrid system in an island system based on maximizing the return of investment and based on maximizing the RES penetration. They concluded that the integration of PHS led to the reduction in LCOE of the wind system and at the same time increased the RES penetration. Another study made by Kaldellis and Kavadias [33] proposed an optimal sizing methodology for wind-hydro systems based on maximizing the energy independence of the local system. They concluded that a significant part of the demand was met by the wind farm while the hydropower system covered energy deficit and reduced the dependency on the local grid.

2.2 PV/wind Hybrid System

As the hybridization of solar and wind resources and the integration of ESSs became shining options to increase the utilization of the RES, enormous number of studies discussed the optimization methodologies of PV/wind hybrid system with and without ESSs [12], [18], [21], [34]–[43]. For instance, Ma et al. [12] examined the technical feasibility of the integration of pumped hydro storage system with standalone PV/wind hybrid system in a remote island in Hong Kong. They concluded that the PHS is the ideal solution to compensate the fluctuation of the energy production from the RES with 100% energy autonomy. Furthermore, Ashok [21] made a model to find the optimal size of PV/wind hybrid system with pumped hydro energy storage system and battery for rural communities based on minimizing the total life cycle cost. Ashok concluded that the system was capable of meeting the demand of the entire village for 24 hours with cost of 6.5 Rs/kWh (0.088 USD/kWh) which is less than the cost of electricity from the extended grid and from the diesel generators. Another study made by Bekele and Tadesse [37] analyzed the feasibility of the installation of PV/wind hybrid system with PHS in Ethiopia using HOMER. They concluded that different sizes of the system have cost of electricity less than 0.16 USD/kWh.

Moreover, Ma et al. [34] evaluated the technical and economical feasibilities of PV/wind hybrid system with battery storage in a remote island in Hong Kong using HOMER software. They concluded that the cost of electricity generation was 0.595 USD/kWh which was higher than the grid tariff. Furthermore, they concluded that the hybrid system has less cost of electricity generation, lower storage capacity and less excess energy than the PV alone. Another study made by Ma et al. [36] compared the feasibility of the integration of batteries and pumped hydro storage system with PV/wind hybrid system for a remote island in Hong Kong. They concluded that the integration of hybrid storage system, i.e. battery + PHS, has lower cost than battery alone.

2.3 Energy Storage Sizing

Several studies focused on studying the optimal methodologies for sizing ESSs for renewable energy and microgrid applications where the optimal sizing plays a vital role in ensuring the economic profits from this integration [44]–[48]. For instance, Le [44] made a study to determine the capacity of ESS for wind turbines farm based on maximizing the economic profit of the integration. Le concluded that the installation of ESS for increasing the dispatchability of wind farms can be profitable. Moreover, Chen et al. [45] proposed a method

for sizing battery ESS for microgrid applications based on cost benefit analysis. They concluded that installing the optimal size of battery ESS for grid connected microgrid could increase the total profits of the system. Another study made by Bahramirad et al. [46] presented a model for estimating the optimal size of ESSs in microgrid based on minimizing the investment cost of the ESS as well as the operation cost of the microgrid. They concluded that larger ESSs do not necessarily have larger economic profits. Furthermore, Borowy and Salameh [47] proposed a methodology for calculating the optimal size of battery ESS for standalone PV/wind hybrid system in Massachusetts, USA based on minimizing the cost of the system. In another study, Kellogg et al. [48] developed an algorithm to find the optimal sizes of a standalone PV/wind hybrid- battery system. The algorithm was used to find the capacity of the components that can meet the hourly average load profile of a home in Montana, USA. In addition, Kaldellis and Zafirakis [43] compared the cost of electricity production of the RES with different ESSs. They concluded that if the RES and the ESSs were properly sized they could form a promising solution.

2.4 RESs in Cyprus and METU NCC

Several studies were considered to determine the feasibility of installing different kinds of PV systems on the island. For instance, Poullikkas [49] studied the feasibility of installing 1 MW grid-tied PV farms in Cyprus in 2009. The study pointed to the unfeasibility of installing such systems in the absence of supportive policies. LCOE for this kind of systems was 0.38 EUR/kWh (0.43 USD/kWh) which was higher than the grid tariff. In 2014, another study was made by Fokaides and Kylili [50] to determine the feasibility of installing 1 MW grid-tied PV farm in Cyprus based on different scenarios with different PV capital cost and different grid tariff. The study concluded that the installation of such plant was feasible if the grid tariff was 0.14 EUR/kWh (0.16 USD/kWh), and the capital cost was 1.15 EUR/W (1.3 USD/W).

In addition to the solar resources, some regions on the island have good wind potential that can be utilized to generate electricity. In 2005, Koroneos et al. [51] said that the wind energy in the southern coastal zone of Cyprus was able to compete with other forms of energy and could become economically viable where the mean wind speed at 10 m height is greater than 5 m/s. Furthermore, Solyali and Redfern [52] examined the cost of electricity production for several locations in Cyprus like: Paphos, Larnaca, Paralimni, Limassol, Akrotiri, Athalassa, Ercan and Polis, where the lowest LCOE was 0.2 EUR/kWh (0.227 USD/kWh) for a 10 MW wind farm in Paralimni. Moreover, Ilkan et al. [53] economically compared installing PV and wind systems in Northern Cyprus for residential application in 2005. They concluded that

although the internal rate of return for wind turbine systems was much higher than the PV systems, there were few locations where wind systems would be economically viable. In addition, Fokaides et al. [54] mentioned in their study the feasibility of Orites wind farm (34.71° N, 32.63° E) in Southern Cyprus with 82 MW in 2014. LCOE for the wind farm was 0.1 EUR/kWh (0.11 USD/kWh) where the feed in tariff and the grid tariff was 0.166 EUR/kWh (0.183 USD/kWh).

Only a couple of studies was made to determine the feasibility of installing hybrid systems in Cyprus. For instance, in 2012, Panayiotou et al. [55] compared the feasibility of installing standalone PV system and PV/wind hybrid system for domestic application in Nicosia, Cyprus. They concluded that PV system was better option; since the wind sources of the examined place was lower compared with the solar resources.

A few papers have studied the feasibility of installing separate PV and wind systems in METU NCC [56]–[58]. For instance, in 2013, Pathirana and Muhtaroğlu [56] found that having 6.81 MW off-grid PV power plant with batteries would meet the demand of the university; however, the cost of electricity generated was 0.24 USD/kWh where the grid tariff was 0.22 USD/kWh, while having a 5.875 MW grid-tied power plant with feed in tariff of 0.22 USD/kWh would reduce the cost of electricity to 0.14 USD/kWh. In addition, in 2015, Sadati et al. [57] determined the feasibility of different sizes of grid-tied PV power plants in METU NCC with energy storage system; having a 4.5 MW PV plant with 15 MWh PHS would meet the demand 83% of the time and have LCOE of 0.24 USD/kWh; where the minimum LCOE, 0.2 USD/kWh, could be achieved with 0.5 MW power plant and no storage system. On the other hand, in 2015, Yenen [58] studied the potential of installing three wind turbines with different hub heights in METU NCC; Vestas V27, V47, V66 with hub height 30, 50, 60 m, respectively, and rated power of 0.225, 0.66 and 1.65 MW, respectively. The author concluded that the installation of these models was not feasible in METU NCC due to relatively low wind resources.

Only one study considered the installation of PV/wind hybrid system in METU NCC [7]; Sadati [7] made a feasibility study for the installation of PV/wind hybrid system with battery storage and PV with battery and PHS in METU NCC. He concluded that 2 MW PV, 3.75 MW wind hybrid system with 1 MWh battery has LCOE of 0.148 USD/kWh while 2 MW PV and 3 MW wind hybrid system without ESSs has LCOE of 0.15 USD/kWh.

2.5 Literature Gap

The ESSs sizing methodologies in the literature was based on only one parameter either technical by achieving 100% RES fraction with the integration [48] or economic by achieving the maximum profits from the integration [44]–[47]. Moreover, the literature lack for studies that analyzed the effect of the integration of short term and long term energy storage system- separate and hybrid ESSs configurations- on the sizing of the RES, i.e. on the COE, Renewable Energy System Fraction (RES fraction) and Demand Supply Fraction (DSF). Furthermore, the literature did not analyze the effect of the DOD of the ESSs on the economic and technical parameters of the RES.

2.6 Software Limitations

The Hybrid Optimization Model for Electric Renewables (HOMER) is the most famous software used in simulating renewable energy systems. HOMER is capable of analyzing the technical and economic feasibilities of different RES configurations. In addition, the software can optimize the size of the RES and can carry out sensitivity analyses for the RES. HOMER has been used extensively in the literature for optimization purposes and diverse case studies. However, HOMER software has several limitations for instance the software does not allow the integration of two energy storage systems the same time and also does not take into account the DOD of the ESSs directly [59]. In addition, the software is limited to the traditional economic parameters like Net Present Cost (NPC) and LCOE that cannot take into account the externalities and the corporation of the fluctuation of the energy generation from the RES. Finally, the software evaluates the technical feasibility of the RES based on one parameter only which is the RES fraction and does not allow the development of other useful parameters like the demand supply fraction [60].

All these limitations of HOMER software were the barrier for using it in this study and in order to fulfill the objectives of this study a new model was developed using Microsoft Excel. The model estimates the hourly energy production from the different RES configurations, i.e. PV, wind and PV/wind hybrid system. In addition, the model estimates the hourly energy stored and the energy available in the ESSs and it allows the integration of two ESSs at the same time and takes into account the DOD of the ESSs. Finally, the model calculates the RES fraction and the demand supply fraction as metrics to assist the technical feasibility of the system and also estimates the LCOE, NPV, Payback Period (PBP) and the COE which

incorporates the fluctuation of the RES energy generation and the mismatching with the demand by taking into account the excess and the deficit energy.

CHAPTER 3

THEORY AND METHODOLOGY

3.1 Solar Geometry

The estimation of the electrical energy production from a PV module requires the estimation of the amount of solar radiation on a tilted surface and this can be achieved by estimating the incident angle. The incident angle is the angle between the surface normal and the beam solar radiation and it is a function of several angles related to three components: the utilization surface, the earth and the sun, and to estimate the incident angle at any time these three components should be geometrically described [61]. Figure 3.1 illustrates the angles required to describe the geometry of the utilization surface and the sun.

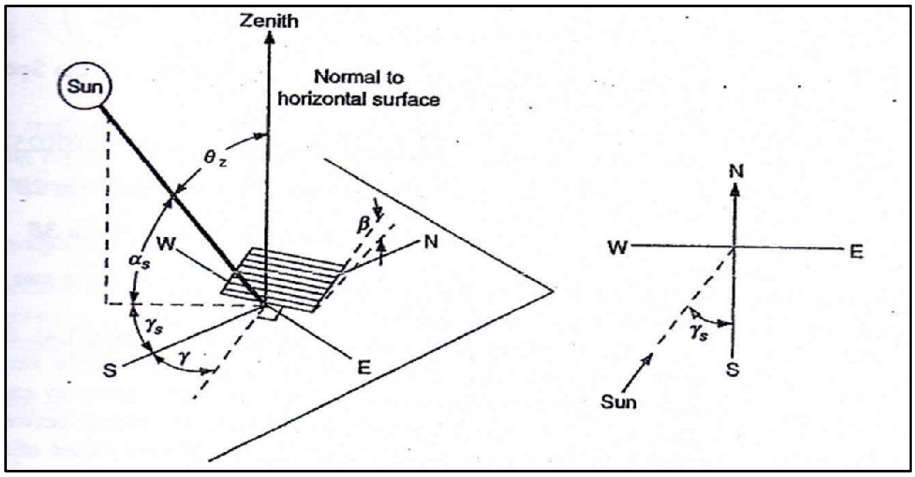

Figure 3.1. Schematic sketch illustrates the angles required to describe the geometry of the beam radiation relative to the specific surface and to describe the geometry of the surface [61].

The sun position changes with time which requires the use of a time that depends only on the apparent angular motion of the sun and does not depend on the location; this time is called the solar time (t_s) and it is used in all the geometric solar relations instead of the local time, Eq. (1) is used to convert the local time to solar time [61].

$$t_s = t_{std} + 4\times(L_{st} - L_{loc}) + E \quad (1)$$

where L_{st} can be calculated using Eq. (2), L_{loc} can be calculated as in Eq. (3) and E can be calculated using Eq. (4) [61].

$$L_{st} = \begin{cases} -T_z \times 15\,, & T_z \leq 0 \\ 360 - T_z \times 15\,, & T_z > 0 \end{cases} \quad (2)$$

$$L_{loc} = \begin{cases} L_{loc} & , \quad if\ L_{loc}\ in\ the\ West \\ 360 - L_{loc} & , \quad if\ L_{loc}\ in\ the\ East \end{cases} \quad (3)$$

$$E = 229.2 \times (0.000075 + 0.001868 \times \cos B - 0.032077 \times \sin B - 0.014615 \times \cos(2 \times B) - 0.04089 \times \sin(2 \times B)) \quad (4)$$

where B and E are constants, B can be calculated using Eq. (5) [61].

$$B = (n - 1) \times \frac{360}{365} \quad (5)$$

As mentioned before the solar time is used in all the geometric relation; however, it is used in the angular form and it is called hour angle (ω) and can be calculated using Eq. (6) [61].

$$\omega = (t_s - 12) \times 15 \quad (6)$$

In order to describe the position of the sun can two angles are used; the zenith angle and the solar azimuth angle. The zenith angle is the angle between the solar beam radiation and the vertical (the zenith) and it can be calculated using Eq. (7). While the solar azimuth angle is the angle between the projection of the beam radiation on the horizontal with south and it can be calculated using Eq. (8) [61]. The solar azimuth angle and the zenith angle both depends on the location and the declination angle (δ) which is the angle between the beam radiation and the equator at solar noon and it can be calculated using Eq. (9) [61].

$$\cos\theta_z = \cos\phi \cos\delta \cos\omega + \sin\phi \sin\delta \quad (7)$$

$$\gamma_s = sign(\omega) \times \left| \cos^{-1}\left(\frac{\cos\theta_z \sin\phi - \sin\delta}{\sin\theta_z \cos\phi} \right) \right| \quad (8)$$

$$\delta = 23.45 \times \sin\left(360 \times \frac{284 + n}{365}\right) \quad (9)$$

Two angles are needed to geometrically describe a certain utilization surface; tilt angle (β) and the azimuth angle (γ); where tilt angle is the angle between the surface and the horizontal. While the azimuth angle is the angle between the projection of the surface normal on the horizontal with south [61]. The incident angle, θ, is estimated using Eq. (10) after obtaining

the zenith and solar azimuth angles at specific hour angle and with the optimal solar geometry of the PV modules. It was reported in [7] that the optimal geometry that maximize the energy production from the PV modules in METU NCC is with 25° tilt angle and 0° surface azimuth angle.

$$\cos\theta = \cos\theta_z \cos\beta + \sin\theta_z \sin\beta \cos(\gamma_s - \gamma) \quad (10)$$

3.2 Solar Resources

The global insolation on a tilted surface, I_T, consist of three components: beam, diffuse and reflected insolation as in Eq. (11) where the reflected insolation is neglected in the analysis [61].

$$I_T = I_{b,t} + I_{d,t} \quad (11)$$

where $I_{b,t}$ can be estimated using Eq. (12) and $I_{d,t}$ can be estimated using Eq. (13) [61] based on the isotropic sky model; which states that the diffuse radiation comes from all directions with the same magnitude [62].

$$I_{b,t} = I_{b,n} \times \cos\theta \quad (12)$$

$$I_{d,t} = I_d \times \left(\frac{1+\cos\beta}{2}\right) \quad (13)$$

The hourly beam and diffuse insolation on a horizontal surface for METU NCC were obtained using Meteonorm v7.1 software which provides the data based on a typical meteorological year.

3.3 PV Energy Production

The efficiency of the PV module is affected by the module temperature; as the module temperature increases the module efficiency decreases and so the energy production. The PV module efficiency can be estimated using Eq. (14) [63] where the effect of the wind and the relative humidity on the module temperature and on the module efficiency is neglected in the analysis.

$$\eta_{PV} = \eta_{PV,Ref} \times (1 - |\beta_{Ref}| \times (T_{PV} - T_{Ref,STC})) \quad (14)$$

Here T_{PV} can be calculated using Eq. (15) [63]. Note in [63] the absolute value of β_{Ref} is not taken and a positive β_{Ref} is assumed. However, in many product literature β_{Ref} is given as a negative value. Therefore, the absolute value of $\beta_{Ref}$is used in Eq. (14) to avoid confusion and possible errors.

$$T_{PV} = T_{amb} + \left(NOCT - T_{Ref,NOCT}\right) \times \frac{I_T}{I_{Ref}} \tag{15}$$

The hourly ambient temperature for METU NCC was obtained using Meteonorm v7.1 software which provides the data based on a typical meteorological year. The specifications of the PV modules- which are necessary to estimate the energy output of the system- were obtained from the manufacturer; PV modules from AXITEC company type AC-250P/156-60S were used. Table 3.1 shows the technical specifications of the PV modules.

Table 3.1. Technical specifications of the AXITEC-250P/156-60S PV modules [64].

Parameter	Value
P (W)	250
$\eta_{PV,Ref}$ (%)	15.37
β_{Ref} (1/°C)	-0.0042
$T_{Ref,STC}$ (°C)	25
$NOCT$ (°C)	45
$T_{Ref,NOCT}$ (°C)	20
G_{Ref} (W/m^2)	800
A_m (m^2)	1.63

After estimating the efficiency of the PV module and the total insolation on the PV module, the hourly total energy output from the PV power plant can be estimated [63] as,

$$E_{gen,PV} = \eta_{PV} \times I_T \times A_m \times N_{modules} \times PR \tag{16}$$

Here PR equals to 85% based on [57], [65], [66] where the missing 15% accounts for the system losses which includes wiring, inverter, shading and dust losses.

3.4 Wind Energy

The estimation of the energy production from wind turbines requires the wind speed at hub height which depends on several factors; wind speed at ground level, the ambient temperature, the height of the hub, the nature of the terrain and time (hour, day, season). All these factors can be represented by one variable called wind profile exponent or wind shear coefficient, α, and the values of it can be estimated using the site-specific data; however, in the absence of the site-specific data α is usually taken as 1/7 [67] where the wind speed at hub height (u_Z) can be calculated as,

$$u_Z = u_1 \times \left(\frac{Z}{Z_1}\right)^{\alpha} \tag{17}$$

The hourly wind speed at ground level for METU NCC were obtained using Meteonorm v7.1 software.

The electrical power generated at each hour can be estimated using Eq. (18) and the hourly electrical energy generated by the wind turbine(s) can be estimated using Eq. (20) by assuming that the energy generated is constant during the hour and each turbine generates the same amount in the case of having multi turbines [67].

$$P_e = \begin{cases} 0 & ,u_Z < u_C \ \ or \ \ u_Z > u_F \\ P_{e,R} \times \frac{(u_C)^K - (u_Z)^K}{(u_C)^K - (u_R)^K} & ,u_c \le u_Z \le u_R \\ P_{e,R} & ,u_R < u_Z \le u_F \end{cases} \tag{18}$$

where K can be calculated based on Justus theory using Eq. (19) [67].

$$K = \{ \ (\sigma/\bar{u})^{-1.086}, \ 1 \le \ K \le 10 \tag{19}$$

$$E_{gen,wind} = N \times P_e \tag{20}$$

Wind turbine model with 2 MW of rated power from GAMESA company (G114-2.0) was used in this study, Table 3.2 shows the technical specifications of the wind turbine model.

Table 3.2. GAMESA G114-2.0 wind turbine technical specifications [68].

Parameter	Value
Rated power (MW)	2
Rotor diameter (m)	114
Hub height (m)	140
Cut-in speed (m/s)	2
Cut-out speed (m/s)	21
Rated speed (m/s)	9

3.5 ESS Model and Electrical Energy Demand

The integration between the ESSs and the RESs, wind and solar systems, provides a reliable power generation system and increases the matching between the RES and the demand. In this study, three configurations of RESs: separate PV system, separate wind system and PV/wind hybrid system will be considered to inspect the effect of the ESSs integration. The RES is assumed to be connected to the electricity grid with two main scenarios: with and without energy storage system (ESS). For scenario #1, without ESS, any deficient in the demand will be compensated by the grid with the local grid tariff, and any excess energy will be dumped into the grid for free where this is called uni-directional metering policy [7]. While for scenario #2, with ESS, the ESS will be charged by the excess energy generation from the RES, where three sub-scenarios of ESSs configuration will be integrated to the RESs; separate short term, separate long term and hybrid short/long term ESSs. The amount of energy demand met by the RES (D_{RES}), the amount of excess energy (D_{excess}) and the energy provided by the grid (D_{grid}) can be estimated for both scenarios as in the energy flow chart in Figure 3.2.

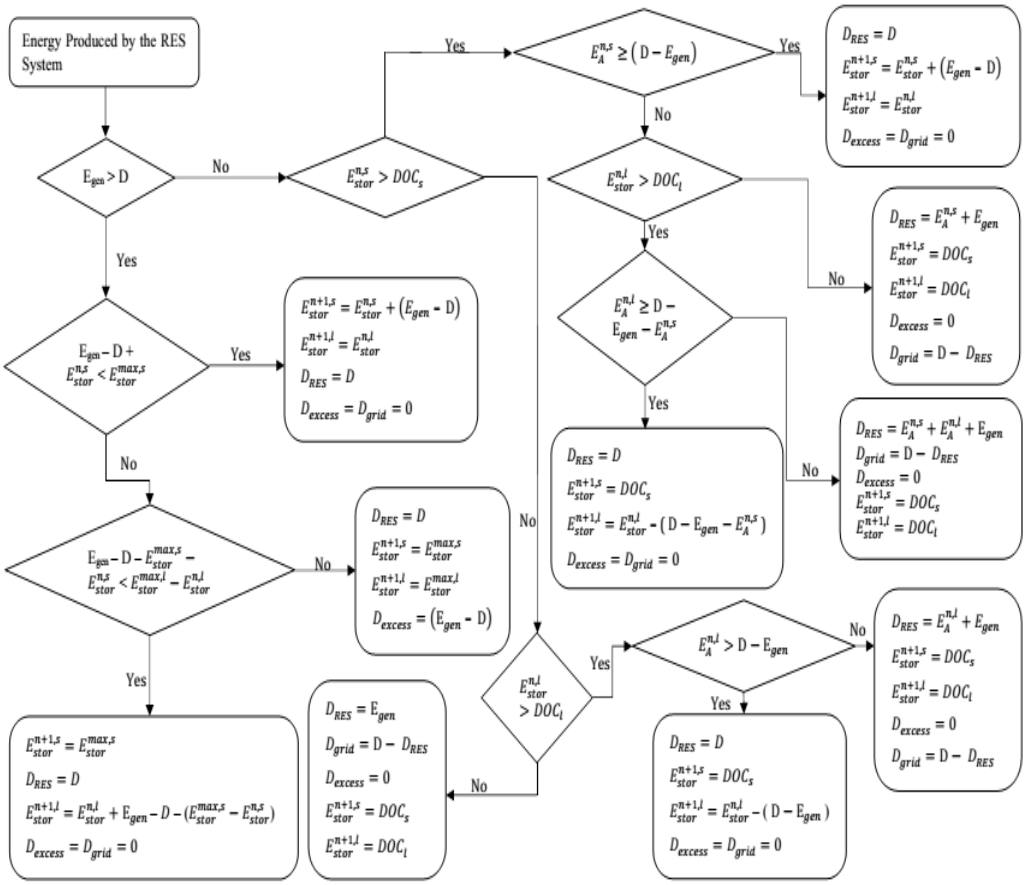

Figure 3.2. The energy flow chart of the renewable energy system.

Several energy storage technologies are available for RES applications as short term and long term ESSs, where in this study the selection of the suitable type for short term ESS was based on the cost, the lifespan and the round-trip efficiency (η_r). The selection of long term ESS was based not just on the cost, the lifespan and the round-trip efficiency but also on the technical feasibility of these systems in the specific location since these technologies- pumped hydro storage (PHS) and underground compressed air energy storage system (UG-CAES)- are highly dependent on the geography of the location [69], [70]. Table 3.3 shows different short term and long term ESSs with their capital cost, the lifespan, the round-trip efficiency and the storage durability.

Table 3.3. Comparison between different short term and long term ESSs based on the capital cost, the lifespan, the round-trip efficiency and the storage durability [69]–[72].

Type	ESS	Cost (USD/kWh)	Lifespan (Years)	η_r (%)	Storage Durability
Short Term	Lead-acid	190-900	5-15	0.7-0.9	min-days
	Nickle- Cadmium	600-1200	10-20	0.6-0.73	min-days
	Lithium-Ion	490-1330	5-20	0.85-0.95	min-days
	Zinc- Barium	190-565	5-10	0.6-0.7	hours- months
	Fuel Cell	500-1500	15-20	0.33-0.42	hours- months
	Flywheels	400-1000	15-20	0.93-0.95	sec-min
Long Term	PHS	9-135	50-60	0.7-0.85	hours- months
	UG-CAES	5-68	20-40	0.7-0.89	hours- months
	Above Ground-CAES	92-140	20-40	0.7-0.9	hours- days

Lithium-Ion battery is used as the short term ESS in this study with constant lifetime of 20 years at 60% rated DOD as provided by the manufacture [71]. While PHS is used as the long term ESS with constant lifetime of 20 years- the real life is more however to simplify the analysis it was taken as 20 years- where the location of METU NCC is suitable for such technology [7]. The optimization of the RES systems with ESS is based on more than two variables; the RES and the ESS capacities where in order to simplify the optimization, the ESSs will be function of either the demand, the deficit or the excess energy. Four different methodologies were used to size the battery in case of separate short term ESS in order to inspect the optimal methodologies to size batteries when integrating them with different RESs based on maximizing the F_{RES} with COE less or equal to the grid tariff. Five methodologies were used to size the PHS in case of separate long term ESS. Table 3.4 shows the methodologies used to size the Lithium-Ion batteries and the PHS in case of separate ESS in METU NCC.

Table 3.4. Methodologies used to size separate short term and long term ESSs.

Scenario	Battery	PHS
1	Average Hourly Deficit	Average Daily Deficit
2	Average Hourly Demand	Average Daily Demand
3	Average Hourly Excess	Average Daily Excess
4	Maximum Hourly Deficit	Maximum Daily Deficit
5	-	Maximum Daily Demand

One of the major drawbacks of PHS is the lag time during the response to the deficit in the energy demand where it was reported in [7] that the PHS has a lag time of 4 minutes. In case of separate PHS, the deficit during the lag is being met by the grid; where this deficit is calculated by assuming the demand is constant during the hour since hourly analysis is carried out in this study. In order to decrease the dependence on the grid and increase the availability and the autonomy of the RES, short term ESS is integrated with the PHS. The short ESS will be charged from the PHS after the response to the 4 minutes deficit if there is energy available in the PHS in order to increase the benefits from it, i.e. increase the autonomy. As mentioned before, in order to simplify the optimization the ESSs will be function of either the demand, the deficit or the excess energy. Twenty sizing methodologies were used to size the hybrid ESS- short term and long term ESSs- in order to inspect the optimal methodologies for sizing the hybrid ESS based on maximizing the F_{RES} with COE less or equal to the grid tariff in case of the integration with different RESs in METU NCC. Table 3.5 shows the methodologies used to size the hybrid ESS when integrated with different RESs.

For both ESS types the DOD and round-trip efficiency (η_r) are the only ESS characteristics considered in this study, where the sizing was based on two major scenarios with 100% DOD and the second scenario was based on DOD <100% as provided in the literature where in both scenarios the lifespan of the ESSs remains constant. Table 3.6 shows the DOD and the round-trip efficiency for the Lithium-Ion battery and the PHS. The size of the short term and long term ESS can be calculated using Eqs. (21) and (22) respectively.

$$E_{stor}^{max,s} = \frac{M_{i,s}}{DOD_s \times \eta_{r,s}} \tag{21}$$

$$E_{stor}^{max,l} = \frac{M_{i,l}}{DOD_l \times \eta_{r,l}} \tag{22}$$

Table 3.5. Methodologies used to size the short term and long-term hybrid ESSs.

Scenario	Hybrid ESS	
	PHS	Battery
1	Average Daily Deficit	Average Hourly Deficit
2		Average Hourly Demand
3		Maximum Deficit in the PHS Lag Time
4		Maximum Demand in the PHS Lag Time
5	Average Daily Demand	Average Hourly Deficit
6		Average Hourly Demand
7		Maximum Deficit in the PHS Lag Time
8		Maximum Demand in the PHS Lag Time
9	Average Daily Excess	Average Hourly Deficit
10		Average Hourly Demand
11		Maximum Deficit in the PHS Lag Time
12		Maximum Demand in the PHS Lag Time
13	Maximum Daily Deficit	Average Hourly Deficit
14		Average Hourly Demand
15		Maximum Deficit in the PHS Lag Time
16		Maximum Demand in the PHS Lag Time
17	Maximum Daily Demand	Average Hourly Deficit
18		Average Hourly Demand
19		Maximum Deficit in the PHS Lag Time
20		Maximum Demand in the PHS Lag Time

Table 3.6. Technical Specification of the Lithium-Ion Batteries and the PHS [71],[72].

Parameter	Battery	PHS
Round-trip Efficiency (%)	95	85
Depth of Discharge (%)	60	89
Discharge Time (h)	1	8

3.6 Performance Assessment of the RES

In order to inspect the matching between the energy production from the RES and the demand, the RES Fraction (F_{RES})- which is the annual fraction of demand met by the system- is used. Furthermore, in order to inspect the autonomy of the system the Demand Supply Fraction (DSF)- which is the fraction of the number of hours in a year where the RES has totally met the demand- is used. F_{RES} and DSF can be calculated as,

$$F_{RES} = \frac{\sum D_{RES}}{\sum D} \tag{23}$$

$$DSF = \frac{H}{24 \times 365} \tag{24}$$

Furthermore, the performance of the RES is assessed using the annual capacity factor (CF) which is the ratio of electricity generated (AC) to the possible energy generated if the RES worked continuously at full nameplate power during the same period [73] and it can be calculated using Eq. (25).

$$CF = \frac{E_{gen}}{(P_{e,R} \times N + P) \times 365 \times 24} \tag{25}$$

3.7 Environmental Assessment of the RES

Renewable energy resources are considered as clean resource and the deployment of these resources will lead to the mitigation in the GHGs like CO_2. The yearly avoided amounts of carbon dioxide emissions from the installation of the RES can be calculated using Eq. (26).

$$A_{CO_2} = R_{CO_2} \times E_{RES} \tag{26}$$

where R_{CO_2} is equal 0.584 [kg/kWh] for Cyprus [74].

3.8 Economic Assessment of the RES

The economic feasibility of any energy system is important as the technical feasibility where in most of the cases, the economic feasibility determines if the project will be established or not. One of the economic parameters that is used to determine the economic feasibility of the energy systems is the levelized cost of electricity (LCOE) which represent the cost of electricity generated by the energy system. The levelized cost of electricity for the RES can be calculated using Eq. (27) where the demand met by the RES was used instead of

the energy generation to incorporate the effect of the mismatching between the energy generation and the demand. Table 3.7 shows all the economic parameters used in this study.

$$LCOE = \frac{C_i + \sum_{t=1}^{L} \frac{M_t}{(1+r)^t}}{\sum_{t=1}^{L} \frac{D_{RES}}{(1+r)^t}} \quad (27)$$

Table 3.7. The economic parameters of the PV, the wind turbine system and the ESSs in addition to the local grid tariff and the annual discount rate for METU NCC.

Parameter	Value	Ref.
PV power plant capital cost (USD/kW)	2150	[75]
PV power plant annual maintenance cost (USD/kW)	24.68	[75]
Wind turbine capital cost (USD/kW)	1980	[76]
Wind turbine annual maintenance cost (USD/kW)	39.53	[76]
PHS capital cost (USD/kWh)	68	[69]
Lithium-Ion Battery Cost (USD/kWh)	495	[69]
System expected lifetime (year)	20	[69], [71], [77]
Local Grid Tariff (USD/kWh)	0.175	[57]
Annual discount rate (%)	9	[78]

Northern Cyprus has a unidirectional metering system where the excess energy from the RES is pumped into the grid for free [7] and so the excess energy is considered as a waste. In addition, the RES cannot meet the demand all the times during the year where the deficit is compensated by the grid with the local grid tariff (GT) which affects the Cost of Electricity (COE) of the RES. The COE of the RES can be calculated as,

$$COE = \frac{D_{RES} \times LCOE + D_{grid} \times \mathrm{GT}}{D} \quad (28)$$

The Net Present Value (NPV) and simple payback period (PBP) are additional economic parameters used to help in the assessment of the RES sizes and configurations. The system is considered feasible if NPV is positive or unfeasible if it is negative. Moreover, as the higher the NPV the higher benefits of the system are or vice versa [79]. NPV and PBP can be calculated using Eq. (29) and Eq. (30) respectively [80].

$$NPV = \sum_{t=1}^{L} \frac{R_t}{(1+r)^t} - C_i \quad (29)$$

$$PBP = \frac{C_i}{R_{t1}} \quad (30)$$

3.9 Case Study: METU NCC

3.9.1 Renewable Energy Resources in METU NCC

Cyprus is a Mediterranean island located between Middle East and Europe where it is considered as the third largest island in the Mediterranean Sea with total area of 9251 km^2 [81]. Figure 3.3 shows the geographical location of Cyprus. Being located on an island with no conventional energy resources, Northern Cyprus uses imported fossil fuels to generate electricity with annual CO_2 emissions of about 850 million kg [82] considering 0.584 kg/kWh which form a tremendous source of pollution [83]. However, Northern Cyprus is rich of renewable energy resources, such as solar energy with about 300 sunny days in a year [49]–[53], [56], [84] and wind energy [49]–[53], [85] which can be utilized to decrease the amounts of fossil fuel used, thus, to reduce the CO_2 emissions and to increase the energy security of the island.

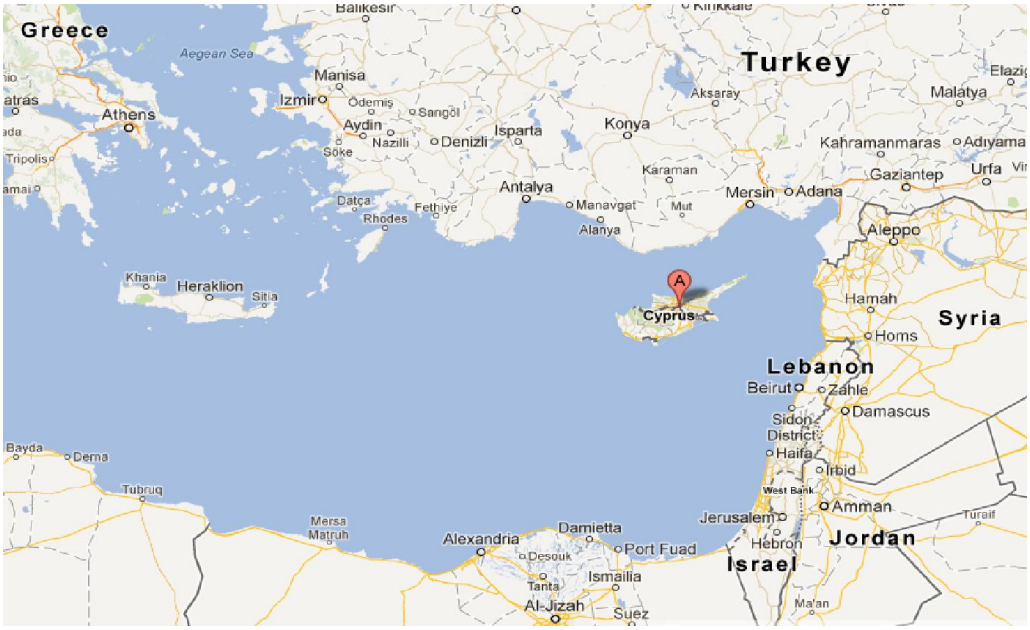

Figure 3.3. The geographical location of Cyprus [87].

METU NCC is located in Guzelyurt in Northern Cyprus (33.017°E and 35.2°W), where its location has good potential of wind resources [7] that can be utilized. Figure 3.4 shows the wind speed ranges at ground level and Figure 3.5 shows the cumulative frequency of the wind speeds at ground level in METU NCC. The average hourly wind speed at ground level (10m) in METU NCC is 2.81 m/s where 39.4% of the time in the year the speed exceeds the average wind speed. Furthermore, with this average wind speed the location of METU NCC is considered as moderate windy region based on the European Wind Classifications [86].

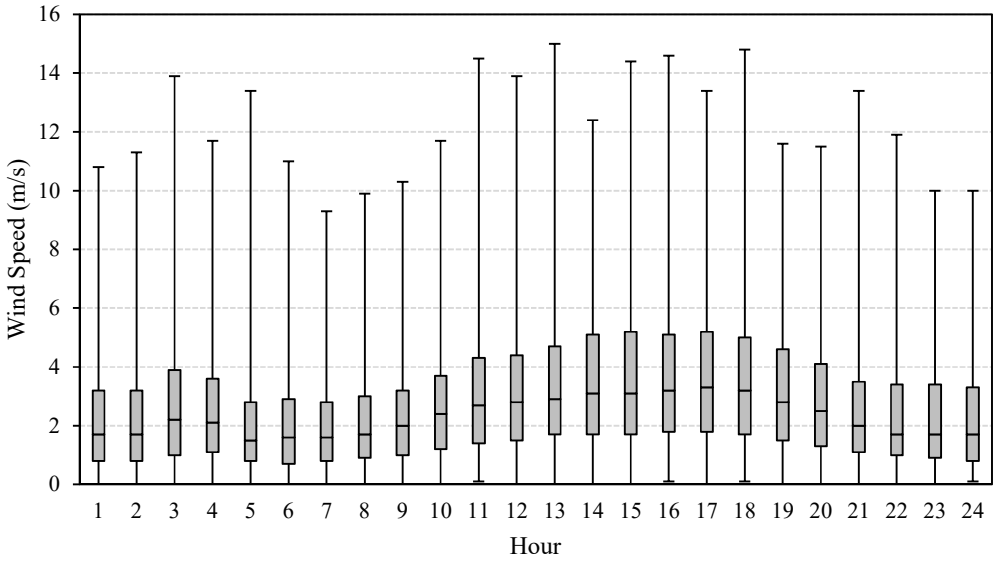

Figure 3.4. The TMY 10m-wind speed ranges at each hour in METU NCC.

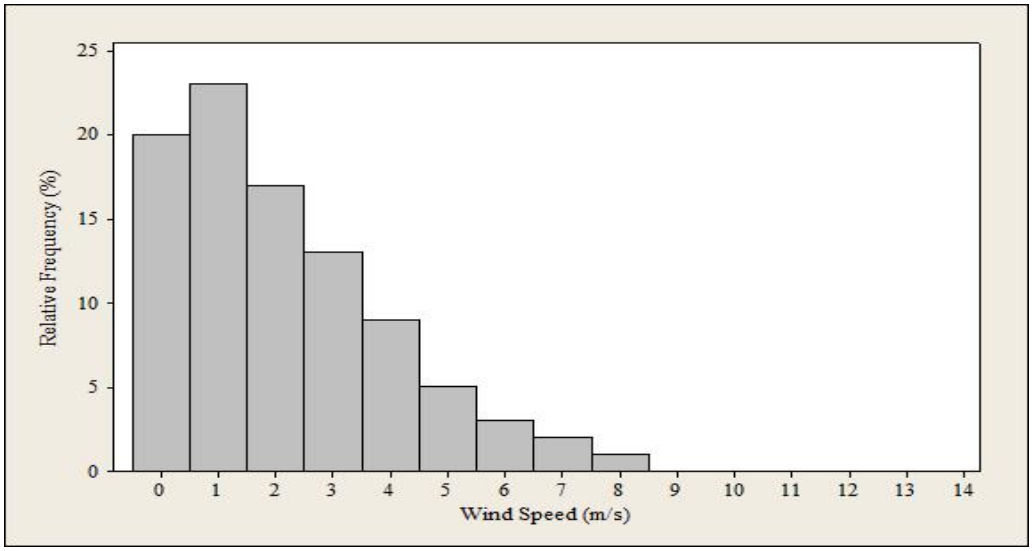

Figure 3.5. The relative frequency of the wind speeds at ground level in METU NCC.

In addition to the potential of wind resources, METU NCC is characterized by hot sunny climate with high solar radiation [58]. The average global solar insolation in METU NCC is 4.93 kWh m^{-2} on a horizontal surface which is high compared with other countries like Spain and USA [7]. Figure 3.6 shows the solar resources map for Cyprus and the location of METU NCC while Figure 3.7 shows the average daily global insolation on a horizontal surface and the average daily wind energy per unit area at 10 m in METU NCC.

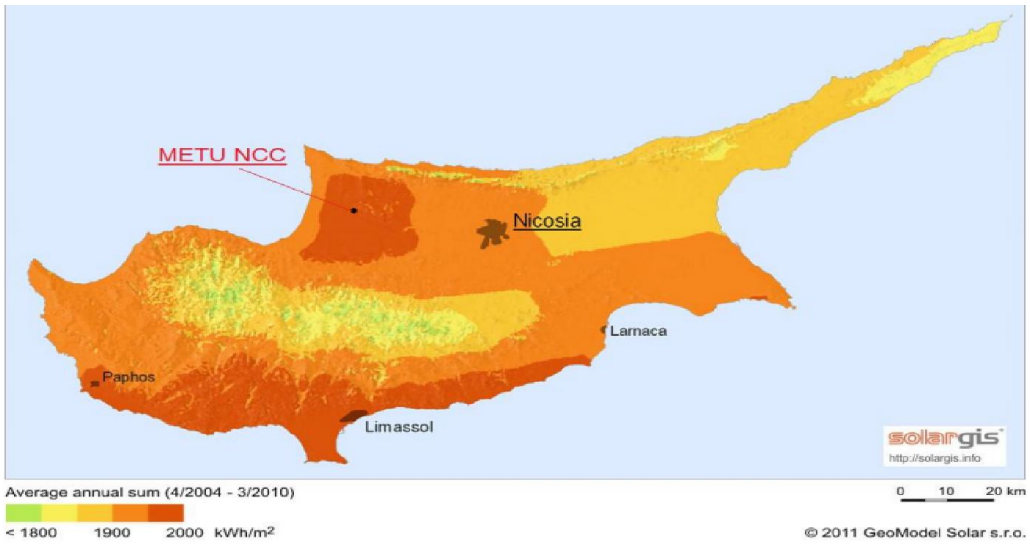

Figure 3.6. Solar resources map of Cyprus [7].

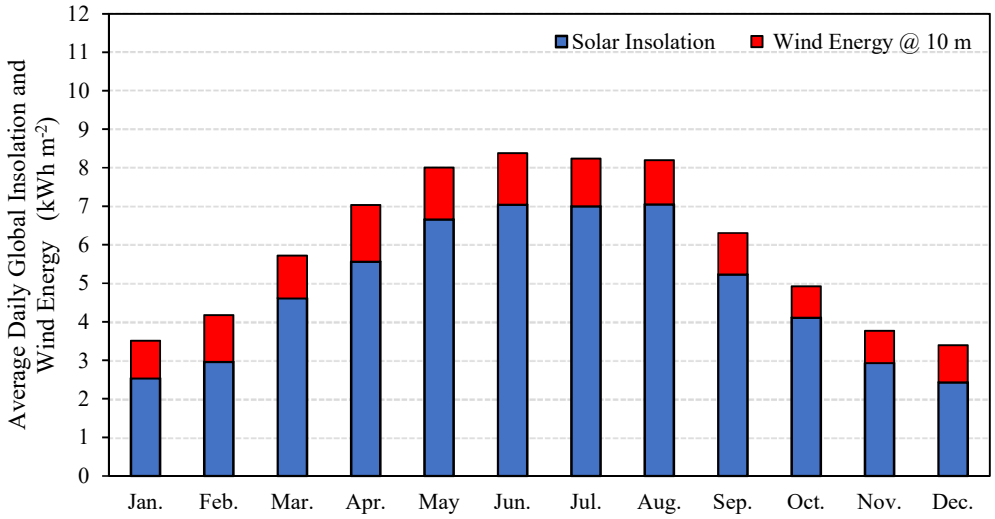

Figure 3.7. The average daily global insolation on horizontal surface and the average daily wind energy per vertical unit area at ground level in METU NCC.

METU NCC represent a perfect example of isolated community that has high potential for the development of microgrid depending on renewable energy resources instead of the electricity grid which mainly depends on fossil fuel for electricity generation [82]. METU NCC is a small community with continuous demand (24/7) throughout the year where the maximum demand occurs in September at the beginning of the fall semester where the temperature is high and the cooling load is supplied by electrical airconditioning units while in winter the heating load in the large buildings- the dormitories and the educational facilities which consumes the highest demand- is supplied by boilers that works on fuel [88], Figure 3.8 shows the average daily demand and the average monthly ambient temperature in METU NCC. Notice that a drop in the demand occurs in August even though the temperature is high where the reason behind this drop is the summer break where the summer school finishes at the end of July and so the students leave the campus.

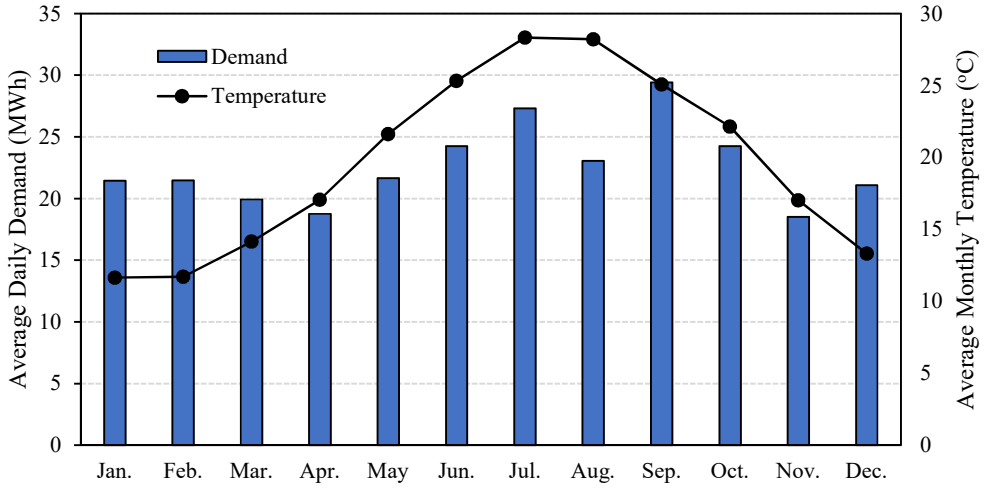

Figure 3.8. The average daily demand of METU NCC in 2015 and the average monthly ambient temperature.

In addition, METU NCC has the site characteristics to establish a pumped hydro storage system where it is near the sea and have higher elevation. The water will be pumped from the sea to the campus with about 100m elevation difference [7] in the time of excess production from the RES, where the water can be stored in a constructed reservoir. While in the deficit times the water will be released to flow to the lower reservoir- the sea- by gravity where the potential energy of the water will be converted to mechanical energy by the turbine and to electrical energy by the generator. Figure 3.9 shows a schematic diagram of a pumped hydro system.

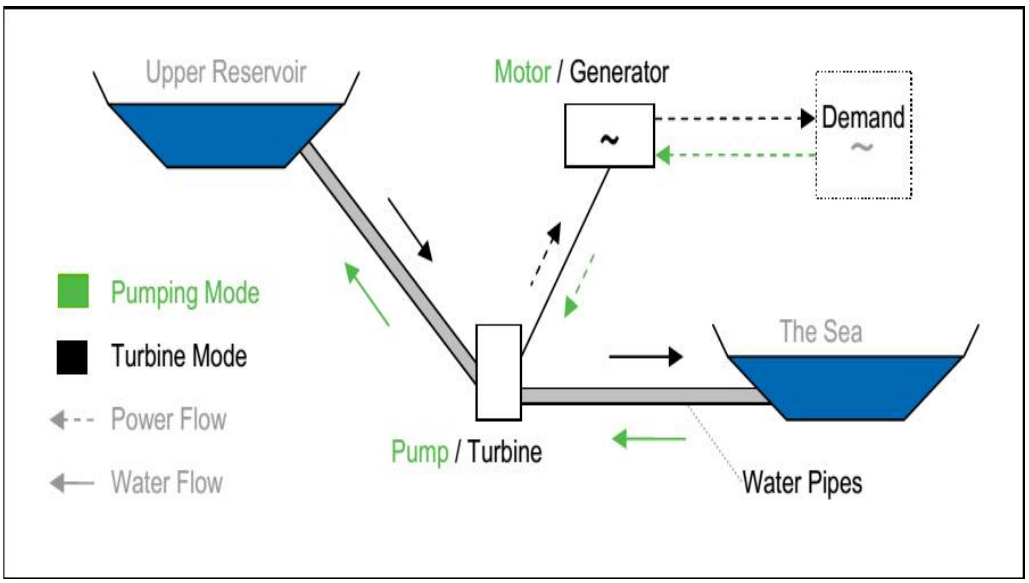

Figure 3.9. Pumped hydro storage system schematic diagram [89].

3.9.2 METU NCC Demand

The average demand throughout the lifespan of the system was forecasted using the hourly demands of 2011, 2014 and 2015 which were obtained from Northern Cyprus Electricity Corporation (Kib-Tek) [90], where the hourly demand of 2011 was generated using the monthly demand data in 2011 and the average hourly demand profile of 2014 and 2015 as shown in Figure 3.10. Linear regression method was used to forecast the peak demand of the 2027 year where the average hourly demand profile of 2014 and 2015 was used to obtain the hourly demand of 2027. Figure 3.11 shows the daily electricity demand in 2011, 2014, and the forecasted demand in 2027 from METU NCC.

Notice in Figure 3.10 that none of the hours has 100% ratio between the demand and the peak demand, the reason behind this is that the peak demand occurs only in one hour in a year and so averaging the hourly values does not give a 100% ratio.

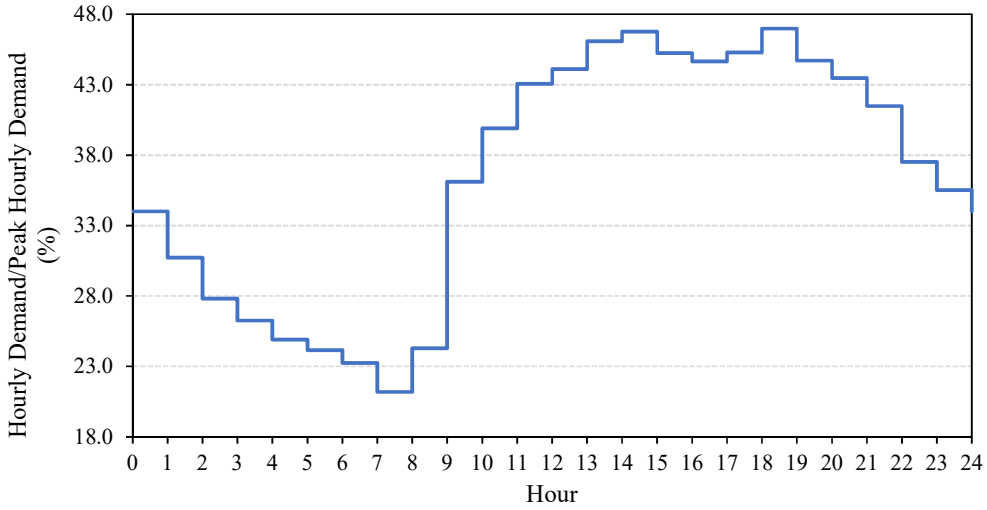

Figure 3.10. Hourly average load profile for METU NCC in 2014 and 2015.

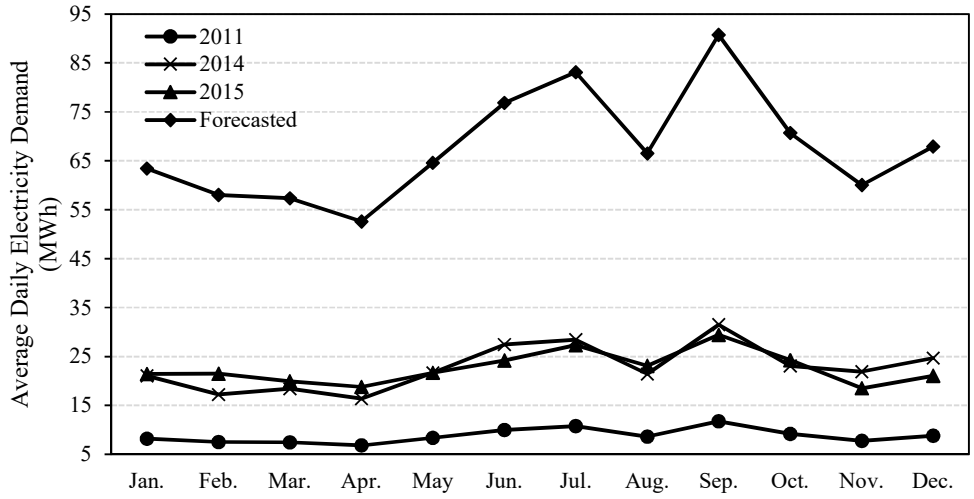

Figure 3.11. The average daily demand of METU NCC in 2011, 2014 and 2015 in addition to the forecasted average demand during the life of the system (year 2027).

3.9.2 Sensitivity Analysis

In this study, a sensitivity analysis of the optimal PV/wind hybrid system with different ESS configurations is carried out to analyze the performance and the sensitivity of the system to any change in the RES resources of the system and the variation in the demand, where in this study the measured solar radiation, wind speeds at 30m and ambient temperature in METU NCC from 2013 to 2016 and the actual demand in 2014, 2015 and the maximum forecasted demand- 2037 demand- will be used. The solar irradiation measurements in METU NCC are carried out using pyrheliometer which measures the Direct Normal Irradiation (DNI) and using pyranometer which measures the Global Horizontal Irradiation (GHI) where the diffuse

irradiation is not measured. The GHI is used to estimate the diffuse solar irradiation using the Orgill and Hollands correlation as in Eq. (31) [61]. Figure 3.12 shows the measured average hourly wind speed at 30m from 2013 and 2016 in METU NCC in addition to the extrapolated TMY data at 30m while Figure 3.13 and Figure 3.14 show the measured average daily GHI and DNI respectively in METU NCC from 2013 to 2016 in addition to the TMY data.

$$\frac{I_d}{I} = \begin{cases} 1 - 0.249 \times k_T, & k_T < 0.35 \\ 1.557 - 1.84 \times k_T, & 0.35 < k_T < 0.75 \\ 0.177, & k_T > 0.75 \end{cases} \quad (31)$$

where k_T can be estimated using Eq. (32).

$$\frac{I}{I_o} = k_T \quad (32)$$

where I_o can be estimated using Eq. (33).

$$I_o = G_{S.C} \times (1 + 0.033 \times \cos(\frac{360+n}{365})) \times \cos\theta z \quad (33)$$

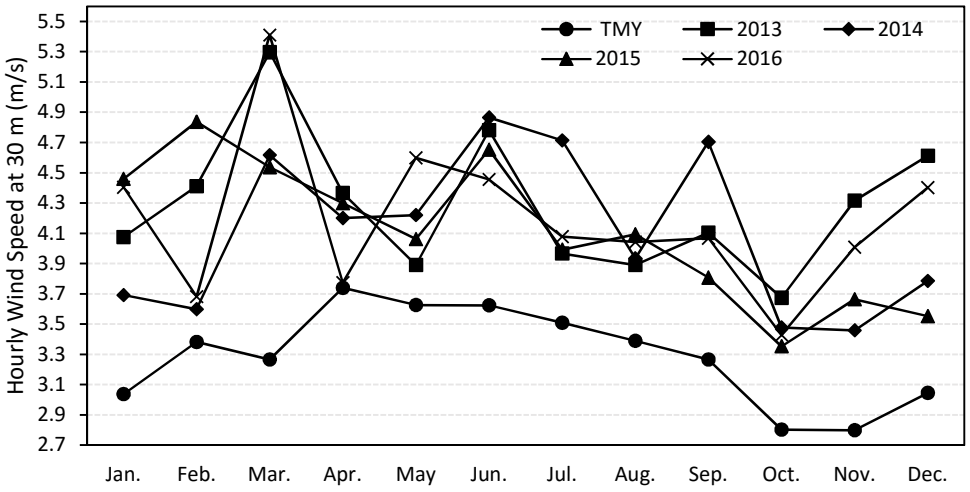

Figure 3.12. The measured average hourly wind speed at 30m in METU NCC from 2013 to 2016 in addition to the extrapolated TMY average hourly speed at 30m.

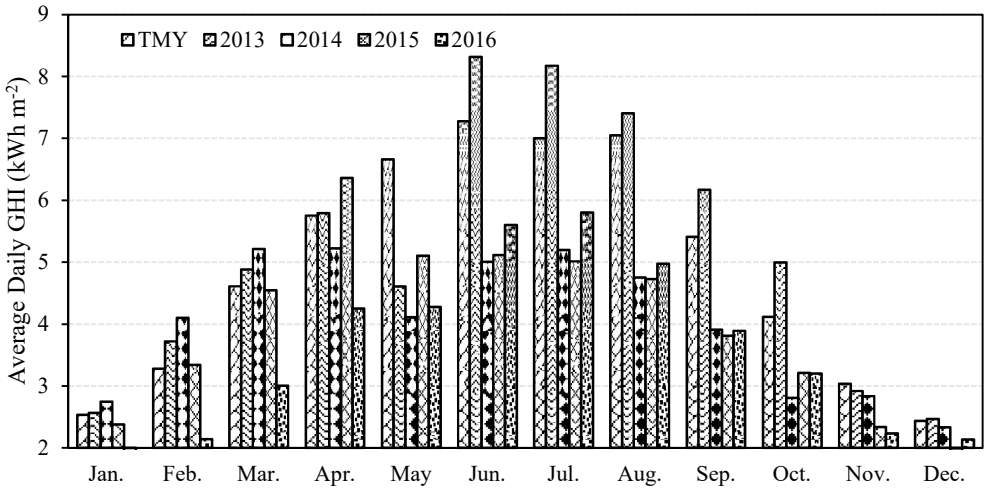

Figure 3.13. The measured average daily GHI in METU NCC from 2013 to 2016 in addition to the TMY GHI.

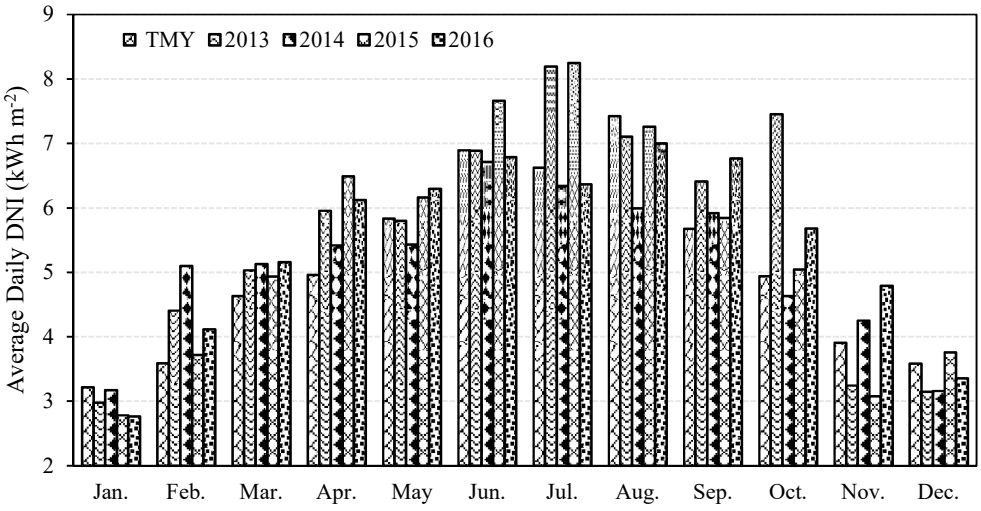

Figure 3.14. The measured average daily DNI in METU NCC from 2013 to 2016 in addition to the TMY DNI.

Notice that in Figure 3.12, Figure 3.13 and Figure 3.14 there are significant differences between the TMY and the measured data; the reason for this difference is that the TMY data are generated using at least 20 years of measured data at specific locations where using the TMY data of these specific locations, the TMY data for other locations are interpolated taking into account several variable like the topography and the elevation [91]. Furthermore, notice that in Figure 3.12 the TMY wind speed is lower than the measured data in the majority of the years and the reason for this in addition to the previous one is that the measured data were

obtained from single wind tower in METU NCC which is placed near a cliff where this location has the highest potential of wind resources, i.e. METU NCC has different microclimates. In addition, the TMY wind speed data at 30m where extrapolated using the 10m TMY data with wind shear coefficient of 1/7 which could be one of the reasons for this deviation since the wind shear coefficient depends on several variable such as the season, terrain and hub height [92]. Moreover, notice that in Figure 3.13 and Figure 3.14 the solar data for 2013 are odd between July and October where this could be due to errors in the measurement or malfunctions in the measuring devices.

In this study, the RES was modeled using Microsoft Excel, where the model estimates the hourly energy production from the RES, the hourly energy stored in ESS, the hourly energy available in the ESS based on the DOD and the round-trip efficiency of the ESS, the annual capacity factor, the annual fraction of demand met by the RES, the annual DSF, the NPV, the PB Pand the COE of the RES. In addition, the model estimates the sizes of the different configurations of the RES- PV, wind and PV/wind hybrid systems- and the capacities of the ESSs based on maximizing the fraction of demand met by the RES with COE less than or equal to the local grid tariff.

CHAPTER 4
RESULTS AND DISCUSSION

4.1 Optimal Sizing Methodologies of ESSs

The sizing of the RES as well as the integrated ESSs plays a vital role in achieving the economic feasibility of the system where the oversizing decreases the economic feasibility while the undersizing leads to inefficient way for the optimal utilization of the RES resources and may also leads to the decrease in the economic feasibility. Therefore, the sizing of the RES and the ESSs in this study was based on maximizing the RES fraction with COE less or equal to the local grid tariff. Table 4.1 shows the optimal sizing methodologies for the ESSs with and without considering the DOD based on maximizing the RES fraction of different RES configurations with COE less or equals to the local grid tariff in METU NCC.

Table 4.1. The optimal sizing methodologies of the battery, PHS and hybrid ESSs with 100% and less than 100% DOD that maximize the RES fraction of the wind, PV and PV/wind hybrid systems with COE less or equal to the local grid tariff in METU NCC.

<table>
<tr><td colspan="2">RES Configuration</td><td colspan="2">PV/Wind</td><td colspan="2">Wind</td><td colspan="2">PV</td></tr>
<tr><td colspan="2">DOD Scenario</td><td><100%</td><td>100%</td><td><100%</td><td>100%</td><td><100%</td><td>100%</td></tr>
<tr><td colspan="2">Battery</td><td colspan="4">Average Hourly Deficit</td><td colspan="2">Average Hourly Excess</td></tr>
<tr><td colspan="2">PHS</td><td>Aver. Daily Demand</td><td>Max. Daily Deficit</td><td>Max. Daily Deficit</td><td>Max. Daily Demand</td><td colspan="2">Average Daily Excess</td></tr>
<tr><td rowspan="2">Hybrid ESS</td><td>Battery</td><td colspan="2">Max. Deficit in 4 min.</td><td>Max. Demand in 4 min.</td><td>Max. Deficit in 4 min.</td><td colspan="2" rowspan="2">Not Feasible</td></tr>
<tr><td>PHS</td><td>Aver. Daily Demand</td><td>Max. Daily Deficit</td><td>Aver. Daily Demand</td><td>Max. Daily Demand</td></tr>
</table>

Table 4.1 indicates that the sizing methodologies are affected by the DOD of the ESSs for PHS and the hybrid ESSs when they are integrated with wind and PV/wind hybrid system. Taking into account the DOD of the ESSs increases the size of the ESS since the size has inverse relationship with the DOD- as in Eqs. (27) and (28) in section 3.5- which requires lower level of the sizing methodologies in order to obtain the feasible system with the maximum RES fraction. While the sizing methodologies for the ESSs with the PV systems do not change with the DOD since they are the only feasible options due to the high capital cost of the PV systems and the low capacity factor compared with the other RES which allows the minimum integration of the ESS to achieve feasible system.

In addition to the effect of the DOD on the sizing methodologies of the ESSs, the DOD also affects the optimal sizes of the RES configurations that maximize the RES fraction with COE equals or less than the gird tariff. Table 4.2, Table 4.3 and Table 4.4 show the optimal configurations of PV, wind and PV/wind hybrid systems respectively that maximize the RES fraction with COE less or equal to the local grid tariff in METU NCC with different ESSs configurations and two DOD scenarios.

Table 4.2. The optimal PV system sizes with and without ESS in METU NCC with two DOD scenarios that maximize the RES fraction with COE less or equals to the grid tariff in addition to the corresponding technical and economic parameters.

ESS	No ESS	Battery		PHS	
Parameter DOD	-	60%	100%	89%	100%
PV Capacity (MW)	4.26	4.17	4.2	4.37	4.39
Battery Capacity (kWh)	-	34.66	21.84	-	-
PHS Capacity (MWh)	-	-	-	0.827	0.761
RES Fraction (%)	25.6	25.14	25.32	26.46	26.6
Capacity Factor (%)	17.5	17.5	17.5	17.5	17.5
COE ($/kWh)	0.175	0.175	0.175	0.175	0.175
NPV ($)	117.23	16404	11694	1123	363
PBP (years)	9.13	9.11	9.12	9.13	9.13
DSF (%)	4.79	4.54	4.67	6.5	6.67
Savings (M$/year)	1.11	1.1	1.1	1.14	1.15
CO2 Emissions (ton)	3809	3728	3760	3916	3939

As shown in Table 4.2, all the scenarios with DOD less than 100% have less PV capacities than 100% DOD scenarios due to the increase in the required ESS capacities. Furthermore, the integration of the PV system with PHS increases the RES fraction by increasing the feasible PV capacity and the match between the demand and the supply. While the integration of the battery reduces the RES fraction and the DSF due to the decrease in the installed capacity of the PV to achieve feasible configuration. It can be noticed in Table 4.2 that the NPV of the PV system increases with the integration of the ESSs where the highest NPV is in the case of the integration of battery storage system where this is due to the decrease in the PV capacity. While in the case of the integration of PHS even though the PV capacity is increased however the NPV is increased and this due to the increase in the RES fraction, i.e. the annual revenues more than the increase in the capital cost.

For wind systems as shown in Table 4.3, only the battery scenario with DOD less than 100% has less wind capacity than the 100% scenario due to the increase in the battery size which requires the decrease in the wind capacities to maintain the economic feasibility. While for the other DOD< 100% scenarios, the wind capacities were not affected however the capacities of the ESSs are decreased due to the change in the sizing methodologies as in Table 4.1. Moreover, the integration of the ESSs in all the configurations increase the RES fraction and the DSF except for the battery with 60% DOD where the integration of 60% DOD battery storage system reduces the feasible wind capacity and so decreases the RES fraction and the DSF. While the integration of 100% DOD battery storage system increases the RES fraction and the DSF by increasing the matching between the demand and the supply. On the other hand, the integration of PHS and hybrid ESS increase not just the matching between the supply and the demand by storing the excess energy but also by increasing the feasible wind system capacity.

Table 4.3. The optimal wind system sizes with and without ESS in METU NCC with two DOD scenarios that maximize the RES fraction with COE less or equals to the grid tariff in addition to the corresponding technical and economic parameters.

Parameter	Scenario	No ESS	Battery		PHS		Hybrid			
	DOD	-	60%	100%	89%	100%	Batt. 60%	PHS 89%	Batt. 100%	PHS
Wind Cap. (MW)		8	6	8	10	10	10		10	
Battery Cap. (MWh)		-	2.76	1.5	-	-	0.871		0.503	
PHS Cap. (MWh)		-	-	-	142.9	149.1	89.51		149.1	
RES Fraction (%)		49.51	46.32	51.82	85.57	87.05	80.28		87.07	
Capacity Factor (%)		28.88	28.88	28.88	28.88	28.88	28.88		28.88	
COE ($/kWh)		0.1713	0.168	0.174	0.172	0.171	0.169		0.174	
NPV (M$)		0.823	2.88	0.99	0.662	0.821	1.77		0.58	
PBP (years)		8.68	7.5	8.6	8.93	8.89	8.55		8.96	
DSF (%)		33.34	30.95	37.89	38.5	38.5	76.71		85.56	
Savings (M$/year)		2.14	2	2.24	3.7	3.77	3.5		3.77	
CO_2 Emissions(ton)		11818	8864	11819	14773	14773	14773		14773	

With the assumptions made in the methodology section, Table 4.3 shows decrease and increase in the NPV for the different scenarios and configurations. The increase in the NPV is caused either by the decrease in the wind capacity as in the 60% DOD battery scenario or by the increase in the matching between the demand and the supply without increasing the wind capacity as in 100% DOD battery scenario or with increasing the wind capacity as in less than 100% DOD hybrid ESS scenario. While the decrease is as a result of the increase in the total capital cost of the system mainly due the PHS system with low revenues compared with the capital cost of such PHS size as in both PHS scenarios and the 100% DOD hybrid ESS scenario. Moreover, the DSF increased with integration of the ESS for all configurations however the increase significantly varies among the three ESS configurations. The largest increase is in the case of the hybrid ESS due to the increase in the wind system size and the existence of the battery where the battery will compensate the deficit in the lag time of the PHS where after the lag time, the PHS is responsible for meeting the deficit. The increase in the DSF in both PHS scenarios is due to the increase in the installed wind capacity where due to the lag time of the PHS the DSF is not increased by the PHS. While for 100% DOD battery scenarios the increase is as a result of the increase in the matching between the demand and the supply.

Table 4.4. The optimal PV/wind system sizes with and without ESS in METU NCC with two DOD scenarios that maximize the RES fraction with COE less or equals to the grid tariff in addition to the corresponding technical and economic parameters.

Parameter \ Scenario	No ESS	Battery		PHS		Hybrid			
DOD	-	60%	100%	89%	100%	Batt. 60%	PHS 89%	Batt. 100%	PHS
PV Cap. (MW)	3.73	3.12	3.53	4.19	1.8	3.44		1.38	
Wind Cap. (MW)	6	6	6	8	10	8		10	
Battery Cap. (MWh)	-	1.22	0.768	-	-	0.833		0.5	
PHS Cap. (MWh)	-	-	-	89.51	116.25	89.51		118.78	
RES Fraction (%)	58.03	57.42	58.73	88.04	90.13	85.63		89.31	
Capacity Factor (%)	24.52	24.98	24.66	24.97	27.14	25.46		27.5	
COE ($/kWh)	0.175	0.175	0.175	0.175	0.175	0.175		0.175	
NPV (k$)	5.72	600	380	0.55	0.431	410		250	
PBP (years)	9.13	8.85	8.96	9.13	9.13	9		9.1	
DSF (%)	34.46	36	37.31	42.58	41.48	80.74		87.18	
Savings (M$/year)	2.51	2.48	2.54	3.81	3.9	3.7		3.86	
CO_2 Emissions (ton)	12203	12038	12024	15567	16383	411308		16010	

As shown in Table 4.4 and similar to the wind systems, the integration of the ESSs increases the RES fraction and the DSF for all ESSs scenarios and configurations except for battery scenario with 60% DOD where the decrease is a result of the decrease in the PV capacity. While the increase is either due to the increase in the matching by utilizing part of the excess energy like the battery scenario with 100% DOD or due to the increase in the installed capacities and the utilization of part of the excess as in the other configurations and scenarios. Furthermore, it can be noticed that the RES fraction for the PV/wind system with PHS alone is larger than the system with hybrid ESS for both DOD scenarios. The reason behind this is that the additional cost of the battery storage system in case of the hybrid ESS requires the decrease in the PV capacities. On the other hand, the system with the hybrid ESS has higher DSF where the battery compensates the deficit during the lag time of the PHS unlike the separate PHS where the deficit is met by the grid. Moreover, notice that the system with PHS for both scenarios is the only configuration that has lower NPV than the system without ESS due to the higher total capital cost of the PHS with lower revenues for such PHS size.

4.2 The Effect of the Integration of Short and Long Term ESSs

4.2.1 PV Systems

The integration of the ESSs affects the technical and economic parameters of the RES; however, these effects vary depending on the type of the RES and the ESS in addition to the capacities of the RES. As one of the economic parameters, the COE of the PV system is affected by the integration of the ESS, Figure 4.1 shows the effect of the integration of different ESS with PV systems on the COE in METU NCC. The integration of the battery and PHS have no significant effect with capacities less than 4 MW where after that, the integration of the PHS decreases the COE while the integration of the battery increases the COE. The reason behind this is the optimal sizing methodology of the ESS where for battery it is sized based on the hourly average excess and the PHS based on the average daily excess. The excess energy from the PV systems with capacities below 4 MW is small and so the size of the ESSs will be small and will not affect the COE. After 4 MW, the ESS size will increase and so increases the matching between the demand and the supply by storing the excess energy which will decrease the COE as in the PHS scenario. While, in the case of battery storage system and due to its high capital cost, it causes the increase in the COE. On the other hand, the integration of the hybrid ESS with the PV causes the increase of the COE for all PV capacities due to the increase in the capital cost with less increase in the revenues caused by the integration of battery storage system mainly. Notice in Figure 4.1 that the integration of battery and PHS does not significantly seems to affect the feasible PV capacities with the assumptions made in the methodology section while the integration of hybrid ESS makes the system economically unfeasible.

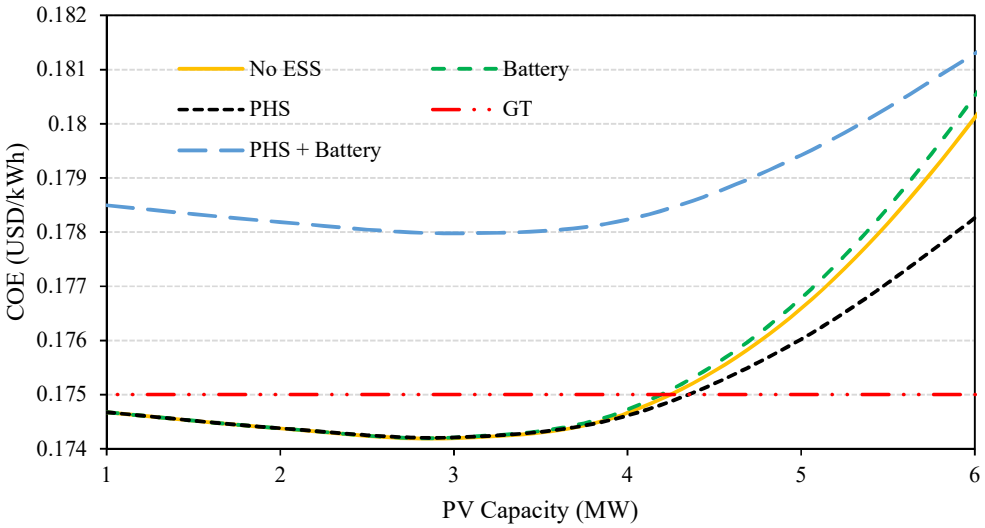

Figure 4.1. The effect of the integration of short and long term ESSs on the *COE* of the PV systems if both ESSs have DOD less than 100% in METU NCC using the optimal ESS sizing methodologies for separate ESS while using the methodology with the lowest COE for the hybrid ESS, i.e. average daily excess for PHS and the maximum deficit in the lag time of the PHS for the battery in addition to the local grid tariff.

The integration of the ESSs with PV systems increases the matching between the supply and the demand by storing the excess and allocating it to meet the deficit. Figure 4.2 shows the effect of the integration of different ESSs on the RES fraction of PV systems in METU NCC. The RES fraction increases with installed PV capacity larger than 6 MW where below this threshold the small excess and the unusable energy due to the DOD of the ESSs prevent the contribution of the ESS in increasing the matching between the demand and the supply. The amount of increase in the RES fraction varies between the ESS configurations where PHS and the hybrid ESS have the largest and almost equal increase where the integration of the battery in the hybrid system does not significantly contribute in increasing the RES fraction since its size is relatively small.

It can be noticed from Figure 4.2 that the RES fraction of the PV system alone and with battery storage system reaches the saturation after almost 16 MW. After 16 MW, the majority of the energy produced by the added PV capacity is excess and in case of the battery its size is not enough to store more excess and so cannot contribute in increasing the RES compared with PHS. While the integration of PHS and hybrid ESS shifts the threshold to larger PV capacities where the size of the PHS in both scenarios, PHS alone and hybrid ESS, is capable of storing the excess and allocate it to meet demand.

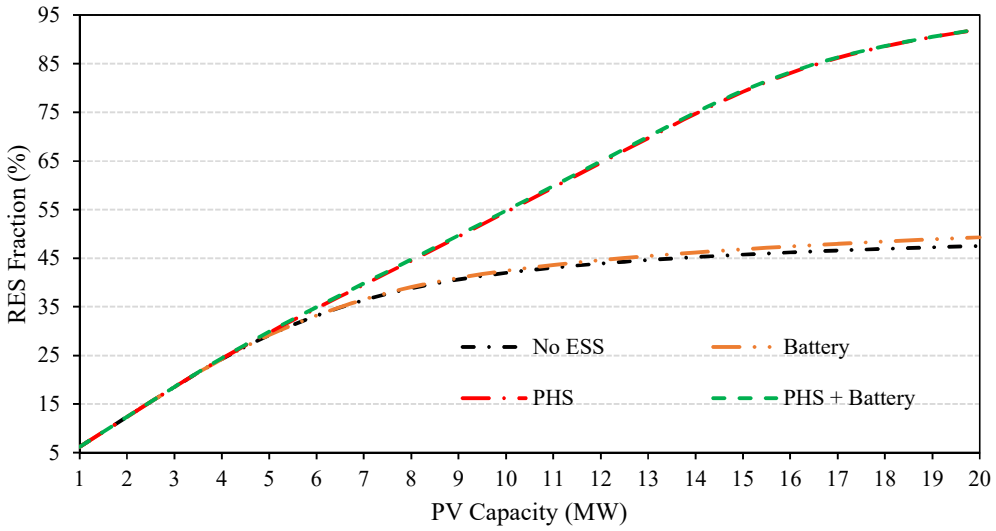

Figure 4.2. The effect of the integration of short and long term ESSs on the RES fraction of the PV systems if both ESSs have DOD < 100% in METU NCC using the optimal ESS sizing methodologies for separate ESS while using for the hybrid ESS the methodologies with the lowest COE, i.e. average daily excess for PHS and the maximum deficit in the lag time of the PHS for the battery.

The integration of the ESS with the PV systems also affects the autonomy of the system where it significantly increases the DSF of the system with installed capacity larger than 4 MW. Even though the system below 4 MW produces considerable amount of energy- with small excess and so the ESSs will not affect the DSF- however it is not sufficient to meet totally the hourly demand in most of the hours in a year and so the system has very low autonomy. However, after 4 MW the number of hours where the demand is totally met by the system starts to increase especially with the integration of hybrid ESS. Figure 4.3 shows the effect of the integration of the ESSs on the DSF of the PV systems in METU NCC.

Notice that in Figure 4.3, the DSF of the PV system is not affected by the integration of the PHS due to the lag time of the ESS which prevent the independency of the system totally from the grid even though the PHS has the capacity to achieve the independency. The integration of the battery storage system was the suggested solution to increase the independency and the autonomy of the system with the help of the PHS where as shown in Figure 4.3 it proves the effectiveness of the such integration. It can clearly be noticed from Figure 4.3 that the integration of hybrid ESS increases the autonomy of the system in a significant way paving the way for the formation of isolated power system or what is known as microgrids. Moreover, notice that the threshold at which the integration of the ESS starts to affect the DSF is not the same threshold at which the integration affect the RES fraction as in Figure 4.2- DSF threshold

is less than the RES fraction one- where increasing the number of hours the demand is met by the system does not necessary require large amount of energy specially with low PV capacities unlike the RES fraction which requires relatively large amount of stored energy to increase it.

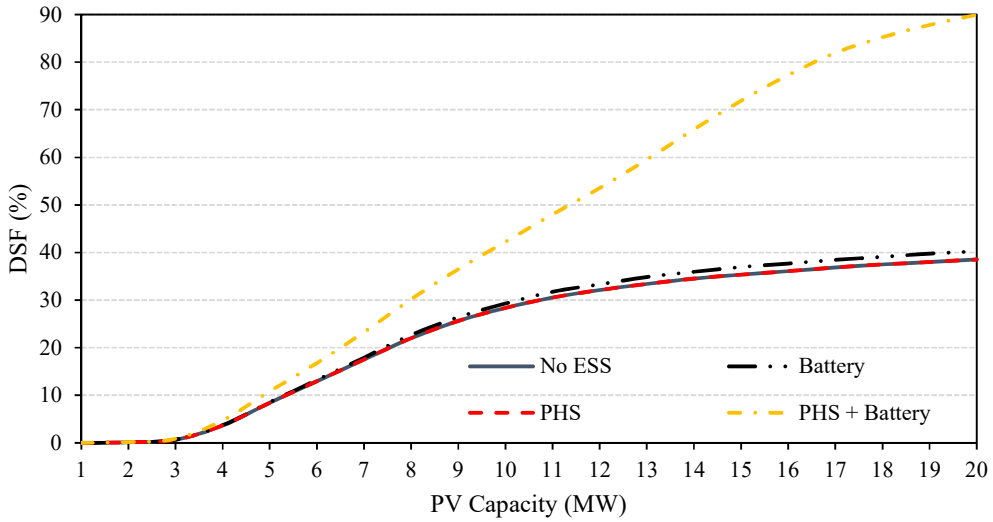

Figure 4.3. The effect of the integration of short and long term ESSs on the DSF of the PV systems if both ESSs have DOD less than 100% in METU NCC using the optimal ESS sizing methodologies for separate ESS while using for the hybrid ESS the methodologies with the lowest COE, i.e. average daily excess for PHS and the maximum deficit in the lag time of the PHS for the battery.

4.2.2 Wind Systems

The integration of the ESSs with wind systems has different effects on the COE than PV systems based on the ESS type and the installed capacity of the wind system. Figure 4.4 shows the effect of the integration of different types of ESSs on the COE of the wind system in METU NCC. The integration of battery storage system with wind systems increases the COE whatever the size of the system due to the high capital cost of the battery with small revenues because of the integration. However, the amount of the increase decreases as the wind capacity increases since the battery capacity is function of the average hourly deficit which reduces the total capital cost of the system. Furthermore, after 10 MW wind capacity the amount of the difference between the COE of the system with battery and system without ESS remains constant where any increase in the installed wind capacity does not match the demand and so does not decrease the deficit.

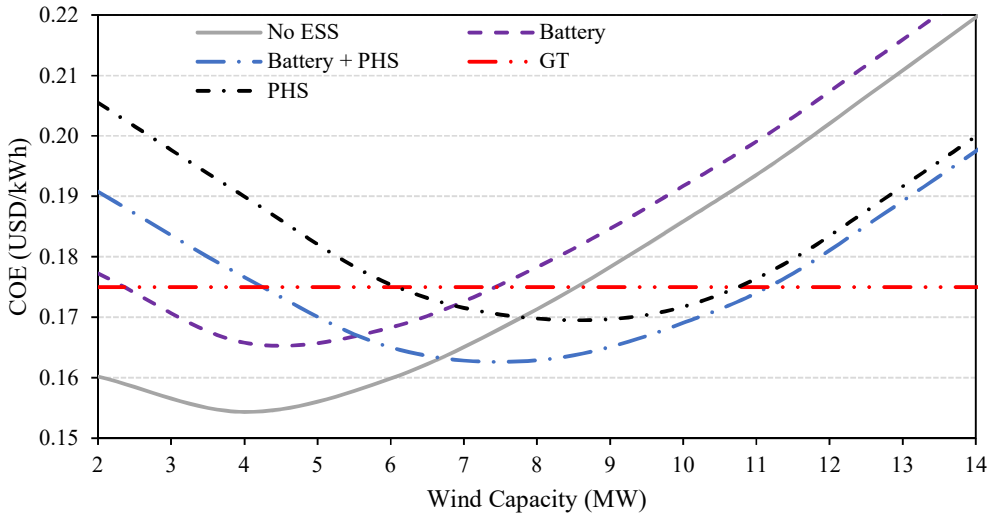

Figure 4.4. The effect of the integration of short and long term ESSs on the COE of the wind systems if both ESSs have DOD less than 100% in METU NCC using the optimal ESS sizing methodologies in addition to the local grid tariff.

The integration of the PHS and hybrid ESS seems to increase the COE up to certain wind capacities, where after these capacities the COE seems that it starts to decrease. The reason behind this is that the capacity of the PHS decreases as the wind capacities increase up to a certain limit since the PHS capacity is function of the deficit which reduces the capital cost. While for the hybrid ESS even though the PHS capacity is constant- function of average daily demand- however the battery is a function of the hourly deficit which decreases the capital cost with the increase in the wind capacities. In addition, due to the relatively small excess from wind capacities less than 7 MW, the integration of the PHS and the hybrid ESS does not have significant revenues and so does not contributes in decreasing the COE. Furthermore, notice that the hybrid ESS has COE less than the PHS even though the hybrid ESS has battery; the main reason behind this is the difference in the PHS capacities where the hybrid ESS has much less installed capacity than the PHS alone- PHS alone is function of the maximum daily deficit while the PHS capacity in the hybrid ESS is a function of average daily demand- which decreases the total capital cost of the system.

Notice that in Figure 4.4, the COE of the system in all the configurations start from high value then decreases to the minimum then start to increase again. The reason behind that is at the beginning the revenues are small compared with the capital cost of the system. While at the minimum COE value, the revenues are the maximum and the optimal compared with the capital cost. After the minimum COE value, the increase in the installed capacity increases the total capital cost with less increase in the revenues due to the mismatch between the supply

from the increased capacities and the demand. Furthermore, notice the integration of the PHS and hybrid ESS increases the feasible wind capacities which means that the integration could help in further deployment of wind systems using these options while the battery storage system did not significantly affect the feasible capacities. Moreover, notice that the integration of PHS and hybrid ESS shifts the minimum COE value to higher wind capacities. The reason behind this is that in the beginning with small wind capacities the revenues from the integration is small compared with the additional cost due to the small excess from these wind capacities. The ESSs can be maximumly utilized in the existence of suitable wind capacity that can provide sufficient excess to ensure the maximum benefits which requires the increase in the wind capacity.

Similar to PV systems, the integration of the ESSs with wind systems increases the RES fraction and the DSF; however, the increase for the wind systems is more than the PV systems. The reason behind this is the sizing methodologies which depend on the capital cost of the systems in addition to the performance and revenues of the wind systems play a major role in this difference. Figure 4.5 shows the effect of the integration of different types of ESSs on the RES fraction of wind systems in METU NCC while Figure 4.6 shows the effect of the integration of different types of ESSs on the DSF of wind systems in METU NCC.

Notice that in Figure 4.5 the PHS alone has higher RES fraction than the hybrid ESS after 5 MW wind capacity where before this threshold the amount of energy stored in the ESS is almost the same even though the ESSs capacities are different where the amount of excess energy is not enough to fill the ESSs. However, after 5 MW and as the PHS alone has bigger capacity than in the hybrid ESS it allocates more excess energy to meet the demand. Moreover, notice that the integration of PHS and hybrid ESS with wind systems increases significantly the RES fraction larger than the PV systems as in Figure 4.2. The reason behind this difference is that the PV system has higher capital cost which allows less integration of ESSs as in the optimal sizing methodologies. Moreover, the PV systems have less performance- less capacity factor and so less energy production- than wind systems.

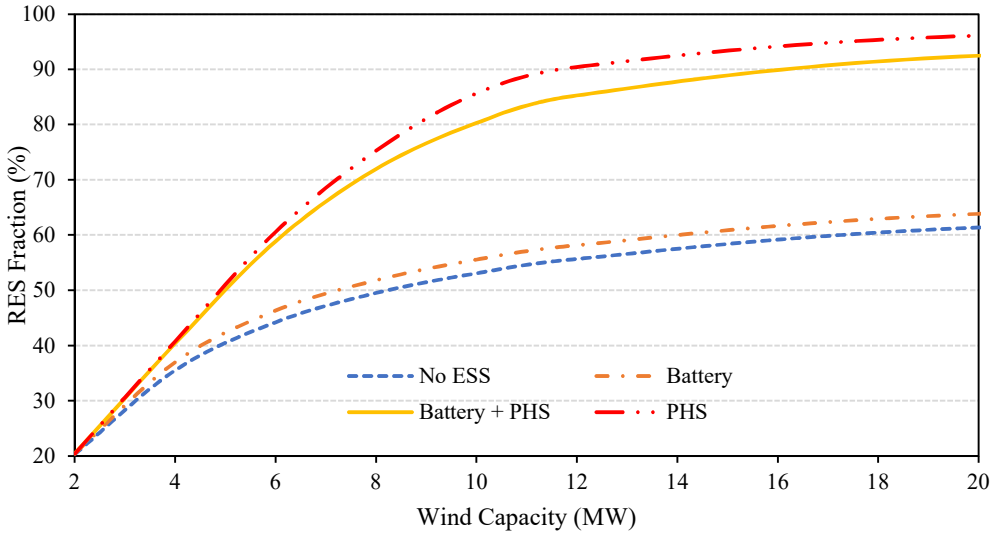

Figure 4.5. The effect of the integration of short and long term ESSs on the RES fraction of the wind systems if both ESSs have DOD less than 100% in METU NCC using the optimal ESS sizing methodologies.

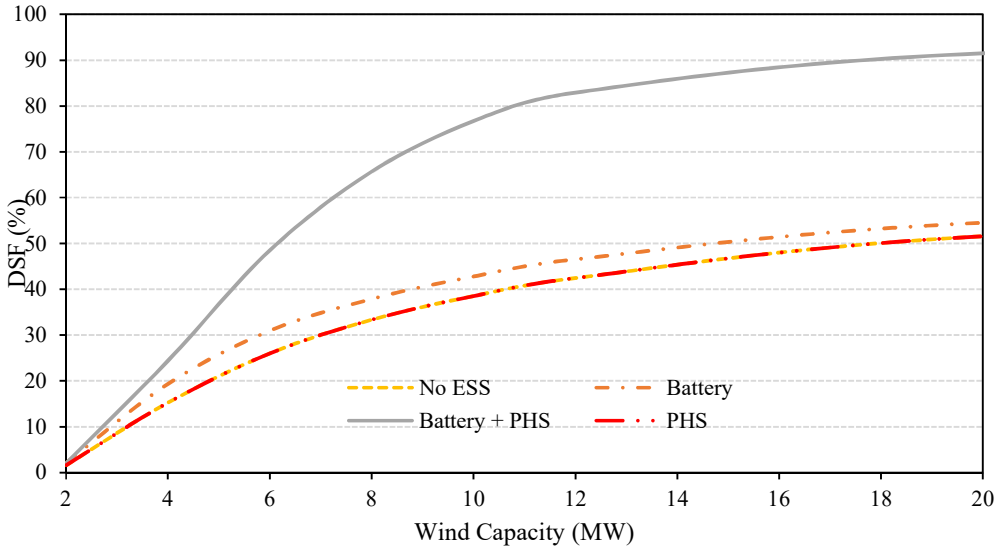

Figure 4.6. The effect of the integration of short and long term ESSs on the DSF of the wind systems if both ESSs have DOD less than 100% in METU NCC using the optimal ESS sizing methodologies.

Notice that in Figure 4.6, unlike the PV system the DSF of the wind system either with ESS or without has value higher than zero with the same installed capacity- 2 MW- and the reason behind this is that wind systems in METU NCC has higher performance than the PV systems, i.e. higher capacity factor which allows higher energy production from the wind

system where the wind system has a 28.88% capacity factor while the PV has 17.5%. In addition, the energy production of wind systems in METU NCC is distributed among the day which increases the probability of meeting the demand totally. Furthermore, similar to PV systems the integration of hybrid ESS with wind systems allows the development of microgrid and increases the availability of the energy system.

4.2.3 PV/Wind Hybrid System

The integration of ESSs with PV/wind hybrid system has different effects on the economic and technical parameter of the system where the type of the ESS and the installed PV/wind system capacities play the major role in these effects. Figure 4.7 shows the effect of the integration of Lithium-Ion batteries on the COE of PV/wind hybrid systems in METU NCC. The integration of battery storage system with PV/wind hybrid system in METU NCC increases the COE whatever is the size of the PV/wind hybrid system. However, this increase varies with the installed capacities of the system components to certain thresholds- 10 MW PV and 20 MW wind- where after these thresholds there are no significant changes on the COE. The reason behind this is at the beginning- with small installed PV and wind capacities- the size of battery storage system is large since the battery is sized based on the average hourly deficit with small revenues from this integration due to the small amount of excess energy from such PV/wind system sizes. After the thresholds, the deficit reaches the saturation phase due to the mismatch between the supply and the demand and so the size of the battery storage system remains almost constant.

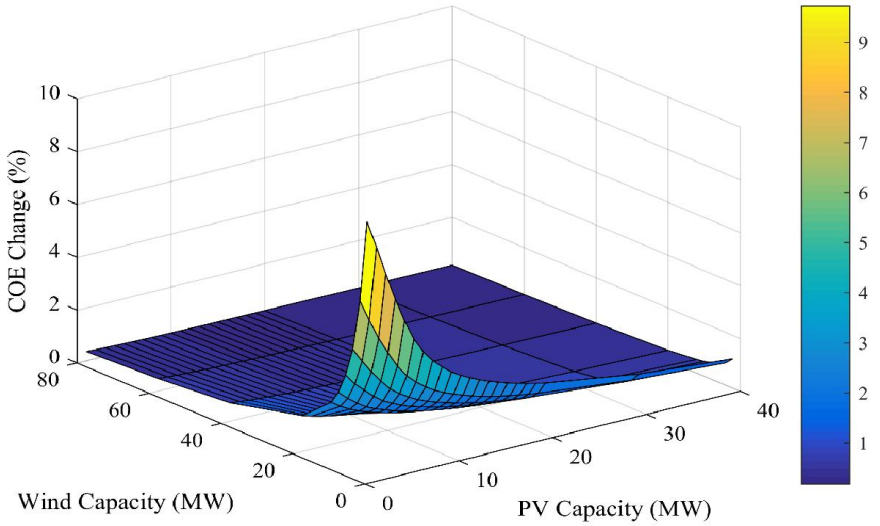

Figure 4.7. The change in the COE of the PV/wind hybrid system as a result of the integration of short term ESS- batteries- with DOD less than 100% in METU NCC where the size of the battery is function of the average hourly deficit.

While the integration of PHS and hybrid ESS increases the COE of the system only at the beginning- with less than 10 MW PV and less than 20 MW wind systems- as shown in Figure 4.8 and Figure 4.9 due to the small revenues from the integration because of the small excess energy from such PV/wind system sizes. Where after that and depending on the installed PV and wind capacities the effect on the COE varies between the decrease in the COE to no change. The reason behind this is the contribution of the ESSs in the revenues is limited to their storing capacities and as the installed PV and wind capacities increase, the excess amount of energy increase and exceeds the storing capacities of the ESSs- since the capacities of the PHS alone and the PHS in the hybrid ESS are constant and do not change with the PV/wind size- where these amounts are dumped into the grid without any revenues.

Furthermore, notice in Figure 4.8 and Figure 4.9 that the integration of PHS decreases the COE more than the integration of the hybrid ESS due to the high capital cost of the battery compared with the PHS alone where both ESS configurations has the same PHS sizes since the sizing methodology is the same with negligible role of the battery in increasing the revenues due to its relatively small size.

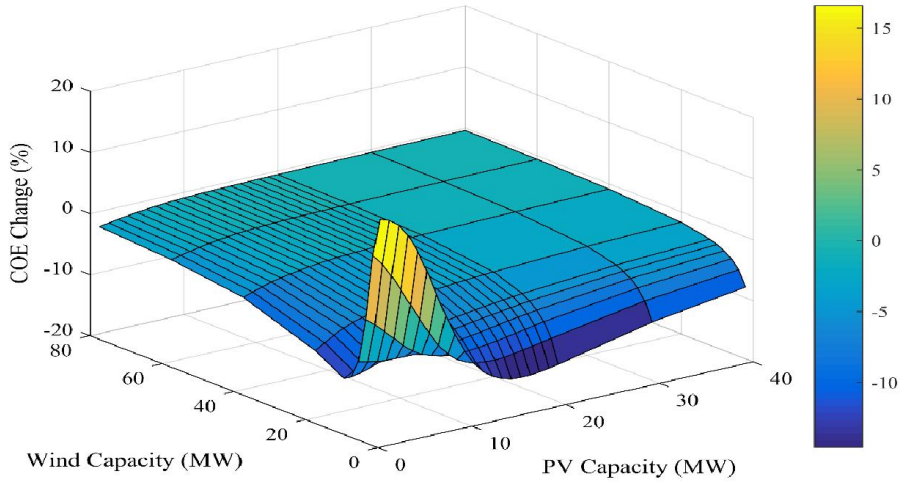

Figure 4.8. The change in the COE of the PV/wind hybrid system as a result of the integration of long term ESS- PHS- with DOD less than 100% in METU NCC where the PHS capacity is a function of the average daily demand, i.e. 89.51 MWh.

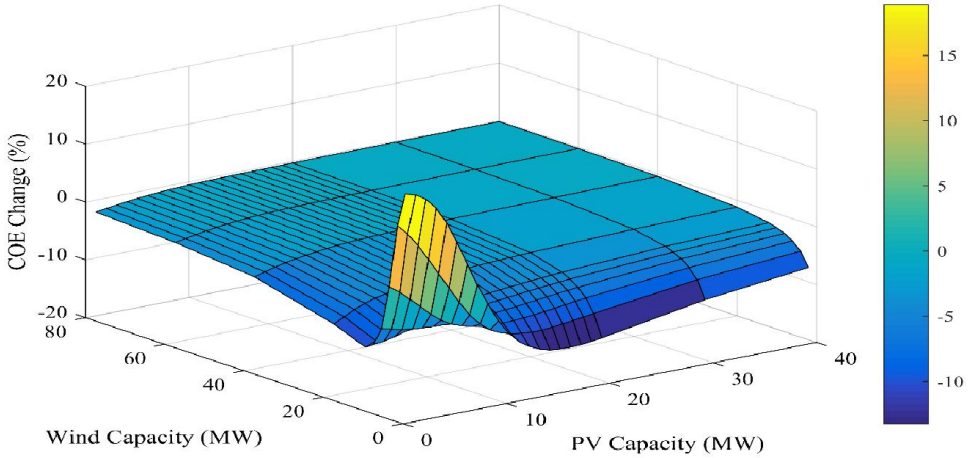

Figure 4.9. The change in the COE of the PV/wind hybrid system as a result of the integration of hybrid ESS- PHS and batteries- with DODs less than 100% in METU NCC using the optimal ESS sizing methodologies.

In order to compare the effect of the integration of different types and configurations of ESSs on the COE of the PV/wind hybrid system 2 representative wind turbine capacities and several PV capacities were taken as shown in Figure 4.10 and Figure 4.11. It can be noticed that the COE of the PV/wind system with the integration of battery storage system is less than the systems with PHS or hybrid ESS only with small installed capacities of wind and PV.

However, as the installed capacities increase the COE of the system with PHS and hybrid ESS decreases. The reason behind this is the small revenues caused by the PHS and the hybrid system with small installed PV and wind capacities since the excess from such PV/wind system is small.

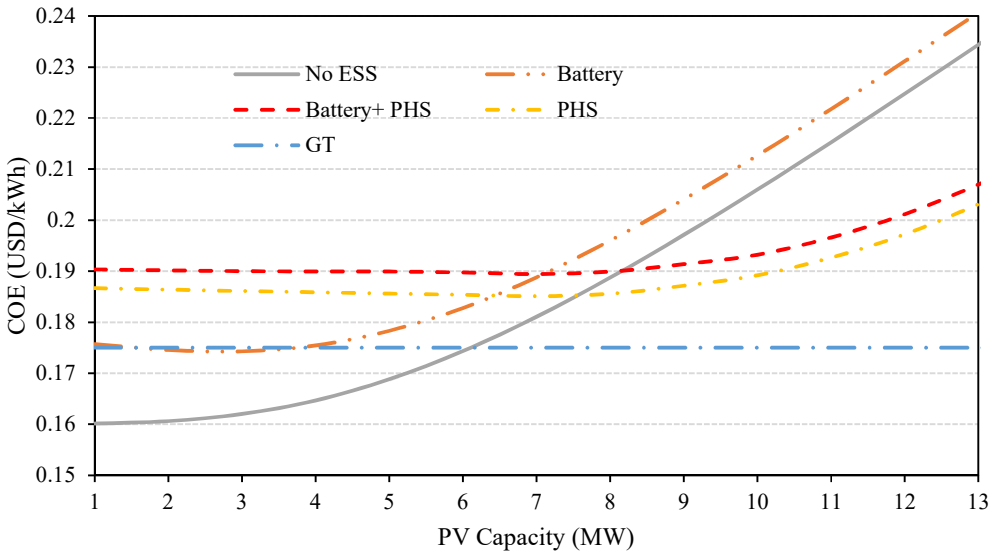

Figure 4.10. The effect of the integration of short and long term ESSs with DOD less than 100% on the COE of the PV/wind hybrid systems - with 1 turbine and several PV capacities- in METU NCC using the optimal ESS sizing methodologies in addition to the local grid tariff.

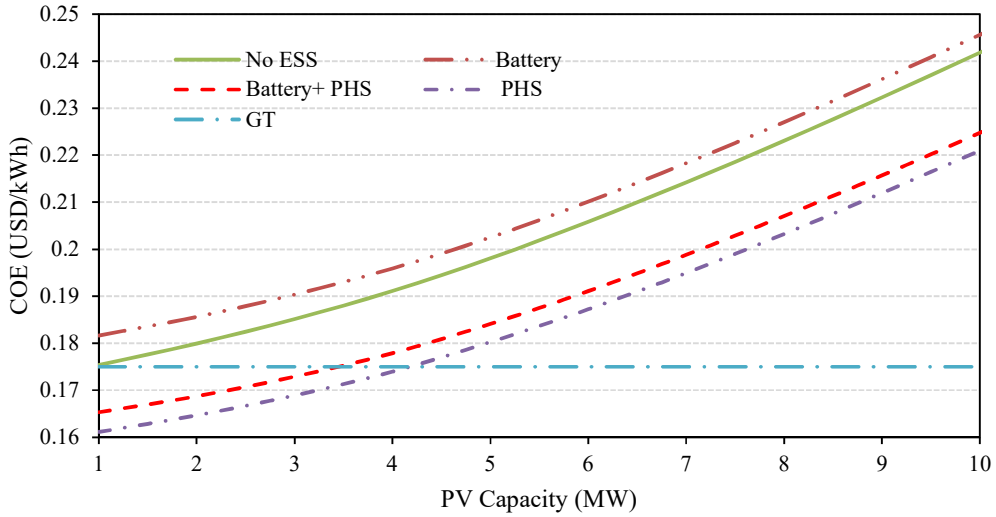

Figure 4.11. The effect of the integration of short and long term ESSs with DOD less than 100% on the COE of the PV/wind hybrid systems - with 4 turbines and several PV capacities- in METU NCC using the optimal ESS sizing methodologies in addition to the local grid tariff.

Furthermore, it can be noticed from Figure 4.10 that the COE of the system with PHS and hybrid ESS has constant COE with PV capacities up to almost 8 MW. The reason behind that is that the increase in the capital cost as a result of the increase in the PV capacities- PHS capacity in both configuration is constant where it is function of the average daily demand- is compensated by the revenues gained by allocating the excess energy to meet more demand by the ESS. While as the wind capacities increase, the capital cost increase in a way that the increase in the revenues cannot compensate the increase in the capital cost.

The integration of short and long term ESS increases the RES fraction of the PV/wind hybrid system. However, the amount of increase varies with the installed PV and wind capacities as well as the type of the ESS and its capacity. Figure 4.12, Figure 4.13 and Figure 4.14 show the effect of the integration of battery, PHS and hybrid ESSs respectively on the RES fraction of PV/wind hybrid system in METU NCC.

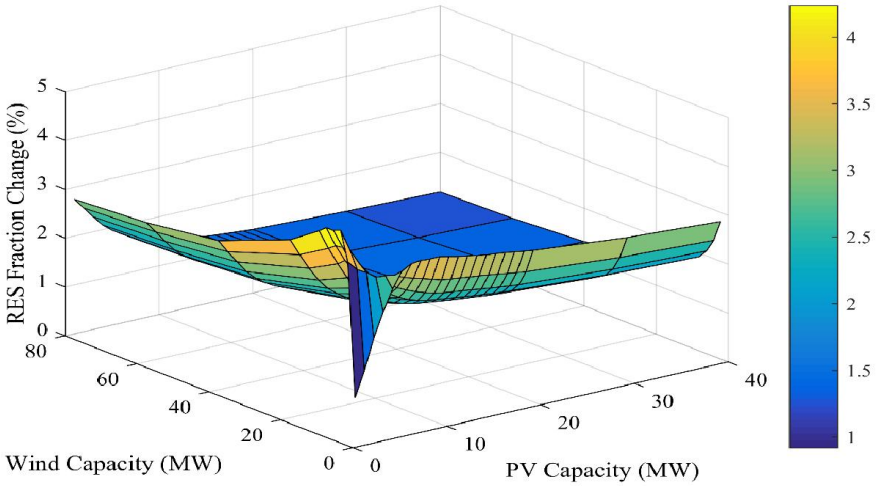

Figure 4.12. The change in the RES fraction of the PV/wind hybrid system as a result of the integration of short term ESS- batteries- with DOD less than 100% in METU NCC where the battery size is a function of the average hourly deficit.

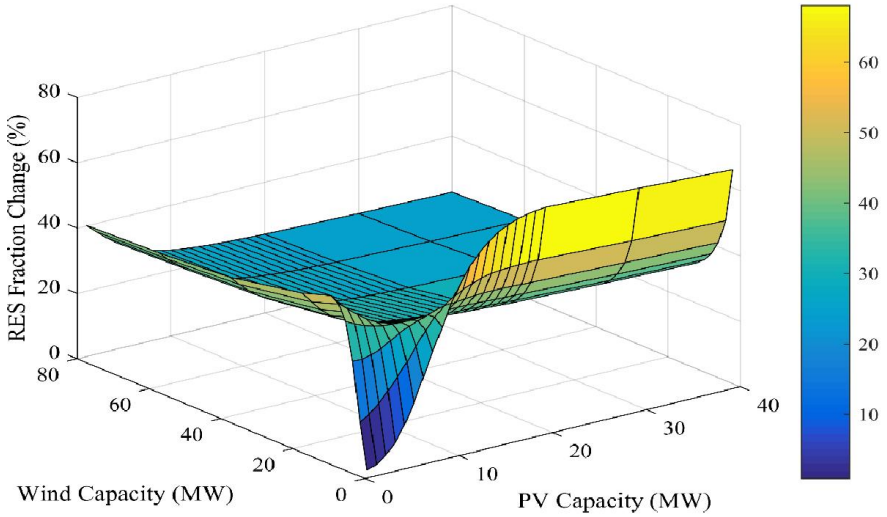

Figure 4.13. The change in the RES fraction of the PV/wind hybrid system as a result of the integration of long term ESS- PHS- with DOD less than 100% in METU NCC where the PHS capacity is a function of the average daily demand, i.e. 89.51 MWh.

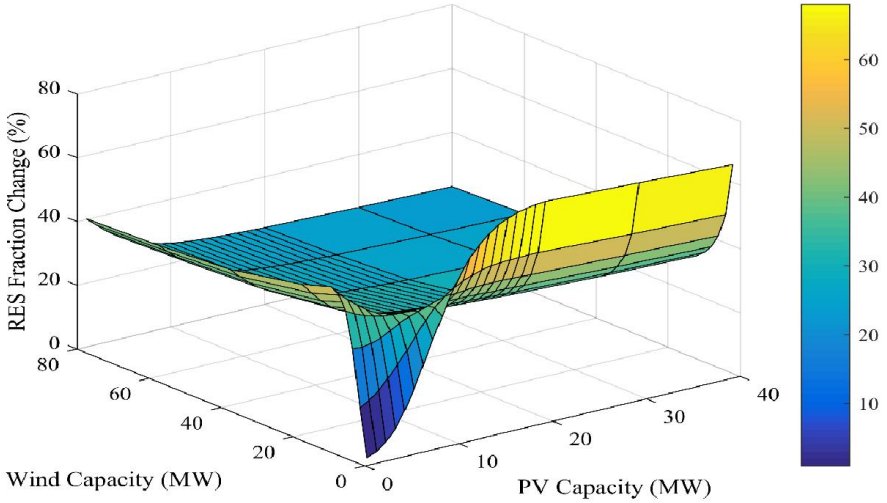

Figure 4.14. The change in the RES fraction of the PV/wind hybrid system as a result of the integration of hybrid ESS- batteries and PHS- with DODs less than 100% in METU NCC using the optimal ESS sizing methodologies.

It can be noticed from Figure 4.12 that the change in the RES fraction varies with the installed capacities where the biggest change in the RES fraction occurs with small PV and wind capacities- 1 MW PV and 10 MW wind. While notice in Figure 4.13 and Figure 4.14 that biggest change occurs with low wind capacity- 2 MW- and PV capacities larger than 10

MW where after these capacities the change in the RES fraction reach the saturation. The reason behind this is that small PV and wind capacities have low RES fraction and the probability of matching more demand is high. Introducing ESSs acts like new energy sources by allocating the excess from these PV and wind systems even though the excess is relatively small. In the case of battery storage system and due to it is small size the benefits from it become smaller as the PV and wind capacities increase while in case of PHS and hybrid ESS and due to their relatively large size it can store more energy and so match more demand. Furthermore, due to the low demand matching- resources availability- characteristic of the PV system compared with wind systems in METU NCC, the highest change occurs with small wind capacities and larger PV capacities where the excess is enough to fill the ESS and the matching is relatively low.

Battery storage system has the smallest effect on the RES fraction where PHS and hybrid ESS have the highest effects. The main reason behind this is the capacity of the ESS where battery storage system is sized based on the average hourly deficit while separate PHS and the PHS in the hybrid ESS are sized based on the average daily demand. PHS and hybrid ESS have almost the same effect since they both have the same sizing methodology with negligible role of the battery in increasing the RES fraction in case of hybrid ESS. In order to compare the effect of the integration of different types and configurations of ESSs on the RES fraction of the PV/wind hybrid system 2 representative wind turbine capacities and several PV capacities were taken as shown in Figure 4.15 and Figure 4.16.

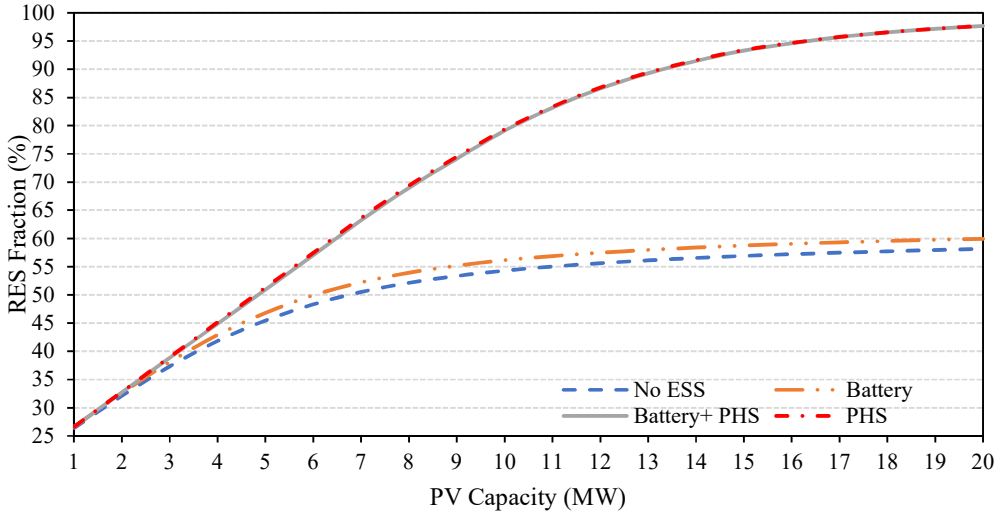

Figure 4.15. The effect of the integration of short and long term ESSs with DOD less than 100% on the RES fraction of the PV/wind hybrid systems - with 1 turbine and several PV capacities- in METU NCC using the optimal ESS sizing methodologies.

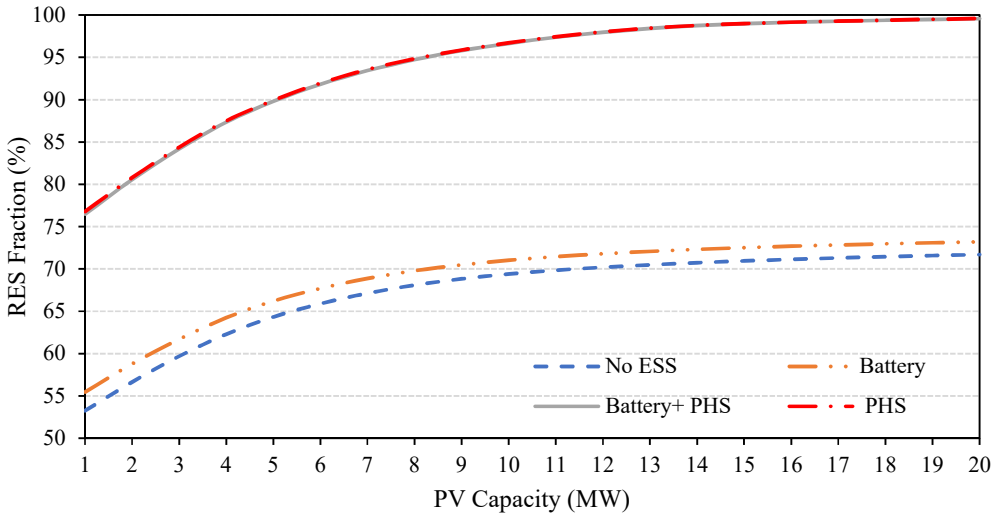

Figure 4.16. The effect of the integration of short and long term ESSs with DOD less than 100% on the RES fraction of the PV/wind hybrid systems - with 4 turbines and several PV capacities- in METU NCC using the optimal ESS sizing methodologies.

Moreover, notice in Figure 4.15 and Figure 4.16 that the integration of PHS and hybrid ESS increases the PV capacity at which the RES fraction reaches the saturation with no significant changes. The main reason for this shift is the ability of the ESSs to store the excess and allocate it to meet the demand where at the PV threshold the ESS is not capable of storing more excess and so the increase in the PV capacity will not increase the matching. Furthermore, notice that 100% RES fraction can be achieved by the integration of PHS and hybrid ESS where without them the system cannot achieve this fraction.

The autonomy of the PV/wind hybrid system is affected by the integration of battery and hybrid ESSs only where the integration of PHS does not affect the autonomy- i.e. the DSF- of the system due to the lag time in the PHS response during the deficit periods. Figure 4.17 shows the change in the DSF of the PV/wind hybrid system in METU NCC because of the integration of battery ESS while Figure 4.18 shows the change in the DSF of the PV/wind hybrid system in METU NCC because of the integration of hybrid ESS.

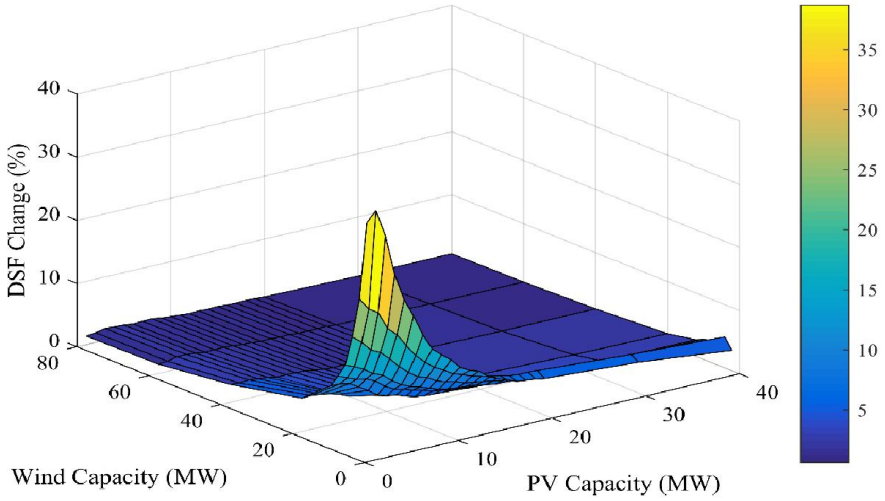

Figure 4.17. The change in the DSF of the PV/wind hybrid system as a result of the integration of short-term ESS- batteries- with DOD less than 100% in METU NCC using the optimal ESS sizing methodology.

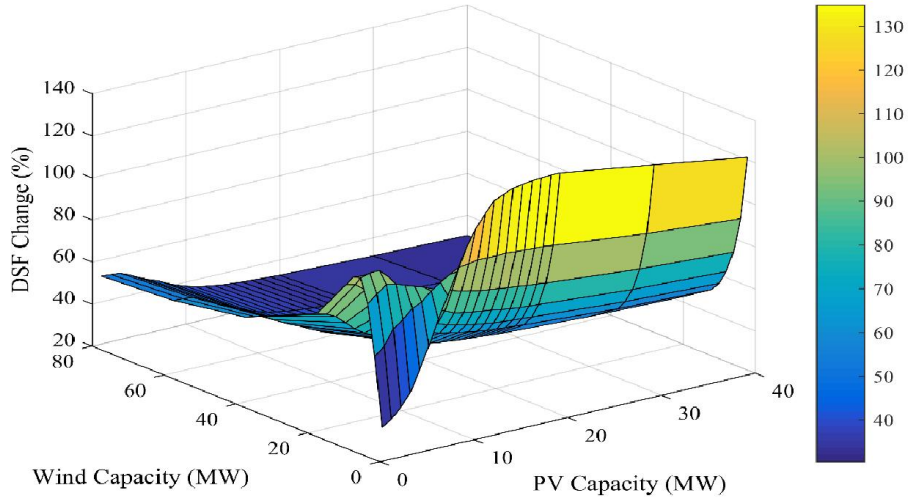

Figure 4.18. The change in the DSF of the PV/wind hybrid system as a result of the integration of hybrid ESS with DODs less than 100% in METU NCC using the optimal ESS sizing methodologies.

Notice that in Figure 4.17 and Figure 4.18 that the pattern of the change in DSF varies based on the ESS type. In the case of battery energy storage system, the largest change in the DSF occurs at the beginning with the lowest installed wind capacity- 2 MW- and PV installed capacity- 1 MW- where after that the effect of the battery start to decrease until it reaches the saturation. The reason behind this in the beginning the system alone achieves low autonomy where the integration of battery increases the number of hours the demand is met totally by the system even though the amount of stored energy is small. However, as the system size increases the system becomes capable of meeting more hours and the benefits of the battery system in increasing the autonomy decrease. Figure 4.19 shows the average hourly electricity generation from 1 MW PV and 2 MW wind capacity and the hourly available energy in 3.64 MWh battery while Figure 4.20 shows the average hourly electricity generation from 15 MW PV and 10 MW wind capacity and the hourly available energy in 1.3 MWh battery. It can be noticed from Figure 4.19 and Figure 4.20 that the number of hours where the demand is met by the system directly increases as the system size increase which reduce the effect of the battery on the autonomy of the system.

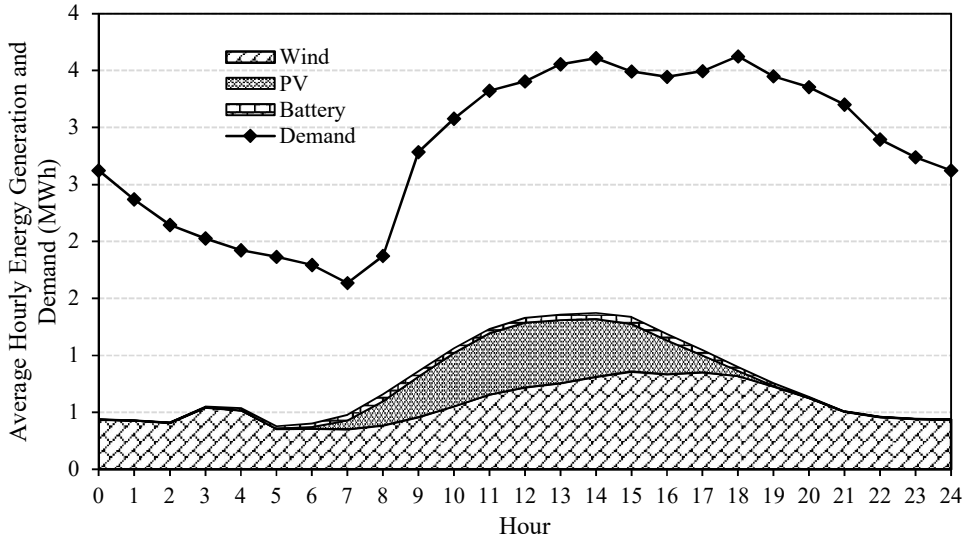

Figure 4.19. The average hourly electricity generation from the hybrid system components, 1 MW PV and 2 MW wind turbine, in addition to the average hourly demand for METU NCC and the hourly available energy in 3.64 MWh battery.

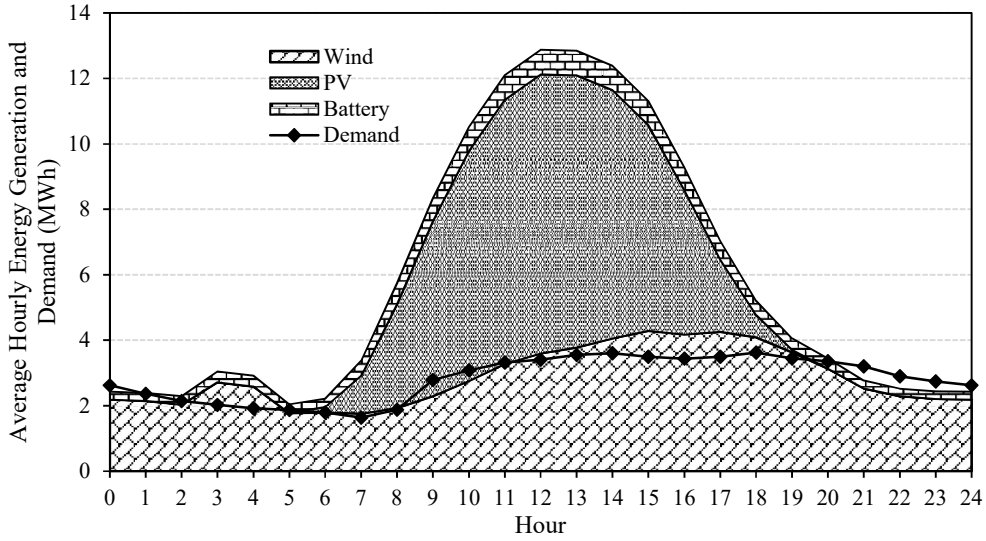

Figure 4.20. The average hourly electricity generation from the hybrid system components, 15 MW PV and 10 MW wind turbines, in addition to the average hourly demand for METU NCC and the hourly available energy in 1.36 MWh battery.

In the case of the hybrid ESS, the highest changes on the DSF occurs with 2 MW wind systems and with PV capacities larger than 10 MW where after 20 MW it start to decrease. Moreover, as the wind capacity increases the effect on the DSF decreases until it reaches the saturation with small change in the DSF at wind capacities more than 20 MW and PV capacities more than 10 MW. The reason behind this is that PV systems have low autonomy due the nature of the solar resources- no energy production during the night- and so having hybrid ESS with large PHS capacity will shift the excess results from the PV system to meet more demand hours. However, after 20 MW PV capacity the hybrid ESS is not capable of storing more energy since it is full which will reduce the effect of the ESS on the DSF. Furthermore, since PV/wind hybrid system with wind capacities larger than 2 MW has high autonomy because wind resources cover in average the whole hours in a day the effect of the ESS decreases as the wind capacity increases. Figure 4.21 shows the average hourly electricity generation from 10 MW PV and 2 MW wind capacity and the hourly available energy in 830.5 kWh battery and 89.5 MWh PHS while Figure 4.22 shows the average hourly electricity generation from 15 MW PV and 10 MW wind turbines and the hourly available energy in 830.5 kWh battery and 89.5 MWh PHS. It can be noticed from Figure 4.21 and Figure 4.22 that the number of hours where the demand is met totally by the system directly increases as the system size increases which reduces the effect of the hybrid ESS on the autonomy of the system. Moreover, it can be noticed that the wind systems in METU NCC have higher

autonomy than the PV systems and so the effect of the hybrid ESS on the PV/wind autonomy is high with low wind capacity.

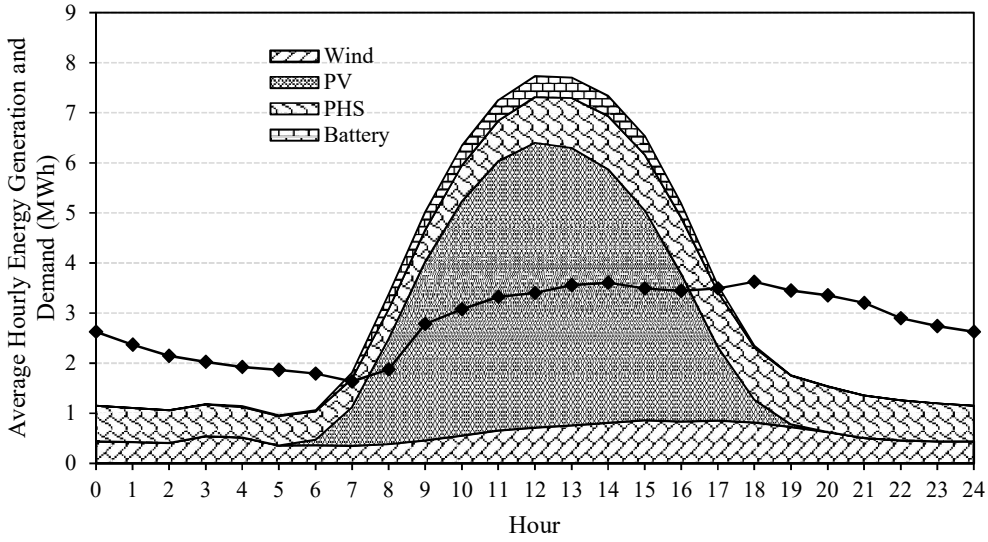

Figure 4.21. The average hourly electricity generation from the hybrid system components, 10 MW PV and 2 MW wind turbine, in addition to the average hourly demand for METU NCC and the hourly available energy in 830.5 kWh battery and 89.5 MWh PHS.

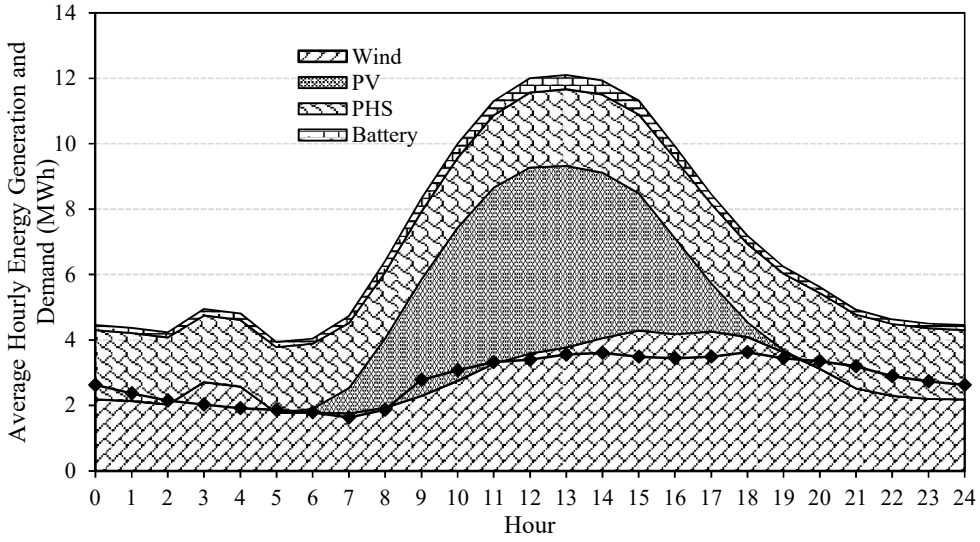

Figure 4.22. The average hourly electricity generation from the hybrid system components, 10 MW PV and 10 MW wind turbines, in addition to the average hourly demand for METU NCC and the hourly available energy in 830.5 kWh battery and 89.5 MWh PHS.

The integration of hybrid ESS with PV/wind hybrid system allows the independency of the power system from the electrical grid and so allows the development of microgrid systems by achieving high autonomy represented by the DSF. While the integration of battery storage

system has small effect on the autonomy of the system and the integration of the PHS alone has no effect due to the PHS lag time in the response where it cannot totally meet the demand in that hour. Figure 4.23 and Figure 4.24 show the effect of the integration of short term and long term ESS on the autonomy of the PV/wind systems with 1 and 4 turbines respectively.

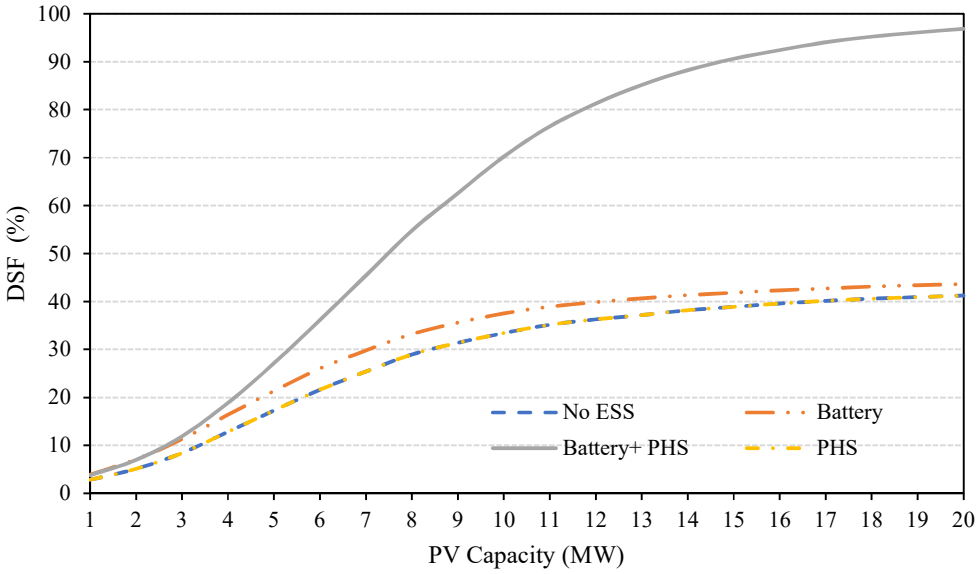

Figure 4.23. The effect of the integration of short and long term ESSs with DODs less than 100% on the DSF of the PV/wind hybrid systems - with 1 turbine and several PV capacities- in METU NCC using the optimal ESS sizing methodologies.

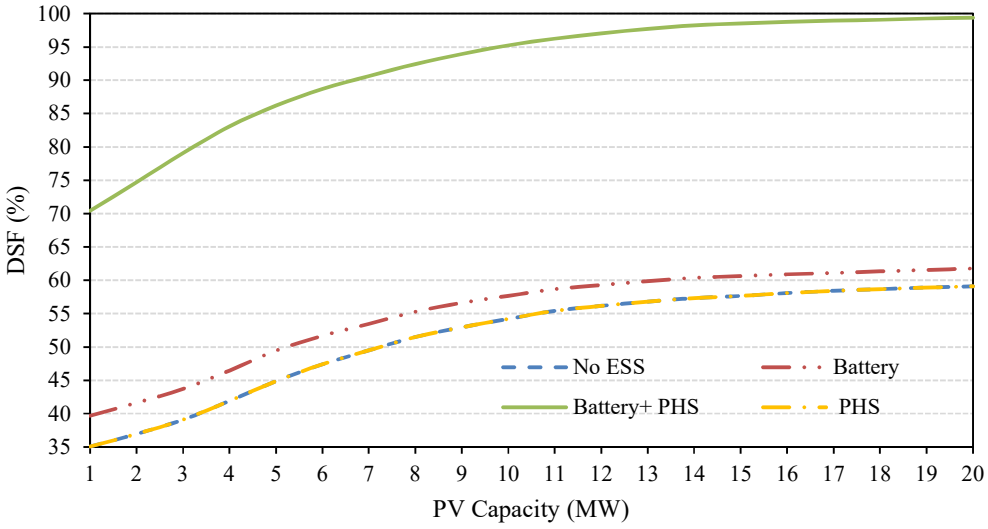

Figure 4.24. The effect of the integration of short and long term ESSs with DODs less than 100% on the DSF of the PV/wind hybrid systems - with 4 turbines and several PV capacities- in METU NCC using the optimal ESS sizing methodologies.

4.3 The Effect of ESS integration on Feasible PV/Wind Hybrid System Sizes

As the integration of ESSs affects the COE of the PV/wind hybrid system, it so affects the economic feasibility of the system and so affects the feasible capacities of the PV/wind hybrid system components where this effect varies depending on the ESS type. Figure 4.25, Figure 4.26, Figure 4.27 and Figure 4.28 show the COE of the PV/wind hybrid system in METU NCC as a function of the number of wind turbines and the PV capacities for four ESS configurations; without ESS, with battery storage system, with PHS and with hybrid ESS respectively. With the assumptions made in the methodology section, it seems that in the absence of any storage system the maximum feasible number of wind turbines in METU NCC is four with maximum PV capacity of 1 MW. On the other hand, the integration of battery storage system with the hybrid system reduces the maximum feasible number of wind turbines to three while it allows the increase in the maximum PV capacity to almost 2.2 MW where the decrease in the wind capacity is to compensate the increase in the total capital cost caused by adding the battery system. The increase in the maximum PV capacity is not because of the integration of battery but because of the decrease in the wind capacity which allows the increase in the PV size to achieve COE equals to the grid tariff. While the integration of PHS and hybrid ESS increases the maximum feasible number of wind turbines to five with maximum PV capacity of 2 MW for PHS alone while for the hybrid ESS and due to the cost of the battery the maximum PV capacity drops to almost 1.4 MW.

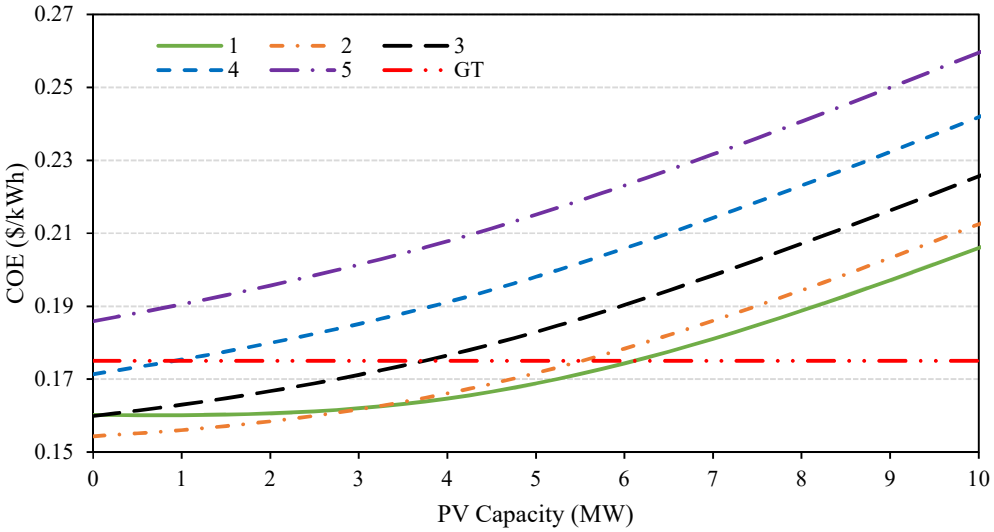

Figure 4.25. The COE of the PV/wind hybrid system as a function of the PV and wind capacities in METU NCC in the absence of any storage system in addition to the local grid tariff.

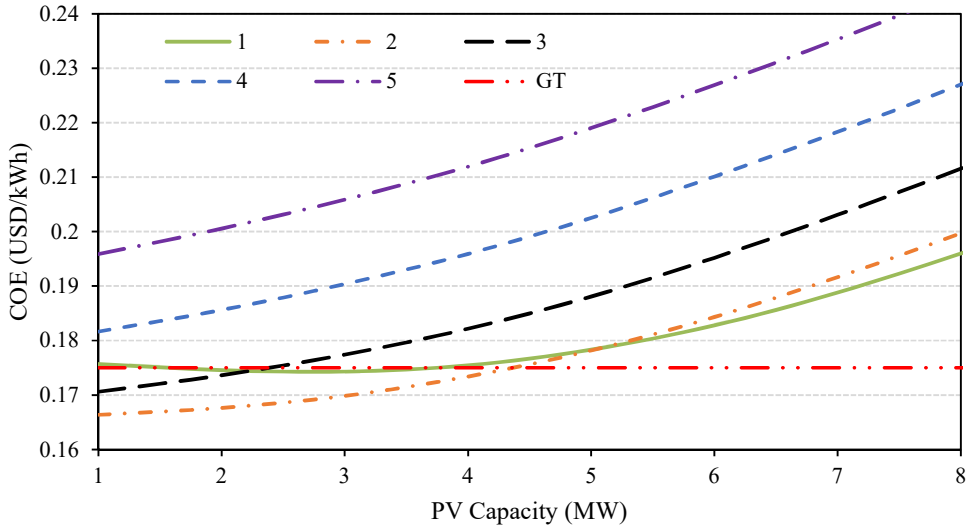

Figure 4.26. The COE of the PV/wind hybrid system as a function of the PV and wind capacities in METU NCC in the presence of Lithium-Ion batteries with DOD less than 100% where the battery capacity is a function of the average hourly deficit in addition to the local grid tariff.

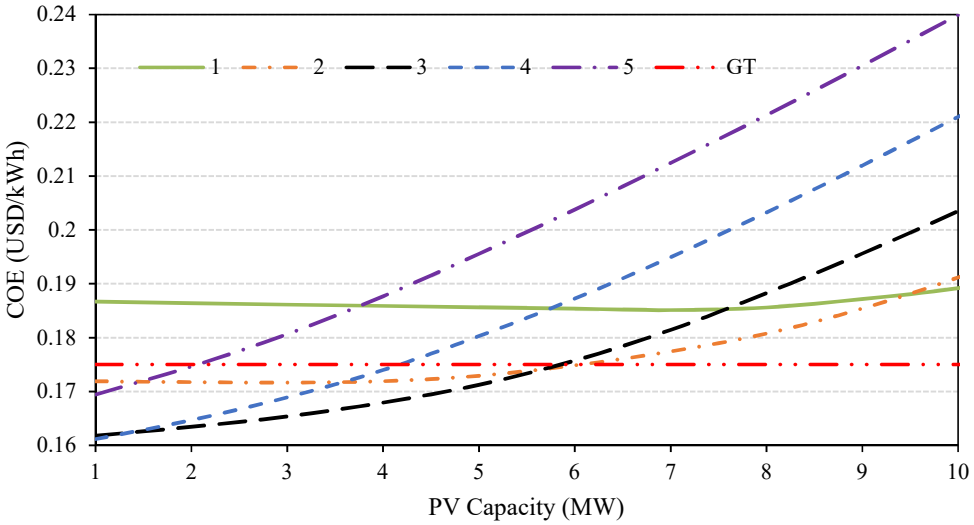

Figure 4.27. The COE of the PV/wind hybrid system as a function of the PV and wind capacities in METU NCC in the presence of PHS with DOD less than 100% where the PHS capacity is a function of the average daily demand- 89.51 MWh- in addition to the local grid tariff.

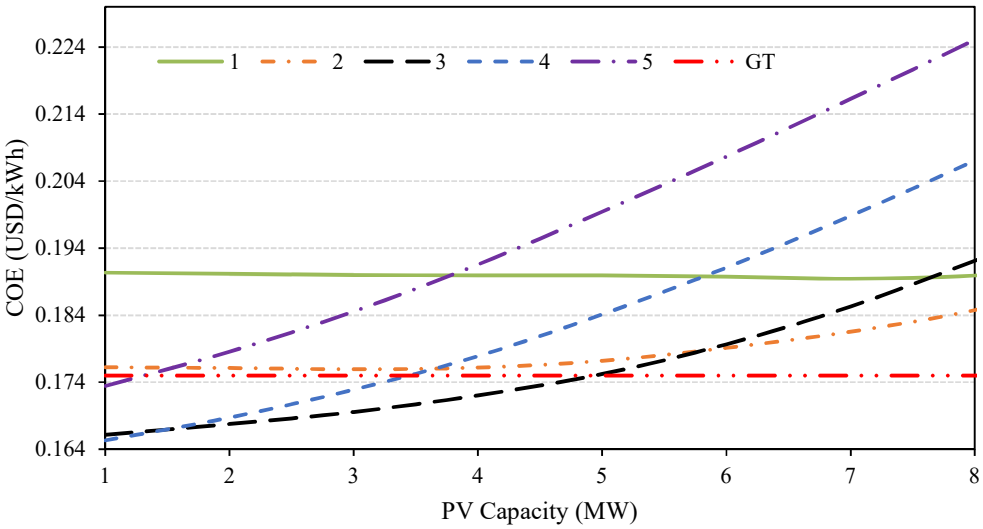

Figure 4.28. The COE of the PV/wind hybrid system as a function of the PV and wind capacities in METU NCC in the presence of PHS/battery hybrid ESS with DODs less than 100% using the optimal ESS sizing methodologies in addition to the local grid tariff.

Notice that in Figure 4.25, Figure 4.26, Figure 4.27 and Figure 4.28 the integration of the battery storage system reduces the feasible PV capacities- with one to three wind turbines- to reduce the capital cost. While the integration of PHS and hybrid ESS makes the installation of one turbine with different PV capacities economically unfeasible in METU NCC, where the

integration caused the increase in the capital cost with small increase in the revenues from storing the excess energy since the excess energy from the hybrid system with one turbine are small. Furthermore, notice that the integration of PHS increases the feasible PV capacities- with two to five wind turbines- since the integration adds more revenues and so allows additional capital cost. While the hybrid ESS caused the unfeasibility of installing two wind turbines where the cost of the battery caused the shift of the COE to up with low revenues from the battery addition. On the other hand, it increases the feasible PV capacities however less than the PHS alone due the cost of the battery.

4.4 Effect of the DOD on the PV/Wind Hybrid System with Hybrid ESS

The DOD of the ESS is a vital parameter that affects the role of the ESS on the economic and technical parameters of the RES. As the DOD increases the amount of stored energy that can be utilized increases and so the benefits of the ESS, while the decrease of the DOD can eliminate the role of the ESS. Figure 4.29 shows the effect of the DOD of 2 MWh battery and 15 MWh PHS hybrid ESS on the RES fraction of PV/wind hybrid system in METU NCC.

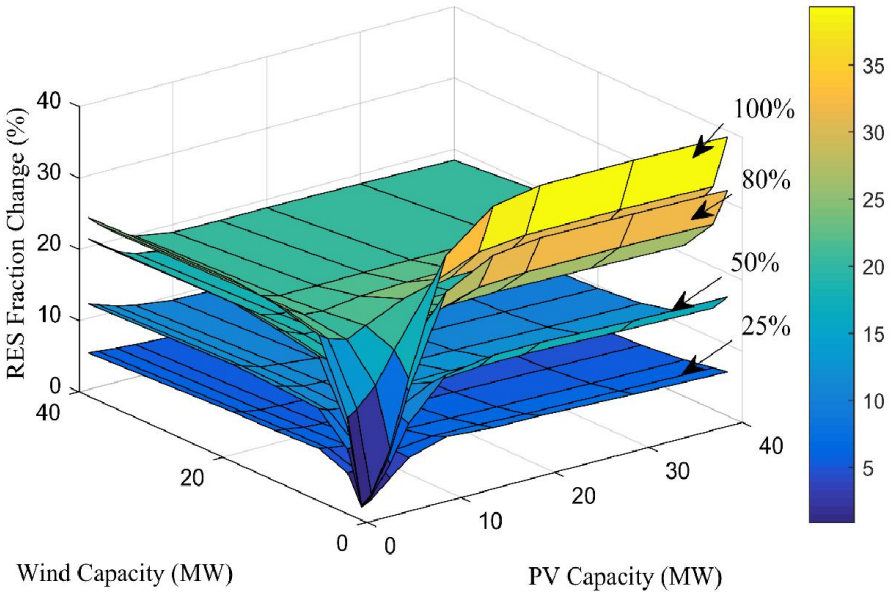

Figure 4.29. The effect of the DOD of the hybrid ESS- 2 MWh battery and 15 MWh PHS- on the RES fraction of the PV/wind hybrid system in METU NCC if both ESSs- battery and PHS- have the same DOD where no ESS scenario is used as the reference case.

It can be noticed from Figure 4.29 that the highest changes in the RES fraction occur with low wind capacity- 2 MW- and PV capacities larger than 10 MW. The nature of the solar resources- available during the daylight only- is the main reason for this where the integration of ESSs help in distributing this energy among the whole day and so increase the matching between the demand and the supply. While the wind resources in METU NCC are distributed among the day and the energy generated from wind systems match the demand more than the solar systems as shown in Figure 4.19, Figure 4.20, Figure 4.21 and Figure 4.22. On the other hand, notice that the ESS with 25% DOD does not affect the RES fraction significantly since the amount of energy that can be utilized is small. Furthermore, it can be noticed from the figure that as the DOD decreases the change in the RES fraction among the PV and wind capacities does not significantly change. As the DOD decreases the space available to store energy decreases- as more energy is trapped and cannot be replaced- and so the required PV and wind capacities needed to fill this space- by their excess production- where increasing the PV and wind capacities will increase only the excess energy.

In addition, the DOD affects the autonomy of the system represented by the DSF where the effect of the DOD on the DSF is larger than its effect of the RES fraction since the DSF depends on the number of hours that the demand met by the hybrid system and any small change in the hourly available energy can significantly change the number of hours. Figure 4.30 shows the effect of the DOD of 2 MWh battery and 15 MWh PHS hybrid ESS on the DSF of PV/wind hybrid system in METU NCC.

As the DOD affects the RES fraction and the autonomy of the system it so affects the economical profits from the ESS integration where this can be noticed by analyzing the effect on the COE of the PV/wind hybrid system. Figure 4.31 shows the change in the COE of the PV/wind hybrid system with 2 MWh battery and 15 MWh PHS hybrid ESS as the DOD changes in METU NCC. It can be noticed from the figure that as the DOD of the ESS decreases the change in the COE increases- it increases the COE of the system compared with the no ESS scenario- where the dependency on the electricity from the grid increases due to the decrease in the amount of energy that can be utlized from the ESS. Figure 4.32 shows the yearly demand met by the PV/wind system components directly - 10 MW PV and 10 MW wind systems- and the yearly demand met by the energy stored in 2 MWh battery and 15 MWh PHS in addition to the yearly demand met by the grid, the yearly excess energy and the yearly energy lost in the PHS and the battery due to their efficiencies for four random ESS DODs where both battery and PHS assumed to have the same DOD in each case.

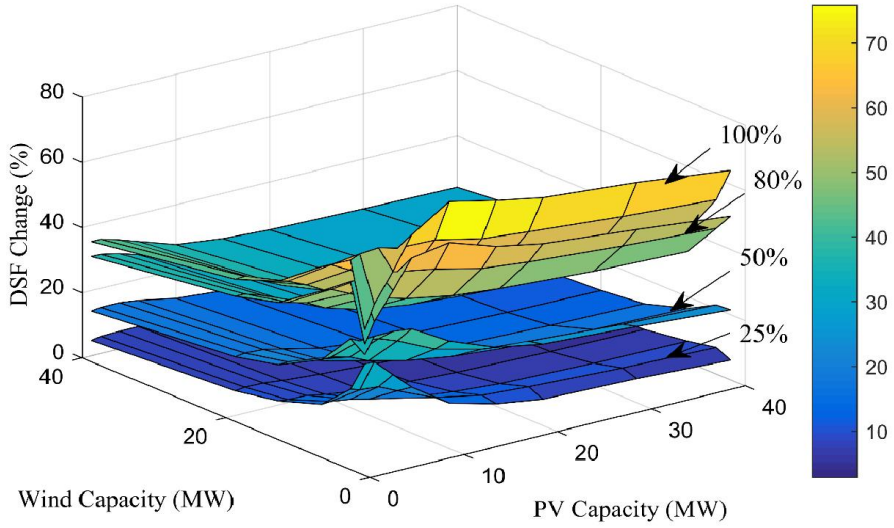

Figure 4.30. The effect of the DOD of the hybrid ESS- 2 MWh battery and 15 MWh PHS- on the DSF of the PV/wind hybrid system in METU NCC if both ESSs- battery and PHS- have the same DOD where no ESS scenario is used as the reference case.

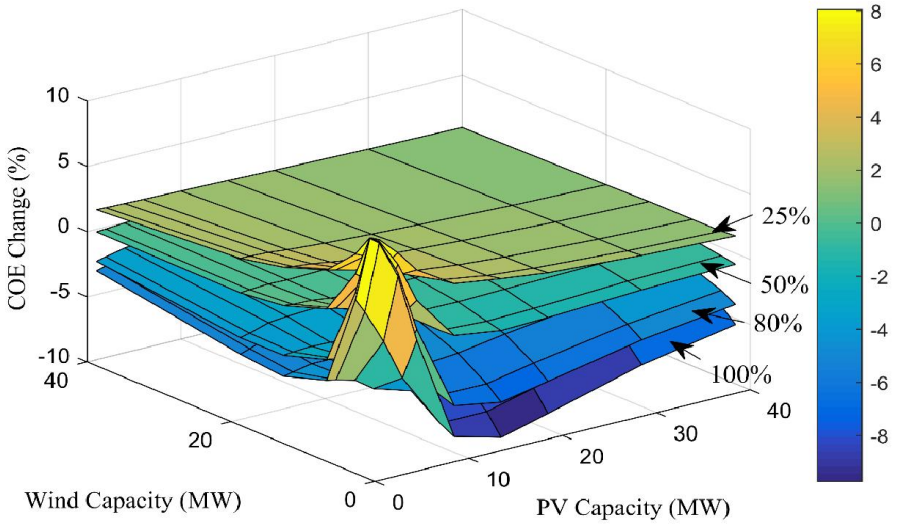

Figure 4.31. The Effect of the DOD of the hybrid ESS- 2 MWh battery and 15 MWh PHS- on the COE of the PV/wind hybrid system in METU NCC if both ESSs- battery and PHS- have the same DOD and no ESS scenario is used as the reference case.

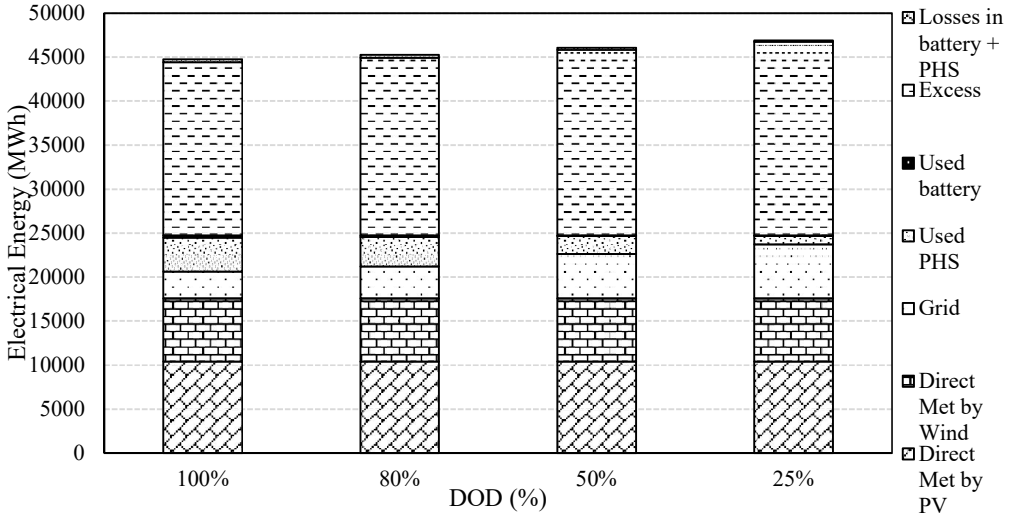

Figure 4.32. The yearly demand met by the PV/wind system components directly - 10 MW PV and 10 MW wind systems- and the yearly demand met by the energy stored in 2 MWh battery and 15 MWh PHS in addition to the yearly demand met by the grid, the yearly excess energy and the yearly energy lost in the PHS and the battery for four random ESS DODs where both battery and PHS assumed to have the same DOD in each case.

It can be noticed from Figure 4.32 that the losses in the battery storage system and the PHS are small where the largest losses belong to the PHS since PHS has lower efficiency (85%) than the Lithium-Ion battery (95%). Moreover, the PHS has bigger capacity than the battery and so the amount of losses is bigger. Furthermore, notice that the amount of excess energy increases as the DOD decreases since the available space for storing the energy- which equals to the amount of energy that can be utilized- is decreased.

4.5 Summary of the Results

The integration of ESS affects the optimal RES sizes- the optimization is based on maximizing the RES fraction with LCOE equals or less than the grid tariff- where the capital cost of the ESS, the RES's performance and capital cost play the major role in this effect while the DOD of the ESS plays a minor role. Table 4.5 and Table 4.6 show the optimal sizes of PV, wind and PV/wind hybrid systems with different ESS configurations in case of 100% and less than 100% DODs respectively in METU NCC based on maximizing the RES fraction with COE less or equal to the grid tariff.

Table 4.5 The optimal sizes of PV, wind and PV/wind hybrid systems with different ESS configurations in METU NCC based on maximizing the RES fraction with COE less or equal to the grid tariff, where the DOD of the ESSs is 100%.

RES Scenario	ESS Scenario	PV Cap. (MW)	Wind Cap. (MW)	Battery Cap. (kWh)	PHS Cap. (MW)	F_{RES} (%)	DSF (%)
PV	No ESS	4.26	--	--	--	25.6	4.79
	Battery	4.2	--	21.84	--	25.32	4.54
	PHS	4.39	--	--	0.761	26.6	6.67
	Hybrid	Not Feasible	--	--	--	--	--
Wind	No ESS	--	8	--	--	49.51	33.34
	Battery	--	8	1500	--	51.82	37.89
	PHS	--	10	--	149.1	87.05	38.5
	Hybrid	--	10	503	149.1	87.07	85.56
Hybrid	No ESS	3.73	6	--	--	58.03	34.46
	Battery	3.53	6	768	--	58.73	37.31
	PHS	1.8	10	--	116.25	90.13	41.48
	Hybrid	1.38	10	500	118.78	89.31	87.18

Table 4.6 The optimal sizes of PV, wind and PV/wind hybrid systems with different ESS configurations in METU NCC based on maximizing the RES fraction with COE less or equal to the grid tariff, where the DOD of the ESSs is less than 100%.

RES Scenario	ESS Scenario	PV Cap. (MW)	Wind Cap. (MW)	Battery Cap. (kWh)	PHS Cap. (MW)	F_{RES} (%)	DSF (%)
PV	No ESS	4.26	--	--	--	25.6	4.79
	Battery	4.17	--	34.66	--	25.14	4.54
	PHS	4.37	--	--	0.827	26.46	6.5
	Hybrid	Not Feasible	--	--	--	--	--
Wind	No ESS	--	8	--	--	49.51	33.34
	Battery	--	6	2760	--	46.32	30.95
	PHS	--	10	--	142.9	85.57	38.5
	Hybrid	--	10	871	89.51	80.28	76.71
Hybrid	No ESS	3.73	6	--	--	58.03	34.46
	Battery	3.12	6	1220	--	57.42	36
	PHS	4.19	8	--	89.51	88.04	42.58
	Hybrid	3.44	8	833	89.51	85.63	80.74

The integration of ESS affects the technical and economic parameters of the system, where the inspection of these effects was based on the change in the DSF, RES fraction and COE of different RES with different ESS configurations which were sized using the optimal sizing methodologies. The effects of the integration of ESSs depends on the RES type, RES capacity and ESS type. For instance, the integration of battery with PV system caused the increase in the COE with PV capacities more than 4 MW where with less than 4 MW the battery did not affect the COE. While the integration of battery with wind system and PV/wind hybrid system increased the COE for all wind capacities. On the other hand, the integration of battery storage system with PV/wind hybrid system in METU NCC increased the COE whatever is the size of the PV/wind hybrid system. However, this increase varies with the installed capacities of the system components to certain thresholds- 10 MW PV and 20 MW wind- where after these thresholds there are no significant changes on the COE.

On the other hand, the integration of PHS with PV systems decreased the COE with capacities larger than 4 MW where below this capacity there was no change in the COE. While the integration of hybrid ESS was not feasible for all the PV capacities due to the cost of the

batteries with less revenues gained from the batteries. On the other hand, the integration of PHS and hybrid ESS with wind systems increased the COE with capacities less than 7 MW for the hybrid and 8 MW for the PHS alone where with capacities larger than these it causes significant drop in the COE. While the integration of PHS and hybrid ESS increases the COE of the system with PV capacities less than 10 MW and wind capacities less than 20 MW due to the small excess energy from such PV/wind system sizes and so small revenues. Where after that and depending on the installed PV and wind capacities the effect on the COE varies between the decrease in the COE to no change.

Furthermore, the integration of all types of ESSs with PV and wind systems increases the RES fraction however with PV capacity larger than 6 MW while with wind capacity larger than 4 MW where the excess energy from the PV and wind systems below these capacities are small. On the other hand, the integration of short and long term ESSs for all the ESS configurations has the same effect on the RES fraction of the PV/wind hybrid system where it increases the RES fraction and the amount of the increase changes until a certain limit- 10 MW PV and 20 MW wind- depending on the type of the ESS. After this limit, the change in the RES fraction reaches the saturation where the ESS are not capable of storing the excess energy and so any increase in the installed capacities of the PV/wind hybrid system components leads to the increase in the excess energy only.

Moreover, the integration of all ESS types increase the DSF with PV capacities larger than 4 MW except for PHS where due to the lag time pf the PHS respond it cannot increase the DSF. While it increases the DSF with wind capacities larger than 2 MW. On the other hand, the integration of ESS with PV/wind hybrid system has different effects on the DSF where the pattern of the change in DSF varies based on the ESS type. In the case of battery energy storage system, the largest change on the DSF occurs in the beginning with the lowest installed wind capacity- 2 MW- and PV installed capacity- 1 MW- where after that the effect of the battery start to decrease until it reaches the saturation. While in the case of the hybrid ESS the highest changes in the DSF occurs with 2 MW wind systems and with PV capacities larger than 10 MW where after 20 MW PV it start to decrease. Moreover, as the wind capacity increases the effect on the DSF decreases until it reaches the saturation.

As the integration of ESSs affects the COE of the PV/wind hybrid system, it so affects the economic feasibility of the system and so affects the feasible capacities of the PV/wind hybrid system components where this effect varies depending on the ESS type. In the absence of any storage system the maximum feasible number of wind turbines in METU NCC is four with

maximum PV capacity of 1 MW. On the other hand, the integration of battery storage system with the hybrid system reduces the maximum feasible number of wind turbines to three while it allows the increase in the maximum PV capacity to almost 2.2 MW, the increase in the maximum PV capacity is not because of the integration of battery but because of the decrease in the wind capacity which allows the increase in the PV size to achieve COE equals to the grid tariff. While the integration of PHS and hybrid ESS increases the maximum feasible number of wind turbines to five with maximum PV capacity of 2 MW for PHS alone while for the hybrid ESS and due to the cost of the battery the maximum PV capacity drops to almost 1.4 MW.

4.6 Sensitivity Analysis for the Optimal PV/Wind Hybrid Systems with Hybrid ESS

The change in the solar and wind resources in addition to the change in the ambient conditions affects the technical and economic parameters of the RES. The sensitivity of PV/wind hybrid system with different ESS configurations to the change in the solar and wind resources in addition to the change in the ambient temperature is investigated using the measured resources in METU NCC between 2013 and 2016 and compared with the results obtained using the TMY data where the assessment of the system's sensitivity is based on the amount of change in the technical and economic parameters of the system. The change in the wind speeds varies between 24.77% and 30.15% while the change in the GHI varies between -27.22% and 4.73% and the change in the DNI varies between -0.33% and 8.65% compared to the TMY data. Table 4.7 shows the changes in the RES fraction, DSF and COE of the PV/wind hybrid system in METU NCC with different ESS configurations and scenarios because of the change in the solar and wind resources as well as the change in the ambient conditions.

It can be noticed from Table 4.7 that the PV/wind system with different ESS configuration is sensitive to the change in the solar and wind resources as well as the ambient conditions where the change in the F_{RES} varies between 7.39% and 17.14 where the system with PHS has the lowest sensitivity to the variation in the resources where the reason behind this is that the system with PHS has the highest F_{RES} among the other configurations; where the increase in the wind resources between 2013 and 2016 is dominant on the decrease in the solar resources and as the F_{RES} increases it becomes more difficult to increase it due to the mismatch between the supply and the demand. While the change in the DSF varies between 10.84% and 25.69% where the system with hybrid ESS has the lowest sensitivity since it has the highest DSF

among the other options and as the DSF increases it becomes more difficult to increase it. On the other hand, the change in the COE varies between -5.49% and -11.09% where the system without ESS has the lowest sensitivity since it has the lowest COE among the other options and as the COE decreases it becomes more difficult to decrease it.

Table 4.7. The sensitivety of the F_{RES}, DSF and COE of the optimal PV/wind hybrid systems with different ESS configurations to the solar and wind resources in additional to the ambient temperature in METU NCC.

Data	ESS Scenario	F_{RES} (%)	F_{RES} Change (%)	DSF (%)	DSF Change (%)	COE ($/kWh)	COE Change (%)
TMY	No ESS	58.03	-	34.46	-	0.175	-
	Battery	57.42	-	36	-	0.175	-
	PHS	88.04	-	42.58	-	0.175	-
	Hybrid	85.63	-	80.74	-	0.175	-
2013	No ESS	66.38	14.39	43.21	25.39	0.1604	-8.34
	Battery	66.93	16.56	45.25	25.69	0.1584	-9.49
	PHS	97.71	10.98	51.72	21.47	0.1581	-9.66
	Hybrid	96.71	12.94	94.71	17.30	0.1556	-11.09
2014	No ESS	63.5	9.43	41.2	19.56	0.1654	-5.49
	Battery	64.01	11.48	42.69	18.58	0.1635	-6.57
	PHS	94.55	7.39	48.13	13.03	0.1636	-6.51
	Hybrid	93.17	8.81	89.49	10.84	0.1618	-7.54
2015	No ESS	63.77	9.89	41	18.98	0.165	-5.71
	Battery	64.19	11.79	42.52	18.11	0.1632	-6.74
	PHS	95.27	8.21	48.13	13.03	0.1623	-7.26
	Hybrid	93.94	9.70	90.82	12.48	0.1605	-8.29
2016	No ESS	67.05	15.54	41.47	20.34	0.1592	-9.03
	Battery	67.26	17.14	43.03	19.53	0.1578	-9.83
	PHS	95.95	8.98	49.93	17.26	0.1591	-9.1
	Hybrid	94.82	10.73	91.97	13.91	0.1589	-9.20

Furthermore, the resources and the ambient conditions are not the only variables that affect the technical and economic parameters of the system, where the variation in the demand affects these parameters and in order to inspect the sensitivity of the PV/wind hybrid system with different ESS configurations to the demand variation, the actual demand of 2011, 2014 and 2015 in addition to the forecasted demand in 2037- i.e. the maximum demand throughout

the system's lifetime- are used. The change in the demand varies between -87% and 53.6% compared with the average demand throughout the life of the systems- the demand of 2027. Table 4.8 shows the sensitivity of the F_{RES}, DSF and COE of the optimal PV/wind hybrid systems with different ESS configurations to the variation in the demand in METU NCC.

Table 4.8. The sensitivity of the F_{RES}, DSF and COE of the optimal PV/wind hybrid systems with different ESS configurations to the change in the demand in METU NCC.

Data	ESS Scenario	F_{RES} (%)	F_{RES} Change (%)	DSF (%)	DSF Change (%)	COE ($/kWh)	COE Change (%)
2027	No ESS	58.03	--	34.46	--	0.175	--
	Battery	57.42	--	36	--	0.175	--
	PHS	88.04	--	42.58	--	0.175	--
	Hybrid	85.63	--	80.74	--	0.175	--
2011	No ESS	80.06	37.96	74.11	115.06	0.819	368
	Battery	85.03	48.08	80.15	122.64	0.787	349.71
	PHS	99.94	13.52	99.92	134.66	1.189	579.43
	Hybrid	99.95	16.72	99.92	23.76	1.157	561.14
2014	No ESS	74.89	29.05	64.62	87.52	0.346	97.71
	Battery	76.58	33.37	66.51	84.75	0.334	90.86
	PHS	99.93	13.51	99.89	134.59	0.458	161.71
	Hybrid	99.89	16.65	99.77	23.57	0.445	154.29
2015	No ESS	74.79	28.88	64.84	88.16	0.348	98.86
	Battery	76.67	33.52	66.96	86	0.336	92
	PHS	99.93	13.51	99.9	134.62	0.462	164
	Hybrid	99.92	16.69	99.86	23.68	0.449	156.57
2037	No ESS	46.63	-19.65	20.26	-41.21	0.1595	-8.86
	Battery	45.32	-21.07	20.29	-43.64	0.1598	-8.69
	PHS	66.56	-24.40	53.45	25.53	0.159	-9.14
	Hybrid	63.76	-25.54	49.3	-38.94	0.161	-8

It can be noticed in Table 4.8 that the system with PHS has the lowest sensitivity in terms of the change in the F_{RES} as a result of the decrease in the demand- as for 2013,2014 and 2015 demands- where the variation varies between 13.51% and 48.08% and the main reason for being PHS configuration the lowest vulnerable is because it has the highest F_{RES} among the other options where decreasing the demand causes the increase RES fraction as the RES resources remain the same. While the system with battery storage system has the lowest

sensitivity to the change in the COE since it has the lowest COE and the lowest RES capacities among the other options where the change in the COE varies between 90.86% and 579.43%. On the other hand, in the case of the increase in the demand- 2037 demand- the system without ESS has the lowest sensitivity to the change in the F_{RES} while the system with hybrid ESS has the lowest sensitivity to the change in the COE. The change in the F_{RES} in the case of the increase in the demand is between -19.65% and -25.54% while the change in the COE is between -8% and -9.14%. Moreover, the system without ESS has the lowest sensitivity to the change in the demand- decreasing or increasing- where the change in the DSF is between -43.64% and 134.66%.

Chapter 5

Conclusions and Future Work

5.1 Conclusions

Several studies in the literature stated that the integration of ESS affects the RES; however, none of these studies analyzed these effects. Moreover, none of these studies considered the DOD of the ESS as one of the factors that affects the role of the ESS integration. The aim of this study is to analyze the effects of the integration of short-term and long-term energy storage systems with PV, wind and hybrid PV/wind systems where the case study was METU NCC. The inspection of these effects was based on the change in the DSF, RES fraction and COE of different RES with different ESS configurations Furthermore, this study aims to determine the optimal PV, wind and PV/wind hybrid system sizes with and without ESSs based on maximizing the RES fraction with cost of electricity equals or less than the local grid tariff with two DOD scenarios. The sizing of RES system with ESS forms a challenging and sophisticated issue where the number of variable of the RES varies between two- in case of separate RES and separate ESS- up to four variables in case of hybrid RES and hybrid ESS where in order to simplify the analysis and the optimization, the capacity of the ESS is sized as a function of either the demand, the excess or the deficit.

According to the results obtained in this study, the following can be said;

- The capital cost of the ESS, the RES's performance and capital cost play the major role in determining the effect of the integration of ESS either it is positive by enhancing the technical parameters and increasing the economic benefits or negative effects by decreasing the feasible RES sizes.
- The DOD of the ESS is a vital parameter that affects the role of the ESS on the economic and technical parameters of the RES. As the DOD increases the amount of stored energy that can be utilized increases and so the benefits of the ESS, while the decrease of the DOD can eliminate the role of the ESS. Moreover, the DOD effects on the autonomy of the system represented by the DSF is larger than its effects on the RES fraction since the DSF depends on the number of hours that the demand met by

the hybrid system and any small change in the hourly available energy can significantly change the number of hours.

Moreover, with the assumptions made in the methodologies used in this study the results obtained indicate that;

- The hybrid system- 1.8 MW PV and 10 MW wind systems- with 116.25 MWh PHS has the highest RES fraction- 90.13%- with DSF of 41.48 while the hybrid system- 1.38 MW PV and 10 MW wind- with 0.5 MWh battery and 118.78 MWh PHS has the highest DSF (87.18%) with RES fraction of 89.31% if the sizing of the ESS was based on 100% DOD.
- The hybrid system of 4.19 MW PV and 8 MW wind systems with 89.51 MWh PHS has the highest RES fraction (88.04%) with DSF of 42.58 while the hybrid system of 3.44 MW PV and 8 MW wind with 0.833 MWh battery and 89.51 MWh PHS has the highest DSF (80.74%) with RES fraction of 85.63% if the sizing of the ESS was based on DOD values specified in the literature, i.e., less than 100% DOD.
- The PV/wind hybrid system is sensitive to the variation in the solar and wind resources where the system with PHS was the least sensitive configuration in terms of the change in the RES fraction while the system with hybrid ESS was the least sensitive in terms of the change in the DSF. On the other hand, the system without ESS has the lowest sensitivity in terms of the change in the COE.
- Similar to the change in the resources, the hybrid system is also sensitive to the change in the demand where the decrease in the demand shows that the system with PHS has the lowest sensitivity in terms of the change in the RES fraction. While in terms of DSF the system without ESS has the lowest sensitivity. On the other hand the system with battery has the lowest sensitivity in terms of the change in the COE. While in case of increasing the demand the system without ESS has the lowest sensitivity in terms of the change in the RES fraction while the system with hybird ESS has the lowest sensitivity in terms of the change in the COE. Moreover, the system with battery has the lowest sensitivity to the change in the DSF similar to the case as in the increase in the demand.

5.2 Future Work

The effect of integration of different types of battery storage system on the technical and economic parameters of PV, wind and PV/wind hybrid systems should be inspected in detail where the effect of the lifespan and the capital cost in addition to the DOD of the battery should be taken into consideration. Furthermore, the relation between the DOD and the lifespan of the ESS should be taken into account in order to determine the effect of the integration of ESSs on the economic parameters of the RES. In addition, the effect of having several bank batteries with an ordered sequence of fully discharging in order to maximize the benefits of the battery should be developed and inspected for it is effectiveness. Moreover, the hybridization of another RES- like biomass systems that can provide baseload- with PV/wind hybrid system and the effect of this hybridization on the effect of the integration of ESSs should be studied. Moreover, an probabilistic approach can be developed to estimate the optimal RES sizes instead of parametric one.

REFERENCES

[1] G. Bölük and M. Mert, "Fossil & renewable energy consumption, GHGs (greenhouse gases) and economic growth: Evidence from a panel of EU (European Union) countries," *Energy*, vol. 74, no. C, pp. 439–446, 2014.

[2] "INDUSTRIAL REVOLUTION." [Online]. Available: http://history-world.org/Industrial Intro.htm. [Accessed: 07-Jan-2017].

[3] "Kyoto Protocol." [Online]. Available: http://unfccc.int/kyoto_protocol/items/2830.php.

[4] M. Carbajales-Dale, C. J. Barnhart, and S. M. Benson, "Can we afford storage ? A dynamic net energy analysis of renewable electricity generation supported by energy storage," *Energy Environ. Sci.*, vol. 7, no. 5, pp. 1538–1544, 2014.

[5] C. Harris, J. P. Meyers, and M. E. Webber, "A unit commitment study of the application of energy storage toward the integration of renewable generation," *J. Renew. Sustain. Energy*, vol. 4, no. 1, 2012.

[6] P. Denholm and R. M. Margolis, "Evaluating the limits of solar photovoltaics (PV) in electric power systems utilizing energy storage and other enabling technologies," *Energy Policy*, vol. 35, no. 9, pp. 4424–4433, 2007.

[7] S. M. S. Sadati, "Assessment of Renewable Energy Based Micro-Grids For Small Communities," Middle East Techincal University Northern Cyprus Campus, 2016.

[8] J. L. Sawin, K. Seyboth, and F. Sverrisson, *Renewables 2016: Global Status Report*. 2016.

[9] B. Bhandari, K. T. Lee, C. S. Lee, C. K. Song, R. K. Maskey, and S. H. Ahn, "A novel off-grid hybrid power system comprised of solar photovoltaic, wind, and hydro energy sources," *Appl. Energy*, vol. 133, pp. 236–242, 2014.

[10] M. K. Deshmukh and S. S. Deshmukh, "Modeling of hybrid renewable energy systems," *Renew. Sustain. Energy Rev.*, vol. 12, no. 1, pp. 235–249, 2008.

[11] K. C. Divya and J. Østergaard, "Battery energy storage technology for power systems-An overview," *Electr. Power Syst. Res.*, vol. 79, no. 4, pp. 511–520, 2009.

[12] T. Ma, H. Yang, L. Lu, and J. Peng, "Technical feasibility study on a standalone hybrid

solar-wind system with pumped hydro storage for a remote island in Hong Kong," *Renew. Energy*, vol. 69, pp. 7–15, 2014.

[13] J. L. Bernal-Agustín and R. Dufo-López, "Simulation and optimization of stand-alone hybrid renewable energy systems," *Renew. Sustain. Energy Rev.*, vol. 13, no. 8, pp. 2111–2118, 2009.

[14] B. Dunn, H. Kamath, and J.-M. Tarascon, "Electrical Energy Storage for the Grid: A Battery of Choices," *Science (80-.).*, vol. 334, no. 6058, pp. 928–935, 2011.

[15] J. K. Kaldellis, D. Zafirakis, and E. Kondili, "Optimum sizing of photovoltaic-energy storage systems for autonomous small islands," *Int. J. Electr. Power Energy Syst.*, vol. 32, no. 1, pp. 24–36, 2010.

[16] P. Denholm and G. L. Kulcinski, "Life cycle energy requirements and greenhouse gas emissions from large scale energy storage systems," *Energy Convers. Manag.*, vol. 45, no. 13–14, pp. 2153–2172, 2004.

[17] M. H. Nehrir *et al.*, "A Review of Hybrid Renewable / Alternative Energy Systems for Electric Power Generation :," *IEEE Trans. Sustain. Energy*, vol. 2, no. 4, pp. 392–403, 2011.

[18] B. Ould Bilal, V. Sambou, P. A. Ndiaye, C. M. F. Kébé, and M. Ndongo, "Optimal design of a hybrid solar-wind-battery system using the minimization of the annualized cost system and the minimization of the loss of power supply probability (LPSP)," *Renew. Energy*, vol. 35, no. 10, pp. 2388–2390, 2010.

[19] L. Xu, X. Ruan, C. Mao, B. Zhang, and Y. Luo, "An improved optimal sizing method for wind-solar-battery hybrid power system," *IEEE Trans. Sustain. Energy*, vol. 4, no. 3, pp. 774–785, 2013.

[20] C. Silva, "Renewable microgrids Reduced LCOE and secured supply Renewable microgrids Agenda," 2016.

[21] S. Ashok, "Optimised model for community-based hybrid energy system," *Renew. Energy*, vol. 32, no. 7, pp. 1155–1164, 2007.

[22] Fraunhofer Institute for Solar systems, "Photovoltaics Report," Freiburg, 2016.

[23] C.-H. Li, X.-J. Zhu, G.-Y. Cao, S. Sui, and M.-R. Hu, "Dynamic modeling and sizing optimization of stand-alone photovoltaic power systems using hybrid energy storage technology," *Renew. Energy*, vol. 34, no. 3, pp. 815–826, 2009.

[24] J. K. Kaldellis, D. Zafirakis, E. L. Kaldelli, and K. Kavadias, “Cost benefit analysis of a photovoltaic-energy storage electrification solution for remote islands,” *Renew. Energy*, vol. 34, no. 5, pp. 1299–1311, 2009.

[25] D. Manolakos, G. Papadakis, D. Papantonis, and S. Kyritsis, “A stand-alone photovoltaic power system for remote villages using pumped water energy storage,” *Energy*, vol. 29, no. 1, pp. 57–69, 2004.

[26] A. Fragaki and T. Markvart, “Stand-alone PV system design: Results using a new sizing approach,” *Renew. Energy*, vol. 33, no. 1, pp. 162–167, 2008.

[27] A. Cherif, M. Jraidi, and A. Dhouib, “A battery ageing model used in stand alone PV systems,” *J. Power Sources*, vol. 112, no. 1, pp. 49–53, 2002.

[28] T. Khatib, A. Mohamed, K. Sopian, and M. Mahmoud, “A new approach for optimal sizing of standalone photovoltaic systems,” *Int. J. Photoenergy*, vol. 2012, 2012.

[29] “GLOBAL STATISTICS | GWEC.” [Online]. Available: http://www.gwec.net/global-figures/graphs/. [Accessed: 30-Jan-2017].

[30] E. D. Castronuovo and J. A. P. Lopes, “Optimal operation and hydro storage sizing of a wind-hydro power plant,” *Int. J. Electr. Power Energy Syst.*, vol. 26, no. 10, pp. 771–778, 2004.

[31] S. V. Papaefthymiou and S. A. Papathanassiou, “Optimum sizing of wind-pumped-storage hybrid power stations in island systems,” *Renew. Energy*, vol. 64, pp. 187–196, 2014.

[32] J. P. Barton and D. G. Infield, “Energy storage and its use with intermittent renewable energy,” *IEEE Trans. Energy Convers.*, vol. 19, no. 2, pp. 441–448, 2004.

[33] J. K. Kaldellis and K. A. Kavadias, “Optimal wind-hydro solution for Aegean Sea islands’ electricity-demand fulfilment,” *Appl. Energy*, vol. 70, no. 4, pp. 333–354, 2001.

[34] T. Ma, H. Yang, and L. Lu, “A feasibility study of a stand-alone hybrid solar-wind-battery system for a remote island,” *Appl. Energy*, vol. 121, pp. 149–158, 2014.

[35] C. Protogeropoulos, B. J. Brinkworth, and R. H. Marshall, “Sizing and techno-economical optimization for hybrid solar photovoltaic/wind power systems with battery storage,” *Int. J. Energy Res.*, vol. 21, no. 3, p. 465—479, 1997.

[36] T. Ma, H. Yang, and L. Lu, “Feasibility study and economic analysis of pumped hydro storage and battery storage for a renewable energy powered island,” *Energy Convers. Manag.*, vol. 79, pp. 387–397, 2014.

[37] G. Bekele and G. Tadesse, “Feasibility study of small Hydro/PV/Wind hybrid system for off-grid rural electrification in Ethiopia,” *Appl. Energy*, vol. 97, pp. 5–15, 2012.

[38] G. Bekele and B. Palm, “Feasibility study for a standalone solar-wind-based hybrid energy system for application in Ethiopia,” *Appl. Energy*, vol. 87, no. 2, pp. 487–495, 2010.

[39] O. Ekren and B. Y. Ekren, “Size optimization of a PV/wind hybrid energy conversion system with battery storage using response surface methodology,” *Appl. Energy*, vol. 85, no. 11, pp. 1086–1101, 2008.

[40] A. N. Celik, “Techno-economic analysis of autonomous PV-wind hybrid energy systems using different sizing methods,” *Energy Convers. Manag.*, vol. 44, no. 12, pp. 1951–1968, 2003.

[41] D. Menniti, a. Pinnarelli, and N. Sorrentino, “A method to improve microgrid reliability by optimal sizing PV/wind plants and storage systems,” *IET Conf. Publ.*, no. April 2016, pp. 816–816, 2009.

[42] A. Maleki and A. Askarzadeh, “Optimal sizing of a PV/wind/diesel system with battery storage for electrification to an off-grid remote region: A case study of Rafsanjan, Iran,” *Sustain. Energy Technol. Assessments*, vol. 7, pp. 147–153, 2014.

[43] J. K. Kaldellis and D. Zafirakis, “Optimum energy storage techniques for the improvement of renewable energy sources-based electricity generation economic efficiency,” *Energy*, vol. 32, no. 12, pp. 2295–2305, 2007.

[44] H. T. Le, “Sizing Energy Storage Systems for Wind Power Firming : An Analytical Approach and a Cost-Benefit Analysis,” *Power Energy Soc. Gen. Meet.*, no. ii, pp. 1–8, 2008.

[45] S. X. Chen, H. B. Gooi, and M. Q. Wang, “Sizing of energy storage for microgrids,” *IEEE Trans. Smart Grid*, vol. 3, no. 1, pp. 142–151, 2012.

[46] S. Bahramirad, W. Reder, and A. Khodaei, “Reliability-constrained optimal sizing of energy storage system in a microgrid,” *IEEE Trans. Smart Grid*, vol. 3, no. 4, pp. 2056–2062, 2012.

[47] B. S. Borowy and Z. M. Salameh, “Methodology for Optimally Sizing the Combination of a Battery Bank and PV Array in a Wind/PV Hybrid System,” *IEEE Trans. Energy Convers.*, vol. 11, no. 2, 1996.

[48] W. D. Kellogg, M. H. Nehrir, G. Venkataramanan, and V. Gerez, “Generation unit sizing and cost analysis for stand-alone wind, photovoltaic, and hybrid wind/PV systems,” *IEEE Trans. Energy Convers.*, vol. 13, no. 1, pp. 70–75, 1998.

[49] A. Poullikkas, “Parametric cost-benefit analysis for the installation of photovoltaic parks in the island of Cyprus,” *Energy Policy*, vol. 37, no. 9, pp. 3673–3680, 2009.

[50] P. A. Fokaides and A. Kylili, “Towards grid parity in insular energy systems: The case of photovoltaics (PV) in Cyprus,” *Energy Policy*, vol. 65, pp. 223–228, 2014.

[51] C. Koroneos, P. Fokaidis, and N. Moussiopoulos, “Cyprus energy system and the use of renewable energy sources,” *Energy*, vol. 30, no. 10, pp. 1889–1901, 2005.

[52] D. Solyali and M. A. Redfern, “Case study of Cyprus: wind energy or solar power?,” *Proc. 11th Int. Sci. Conf. Electr. Power Eng. 2010*, no. May, pp. 283–290, 2010.

[53] M. Ilkan, E. Erdil, and F. Egelioglu, “Renewable energy resources as an alternative to modify the load curve in Northern Cyprus,” *Energy*, vol. 30, no. 5, pp. 555–572, 2005.

[54] P. A. Fokaides, I. C. Miltiadous, M. K. A. Neophytou, and L. P. Spyridou, “Promotion of wind energy in isolated energy systems: The case of the Orites wind farm,” *Clean Technol. Environ. Policy*, vol. 16, no. 3, pp. 477–488, 2014.

[55] G. Panayiotou, S. Kalogirou, and S. Tassou, “Design and simulation of a PV and a PV-Wind standalone energy system to power a household application,” *Renew. Energy*, vol. 37, no. 1, pp. 355–363, 2012.

[56] W. P. M. R. Pathirana and A. Muhtaroğlu, “Multifaceted Feasibility Analysis of PV Solar Application in Northern Cyprus,” *Int. J. energy*, vol. 3, no. 4, 2013.

[57] S. M. S. Sadati, E. Jahani, and O. Taylan, “Technical and economic analyses for sizing PV power plant with storage system for METU NCC,” in *ASME International Mechanical Engineering Congress and Exposition*, 2015.

[58] M. Yenen, “Modeling Electrical Energy Production in Northwestern Cyprus Based on Solar And Wind Measurements,” Middle East Technical University Northern Cyprus Campus, 2015.

[59] S. Sinha and S. S. Chandel, “Review of software tools for hybrid renewable energy systems,” *Renew. Sustain. Energy Rev.*, vol. 32, pp. 192–205, 2014.

[60] NREL, “Getting Started Guide for HOMER Legacy (Version 2.68),” Colorado, 2011.

[61] J. A. Duffie and W. A. Beckman, *Solar engineering of thermal processes*, 3rd ed. Hoboken, N.J: Wiley, 2006.

[62] P. G. Loutzenhiser, H. Manz, C. Felsmann, P. A. Strachan, T. Frank, and G. M. Maxwell, “Empirical validation of models to compute solar irradiance on inclined surfaces for building energy simulation,” *Sol. Energy*, vol. 81, no. 2, pp. 254–267, 2007.

[63] S. Dubey, J. N. Sarvaiya, and B. Seshadri, “Temperature dependent photovoltaic (PV) efficiency and its effect on PV production in the world - A review,” *Energy Procedia*, vol. 33, pp. 311–321, 2013.

[64] AXITEC Solar, “AXIplus SE 60,” USA.

[65] Y. Ueda, K. Kurokawa, K. Kitamura, M. Yokota, K. Akanuma, and H. Sugihara, “Performance analysis of various system configurations on grid-connected residential PV systems,” *Sol. Energy Mater. Sol. Cells*, vol. 93, no. 6–7, pp. 945–949, 2009.

[66] N. H. Reich, B. Mueller, A. Armbruster, W. G. J. H. M. Van Sark, K. Kiefer, and C. Reise, “Performance ratio revisited: is PR>90% reaslistic?,” *Prog. Photovolt Res. Appl.*, vol. 20, no. 6, pp. 717–726, 2012.

[67] J. F. Manwell, J. G. McGowan, and A. L. Rogers, *Wind energy explained: theory, design and application*, 2nd ed. Chichester, U.K: Wiley, 2009.

[68] Gamesa, “G114-2.0 MW: greater energy produced from low and medium wind sites,” Madrid, 2014.

[69] B. Zakeri and S. Syri, “Electrical energy storage systems: A comparative life cycle cost analysis,” *Renew. Sustain. Energy Rev.*, vol. 42, pp. 569–596, 2015.

[70] S. M. Schoenung and W. V. Hassenzahl, “Long- vs . Short-Term Energy Storage Technologies Analysis A Life-Cycle Cost Study A Study for the DOE Energy Storage Systems Program,” *Power Qual.*, vol. SAND2011-2, no. August, p. 84, 2003.

[71] SAFT, “A range of ready- to- install containerised energy storage for renewable energies and grid management,” 2013.

[72] N. Erniza, M. Rozali, S. Rafidah, and W. Alwi, “Optimisation of Pumped-Hydro Storage System for Hybrid Power System Using Power Pinch Analysis,” *Chem. Eng. Trans.*, vol. 35, pp. 85–90, 2013.

[73] “NRC: Glossary -- Capacity factor (net).” [Online]. Available: http://www.nrc.gov/reading-rm/basic-ref/glossary/capacity-factor-net.html.

[74] F. Breu, S. Guggenbichler, and J. Wollmann, “Carbon dioxide intensities of fuels and electricity for regions and countries,” 2003.

[75] A. J. Sangster, “Solar Photovoltaics,” *Green Energy Technol.*, vol. 194, no. 4, pp. 145–172, 2014.

[76] P. Breeze, “Wind Power,” *Power Gener. Technol.*, vol. 1, no. 5, pp. 223–242, 2014.

[77] Y. Sawle, S. C. Gupta, A. Kumar Bohre, and W. Meng, “PV-wind hybrid system: A review with case study,” *Cogent Eng.*, vol. 3, no. 1, p. 1189305, 2016.

[78] J. Steinbach and D. Staniaszek, “Discount rates in energy system analysis Discussion Paper,” no. May, 2015.

[79] N. Rule and S. A. Ross, “Contemporary Issues Uses , Abuses , and Alternatives to the,” *Alternatives*, vol. 24, no. 3, pp. 96–102, 1995.

[80] “Net Present Value - The Environmental Literacy Council.” [Online]. Available: https://enviroliteracy.org/environment-society/economics/net-present-value/. [Accessed: 10-Feb-2017].

[81] “Cyprus - Island Profile - Nations Online Project.” [Online]. Available: http://www.nationsonline.org/oneworld/cyprus.htm. [Accessed: 17-Feb-2017].

[82] Northern Cyprus Electricity-corporation, “Statistics.” [Online]. Available: https://www.kibtek.com/statistikler/. [Accessed: 13-Jan-2017].

[83] “Specific carbon dioxide emissions of various fuels.” [Online]. Available: http://www.volker-quaschning.de/datserv/CO2-spez/index_e.php.

[84] A. A. BABATUNDE and S. ABBASOĞLU, “Evaluation of field data and simulation results of a photovoltaic system in countries with high solar radiation,” *Turkish J. Electr. Eng. Comput. Sci.*, vol. 23, pp. 1608–1618, 2015.

[85] D. Solyali, M. Altunç, S. Tolun, and Z. Aslan, “Wind resource assessment of Northern Cyprus,” *Renew. Sustain. Energy Rev.*, vol. 55, pp. 180–187, 2016.

[86] K. Radics and J. Bartholy, “Estimating and modelling the wind resource of Hungary,” *Renew. Sustain. Energy Rev.*, vol. 12, no. 3, pp. 874–882, 2008.

[87] “My epic Cyprus road trip! – TravelReportage.com by Giulia Cimarosti.” [Online]. Available: http://www.travelreportage.com/2012/08/08/my-epic-cyprus-road-trip/. [Accessed: 17-Feb-2017].

[88] S. M. H. Ali, “Optimal Photovoltaic Size Estimation for a Campus Area Considering Uncertainties in Load, Power Generation and Electricity Rates,” Middle East Technical University Northern Cyprus Campus, 2015.

[89] S. Project, “Facilitating energy storage to allow high penetration of intermittent renewable energy Report summarizing the current Status , Role and Costs of Energy Storage Technologies,” *http://www.store-project.eu/documents/results/en_GB/report-summarizing-the-current-status-role-and-costs-of-energy-storage-technologies*, 2012.

[90] “Northern Cyprus Electricity-corporation.” [Online]. Available: https://www.kibtek.com/. [Accessed: 31-Jan-2017].

[91] S. Wilcox and W. Marion, “Users manual for TMY3 data sets,” *Renew. Energy*, no. May, p. 51, 2008.

[92] S. Rehman and N. M. Al-Abbadi, “Wind shear coefficients and energy yield for Dhahran, Saudi Arabia,” *Renew. Energy*, vol. 32, no. 5, pp. 738–749, 2007.